Signal Processing and Microwave Remote Sensing WS 19/20

I. Microwave Remote Sensing

Prof. Dr. Michael Eineder

Institut für Methodik der Fernerkundung
Deutsches Zentrum für Luft- und Raumfahrt DLR

Microwave Satellite Remote Sensing

Atmospheric Transmittance

→ influenced by gases, frequency-dependent

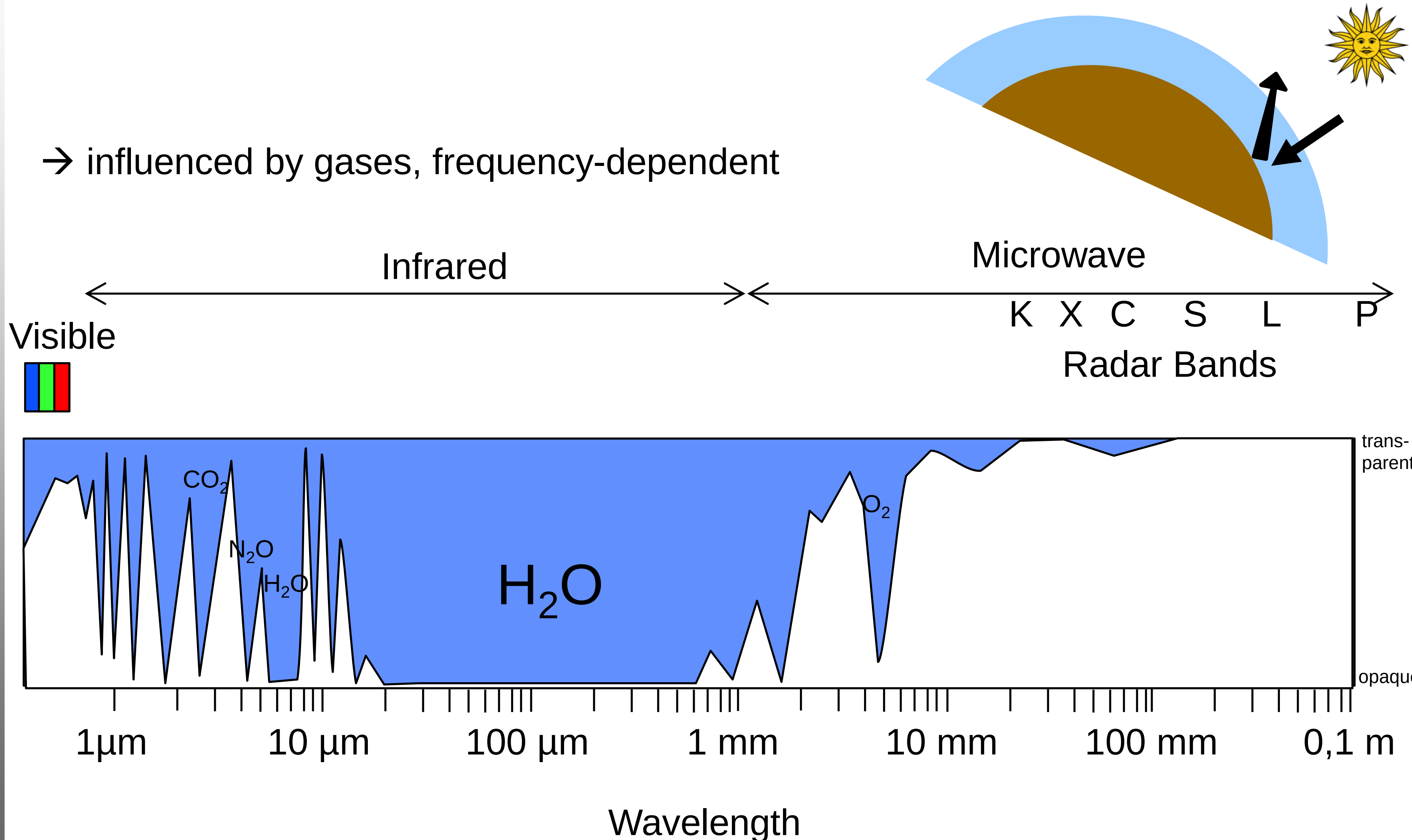

Microwaves in Remote Sensing

- Sensors: High-frequency electronics instead of optics
- Mainly penetrating atmosphere and clouds
- Partial penetration of vegetation, soil, snow and ice
- Emission and reflectance are mainly controlled by the complex dielectric constant (mainly due to water content)
- Scattering ("reflection behaviour") is mainly influenced by
  - Volumetric distribution of objects ("scatterers", e.g. vegetation)
  - Surface roughness: e.g. Bragg-scattering
- Coherent measurement of signal return phase possible
  - mandatory for Synthetic Aperture Radar, Interferometry, etc

Microwave Frequency and Wavelength Bands

Definitions by IEEE , NATO and ITU

band	frequency f_0	wavelength $\lambda = c/f_0$	typical application
Q-D	33–170 GHz	1.8 –9.0 mm	passive microwave sounding
Ka	27 – 40 GHz	1.1 – 0.8 cm	airport surveillance
K	18 – 27 GHz	1.7 – 1.1 cm	little used (H_2O absorption)
Ku	12 – 18 GHz	2.4 – 1.7 cm	**satellite altimetry**
X	8 – 12 GHz	3.8 – 2.4 cm	**SAR**, marine radar, weather radar
C	4 – 8 GHz	7.5 – 3.8 cm	**SAR**, weather radar
S	2 – 4 GHz	15 – 7.5 cm	long-range weather radar
L	1 – 2 GHz	30 – 15 cm	**SAR**, traffic control
P	0.3 – 1 GHz	100 – 30 cm	experimental SAR

Microwave Satellite Remote Sensing

Microwave Reflector and Horn Antennas

- Conversion of electrical energy to high frequency EM radiation (microwaves)
- Directed illumination of scene with antenna diagram
- Reception of reflected EM energy and conversion to electrical signal

- → passive antennas, e.g. planar, parabolic, horn

Sensitivity Diagram of a Flat Antenna

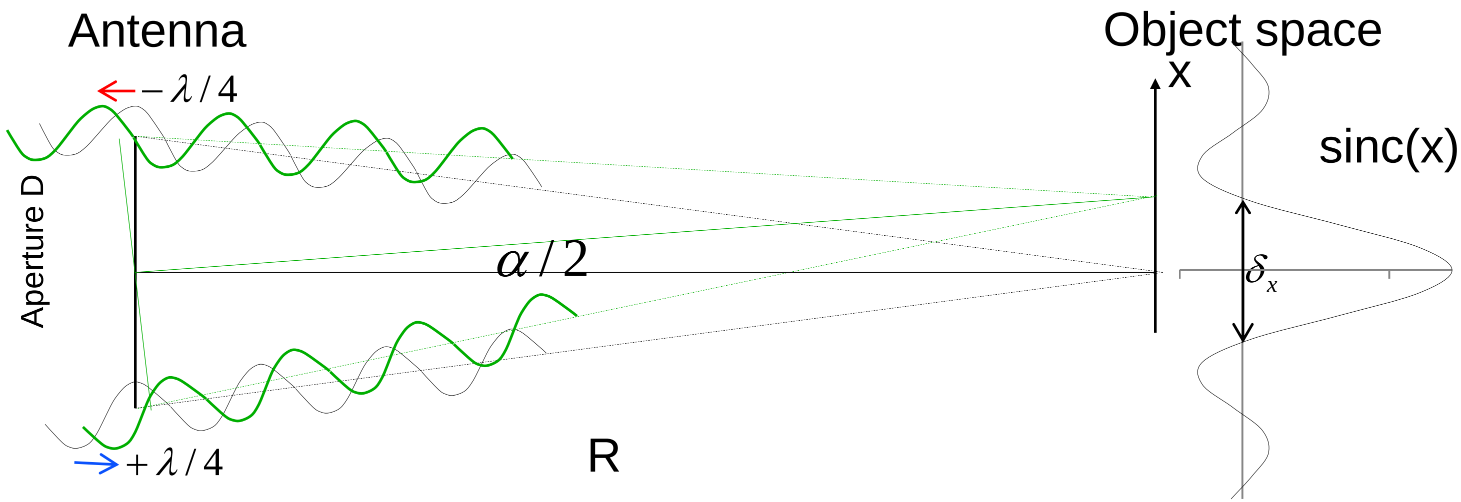

Antenna beam width:

$$\boxed{\begin{aligned} &\alpha \approx \lambda / D \\ &\delta_x = R\alpha = R\lambda / D \end{aligned}}$$

→Pointing characteristics depends on wavelength and size of antenna

Angular Resolution of an Optical Imaging System

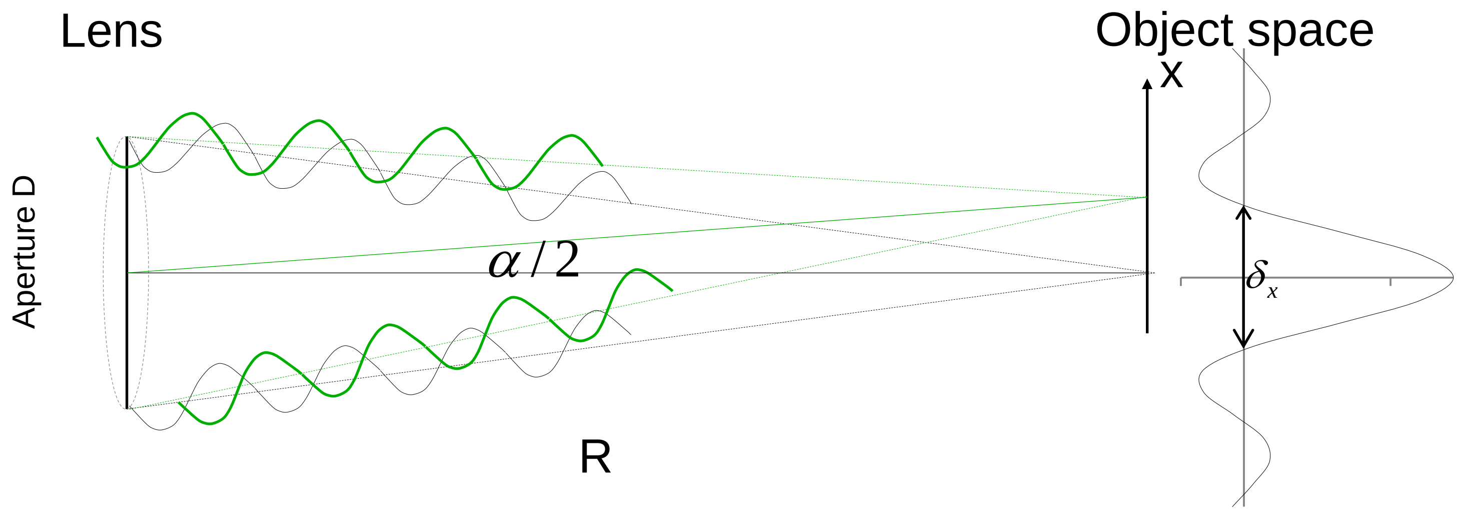

Diffraction limit (angle): $\alpha \approx \lambda / D$

Diffraction limit (): $\delta_x = R\alpha = R\lambda / D$

→Diffraction limits resolution of sensors and transmitters!

Examples:

Human eye:	1000 km * 500 nm/5 mm = 100 m
Satellite dish antenna (Ku):	1000 km * 2 cm / 60 cm = 33 km (!)

Planar Antennas

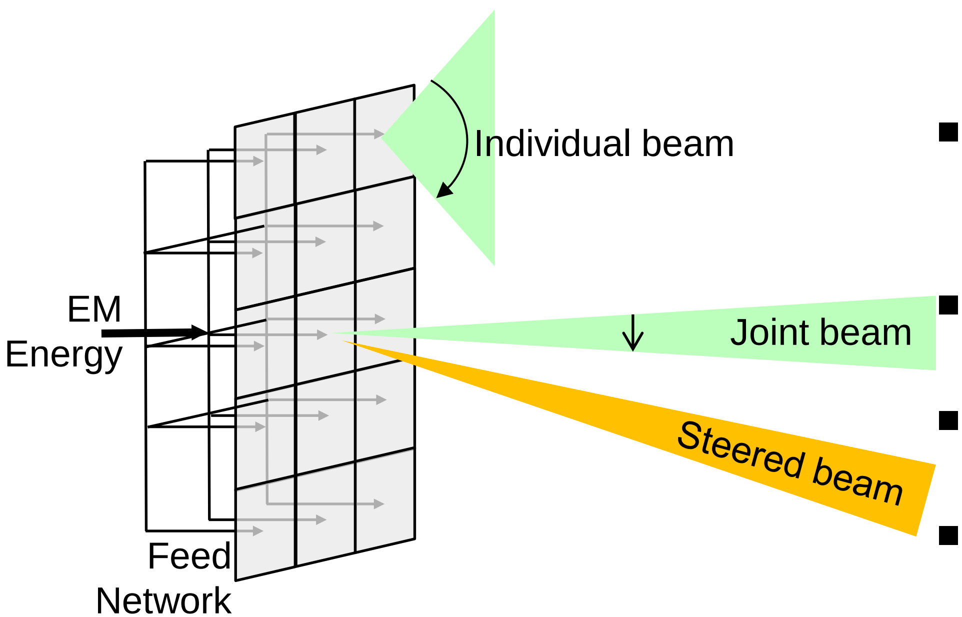

- Antenna is composed from several smaller elements, e.g. microstrip, slotted waveguides (“array antenna”)
- Together they form a larger antenna with smaller beam width (higher directivity)
- Beam steering possible by phase shifting of individual elements
- Same principle for transmit and receive
- Examples: Most Synthetic Aperture Radars

Phased Array Antennas

- Electronic antenna beam steering with phase shifters

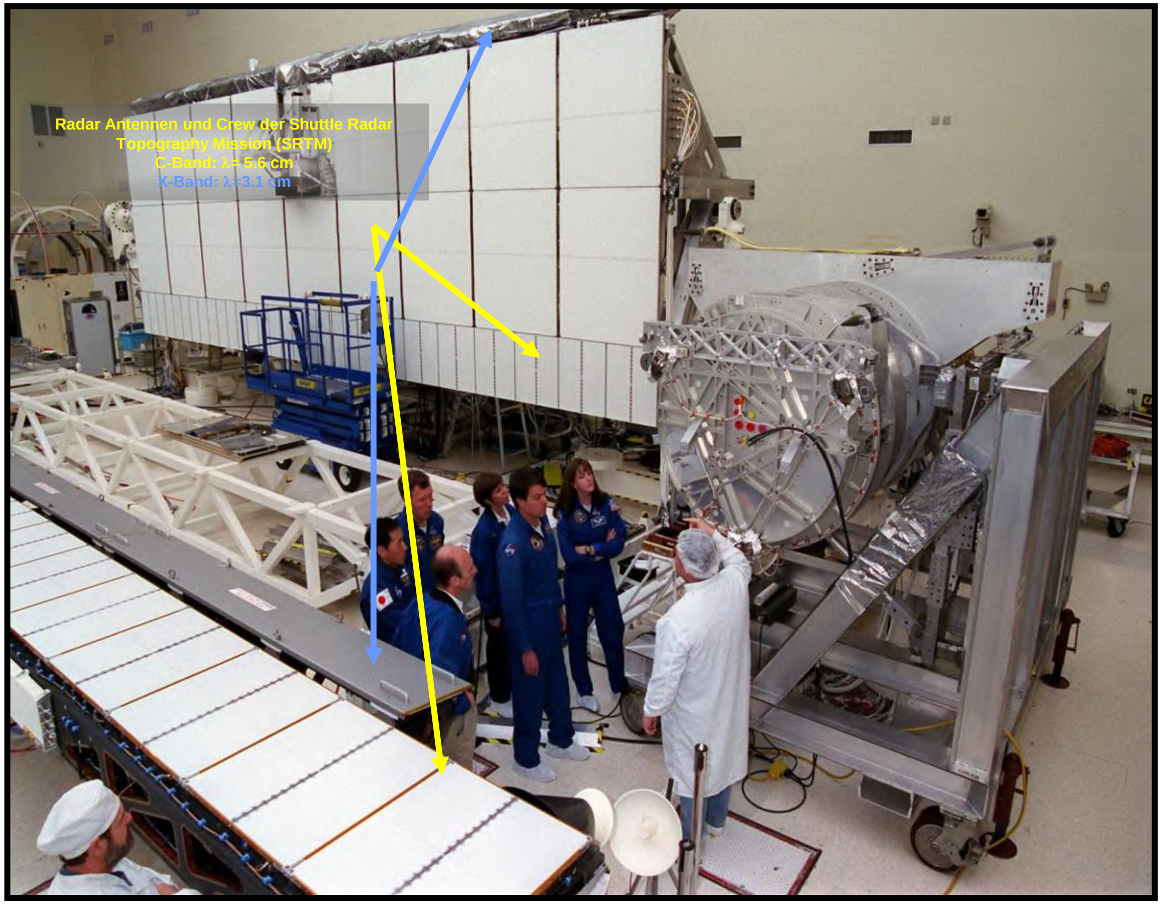

(Photo: NASA/JPL)

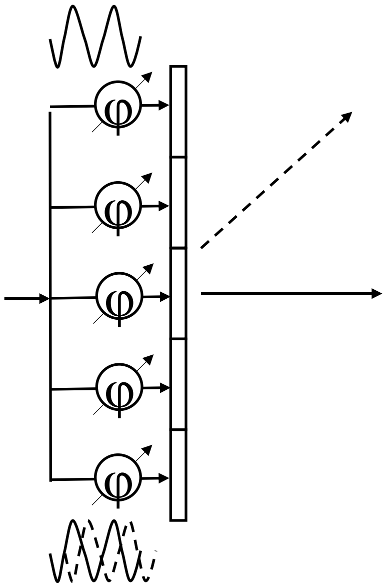

Reflector Antennas

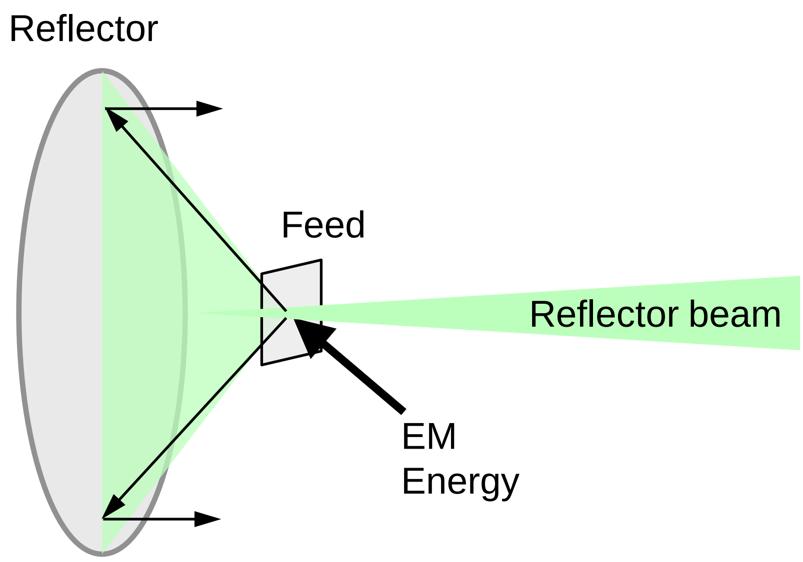

- Small, high power element illuminates larger parabolic reflector
- Size of reflector determines beam width
- Orientation of reflector determines beam pointing

- Examples: communication, Sat-TV, simple radars, radar altimeters

New: Reflector Antennas with Feed Array

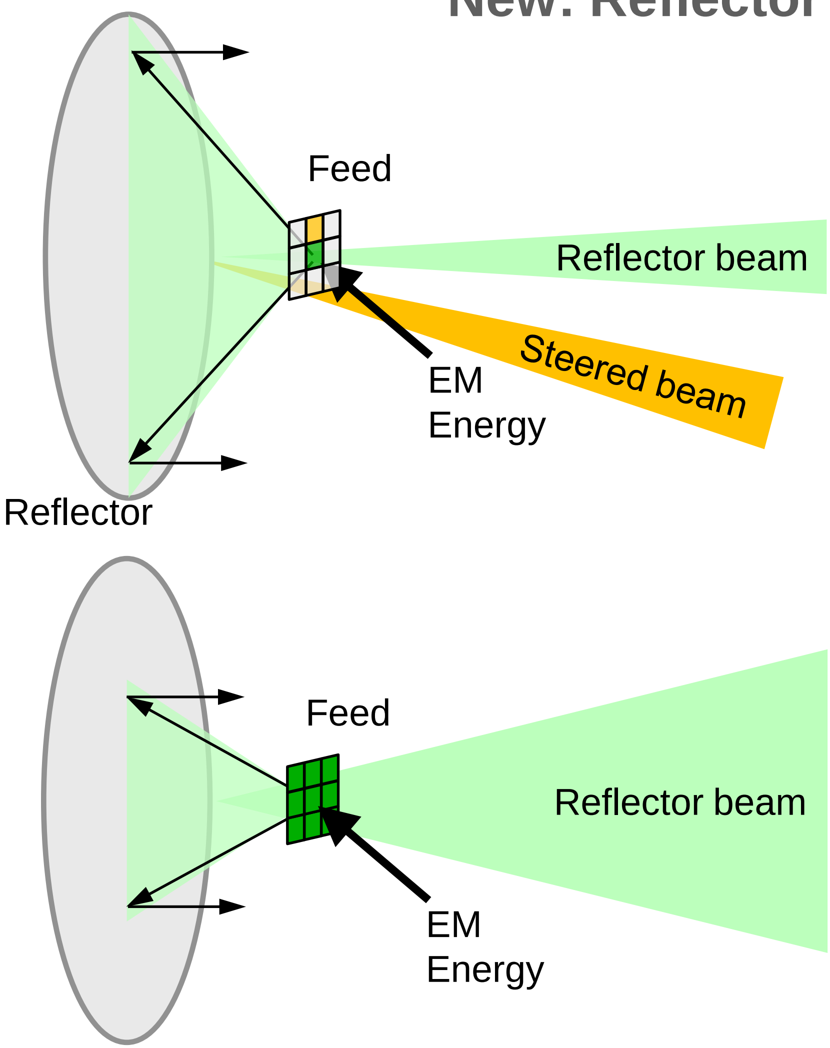

- Beam width can be electronically changed by using one or multiple array elements
- Beam pointing can be electronically changed (steered) by using different array elements ("feed offset")

- Examples: e.g. Innovative SARs (e.g. Biomass, DLR's Tandem-L proposal)

EM-Wave Scattering at Rough Surfaces (simplified)

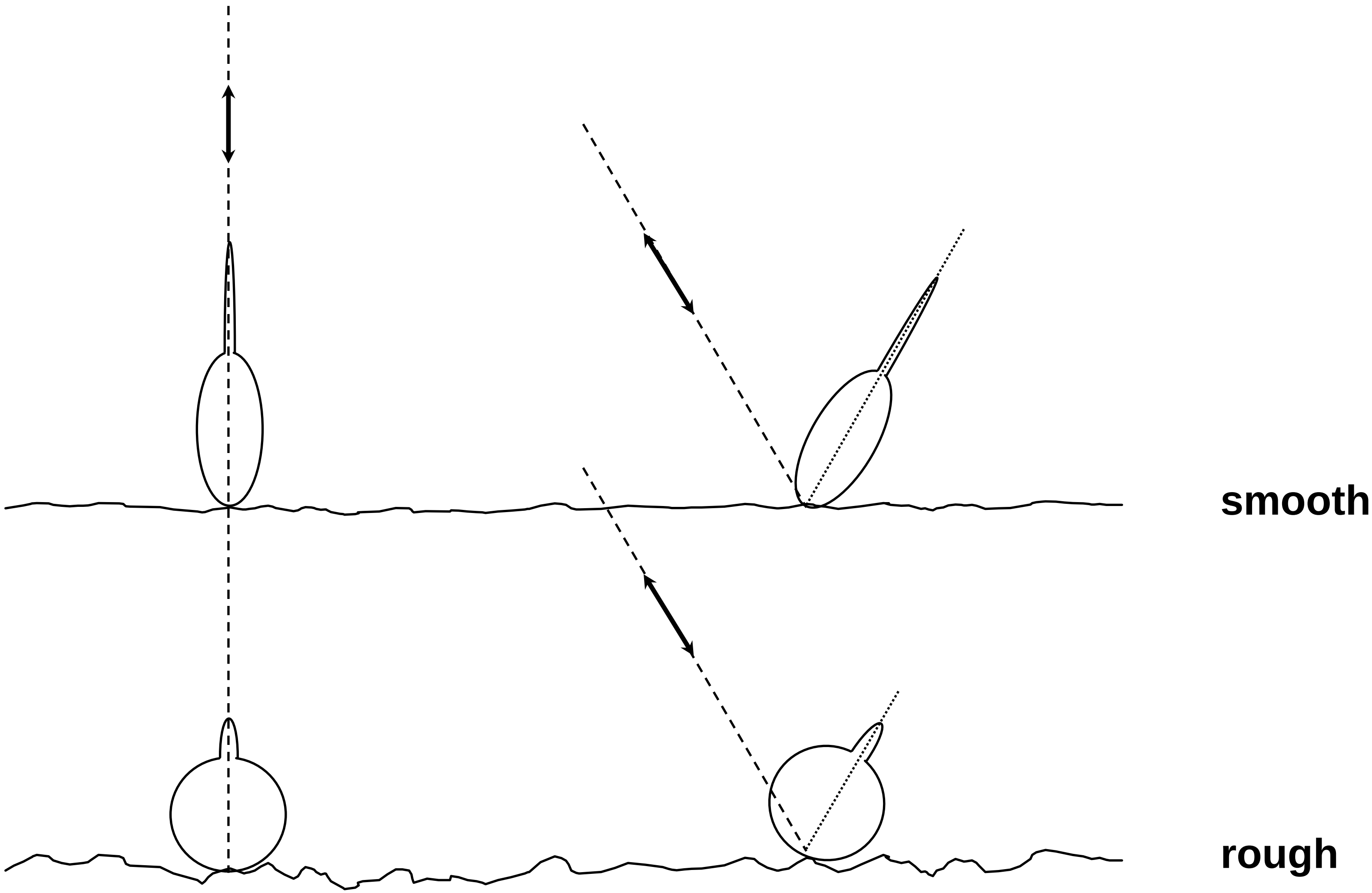

Wavelength and Surface Roughness

$$\lambda = 2\,\text{cm} \ldots 25\,\text{cm}$$

rough **smooth**

Phasor Representation of a Wave Signal

complex representation: $A \cdot \cos(2\pi \nu_0 \tau + \phi) \rightarrow A \cdot \exp(j\,(2\pi \nu_0 \tau + \phi))$

after demodulation: $u = A \cdot \exp(j \cdot \phi)$

amplitude: $A = |u|$

intensity, power: $A^2 = |u|^2$

phase: ϕ

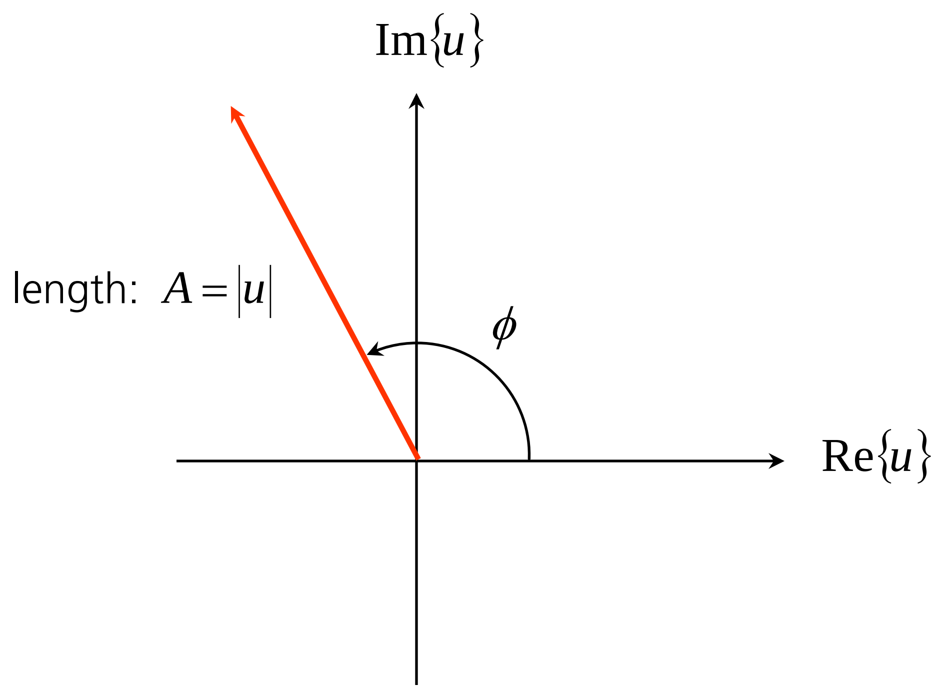

Phase and Frequency Basics

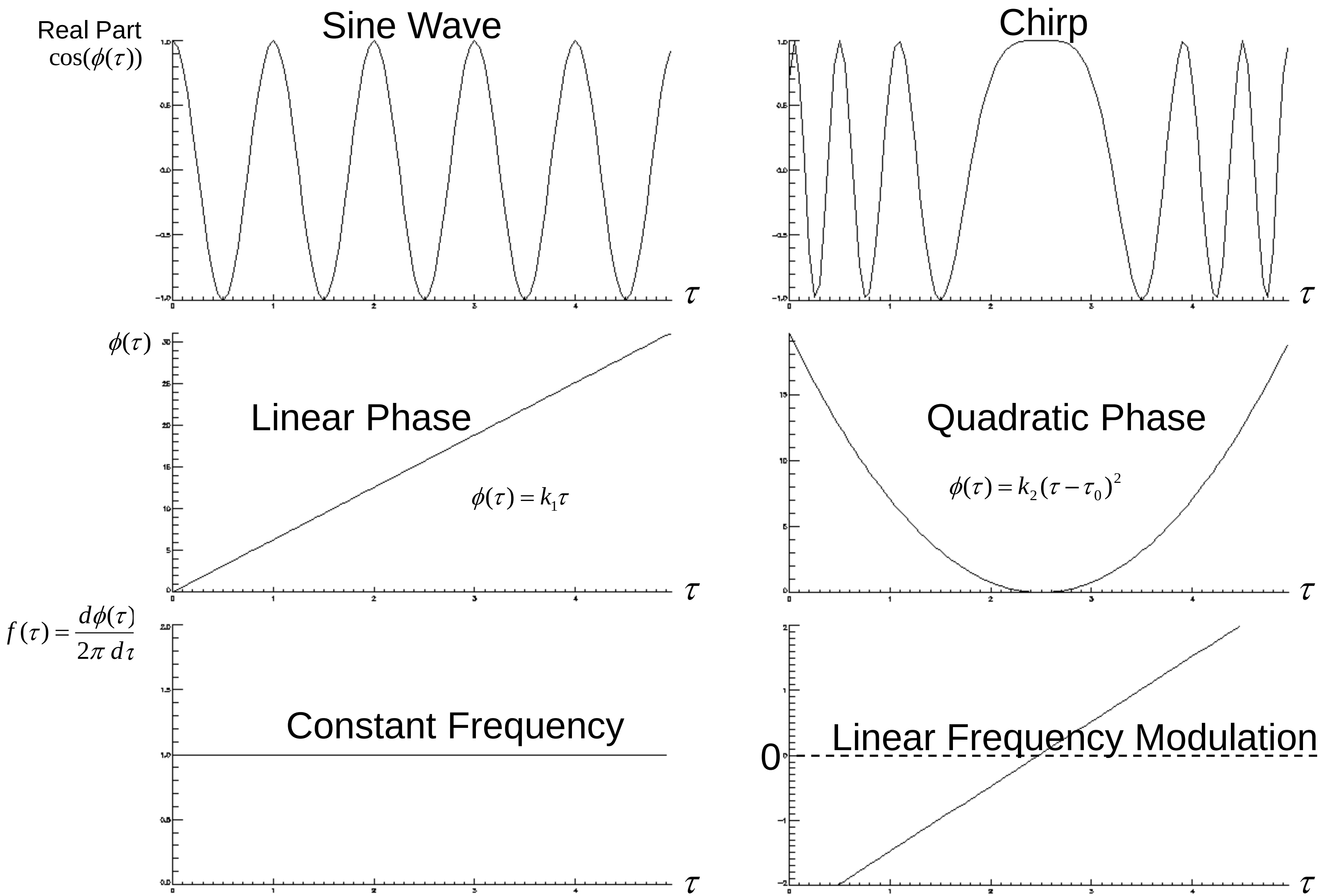

Microwave Satellite Remote Sensing

Microwave Radiometers

- Passive instrument, measures
- the emission of the Earth surface caused by surface temperature
- atmospheric parameters
- Example: Microwave Humidity Sounder (MHS) on ESA's MetOp-A (2006)

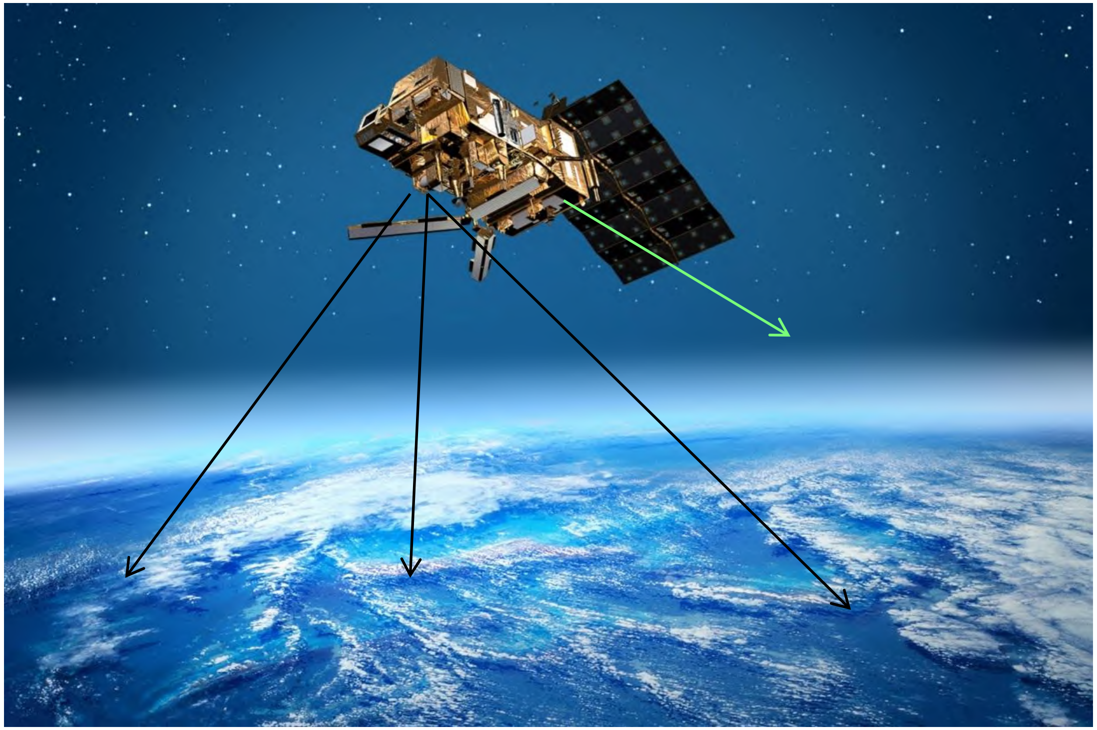

MetOp-1 © ESA

MHS Instrument

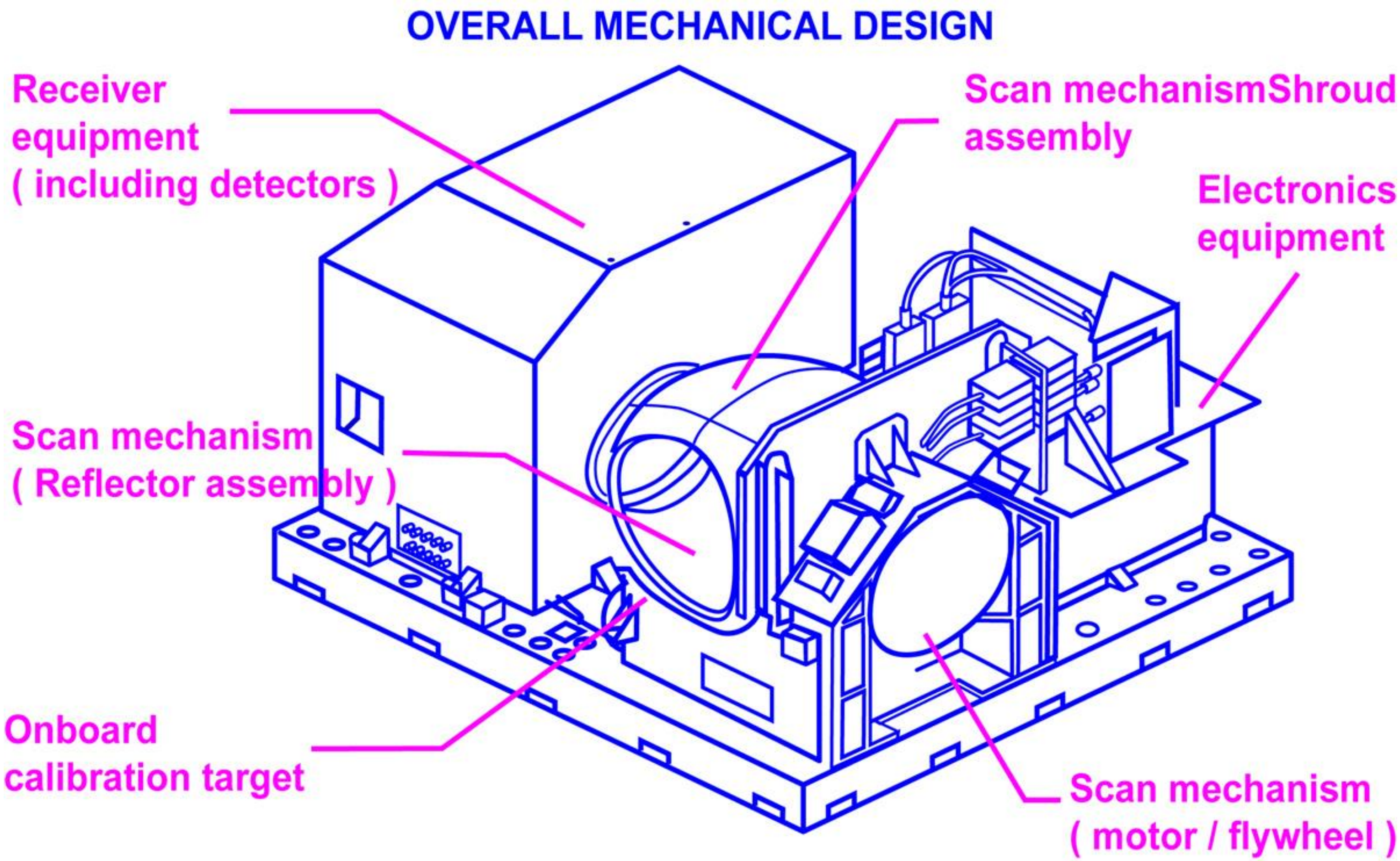

Microwave Humidity Sounder: 5-Channel Radiometer

Absorption curves of Water Vapor and Oxygen

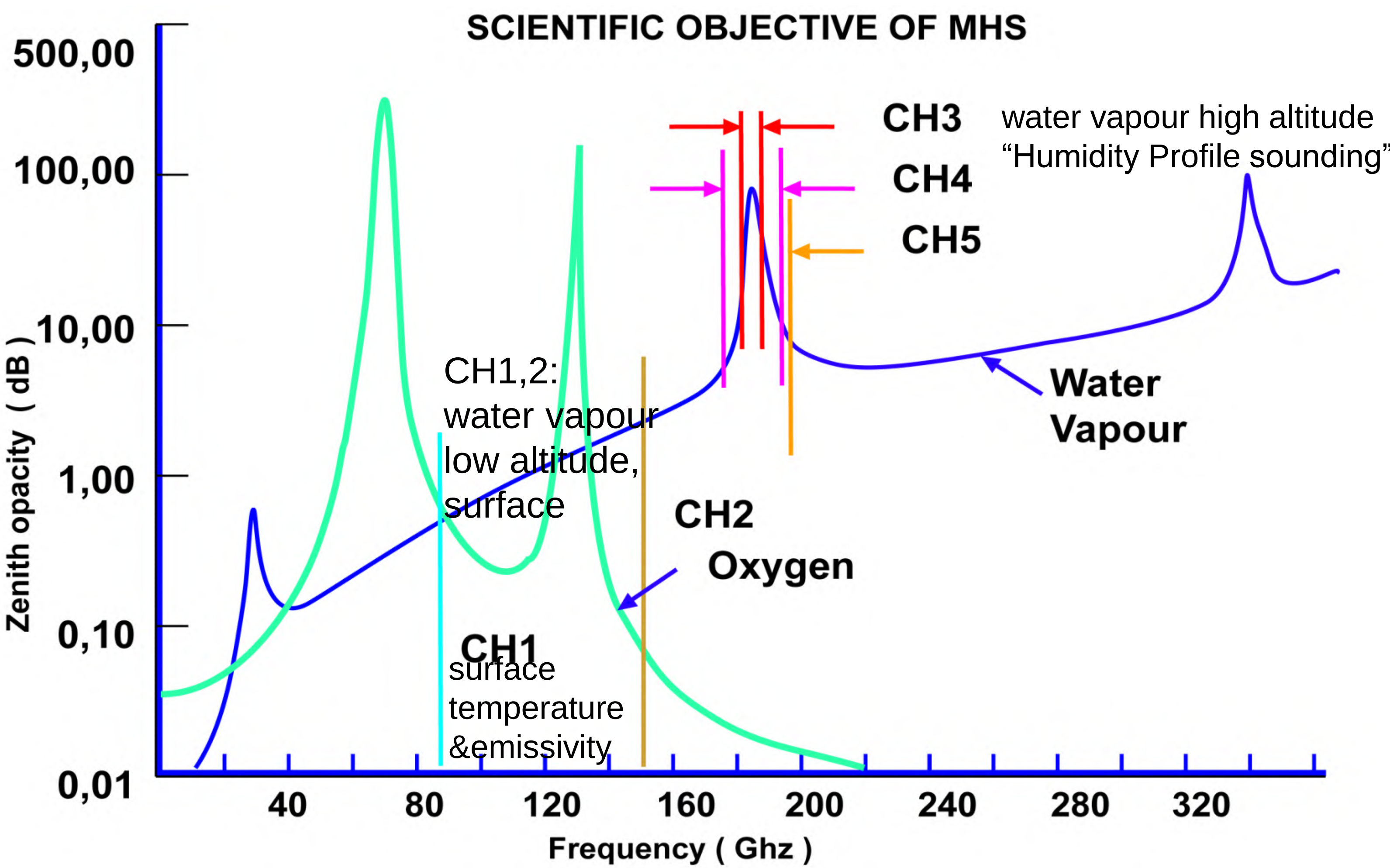

Graphics: © ESA

MetOp MHS 89GHz (CH1) World view

Data acquired over one complete satellite orbit

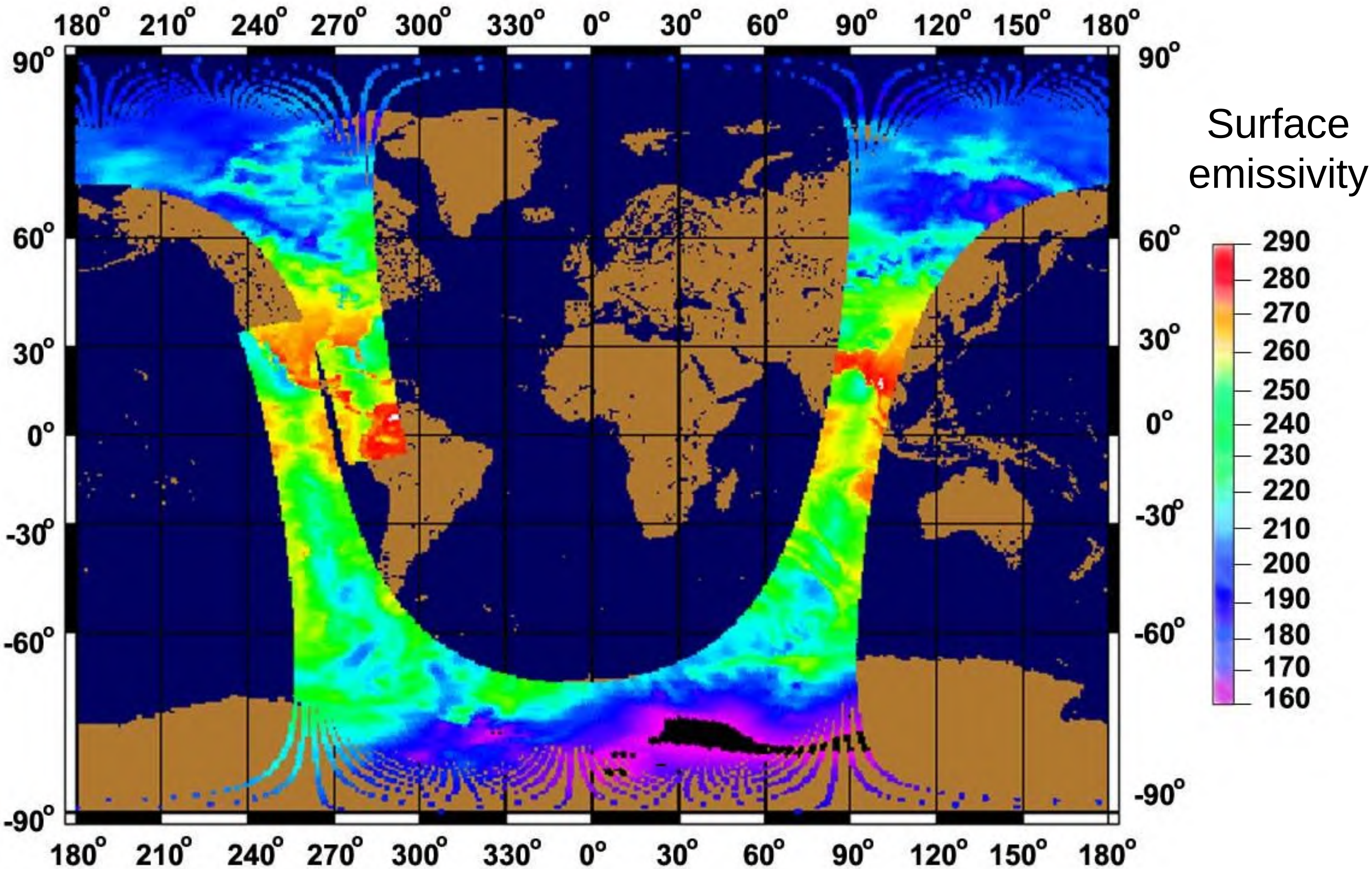

Other Passive Satellite Microwave Radiometers (I)

Instrument		Satellite	
SMMR	Scanning Multichannel Microwave Radiometer	SEASAT, NIMBUS-7	’78-’87
SSM/I	Special Sensor Microwave / Imager	DMSP	’87-
TMI	TRMM Microwave Imager	TRMM	’97-
MWR	Microwave Sounder	ERS, ENVISAT	’91-
AMSU-A / -B	Advanced Microwave Sounding Unit	NOAA, METOP	’98-
MHS	Microwave Humidity Sounder	METOP, NOAA	’05-

Examples: Passive Microwave Radiometers (II)

name	frequencies [GHz]	number of channels	swath [km]	EFOV [km]
SMMR	6.63, 10.69, 18.0, 21.0 37.0 GHz; H and V	10	1846	
SSM/I	19.3, 37, 85.5;H and V 22.2 V	7	1394	43 x 69 … 13 x 15
TMI	10.7, 19.[illegible] 37, 85.5	10	780	63 x 37 … 7 x 5
MWR	23.8, 3[illegible]	[illegible]	[illegible]	[illegible]
AMSU-A	23.8V, [illegible] 52.8V, 53.6H, 54.4H, 54.94V, 55.5H, 57.29H, 89,0V	15	2343	50 (nadir)
AMSU-B	89.0, 150.0, 183.0	5	2350	16,3 (nadir)
MHS	89.0, 157.0, 183.311	5	-	16

Special Sensor Microwave/Imager (SSM/I): measures surface/atmospheric microwave brightness temperatures …

Sea Ice Concentration from SSM/I Temperature Data

March 3, 2002

Antarctica

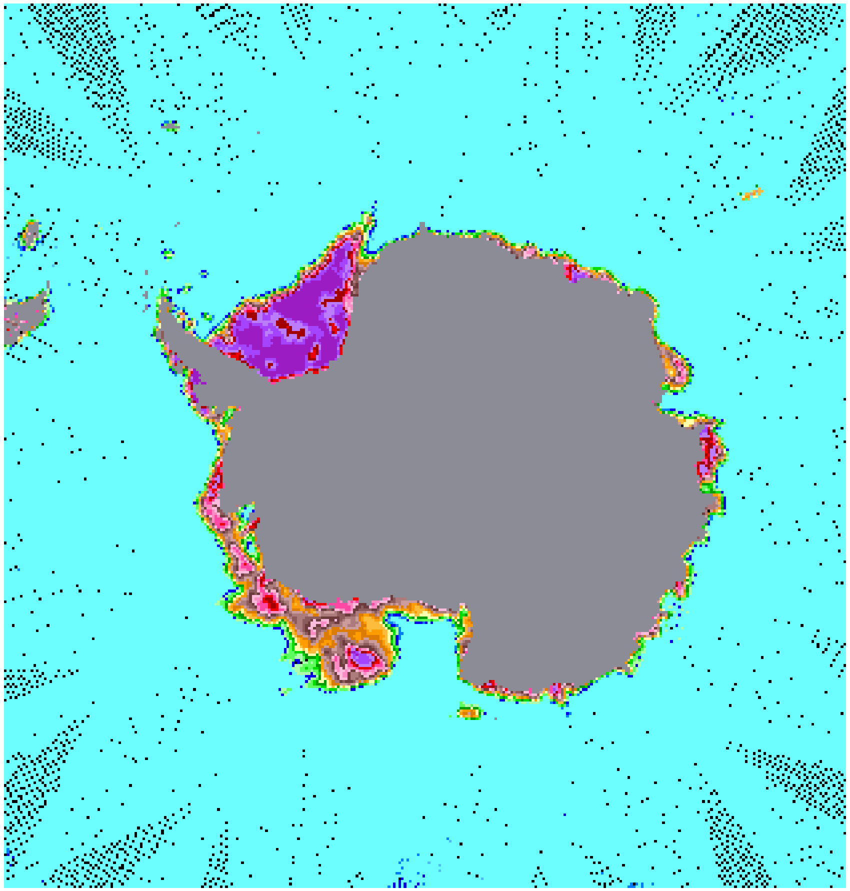

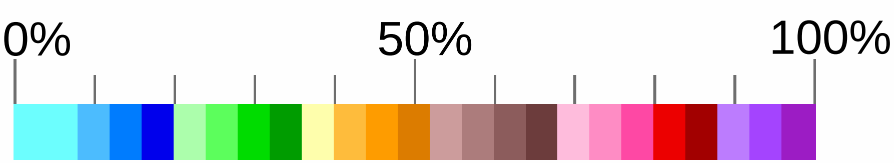

Arctica

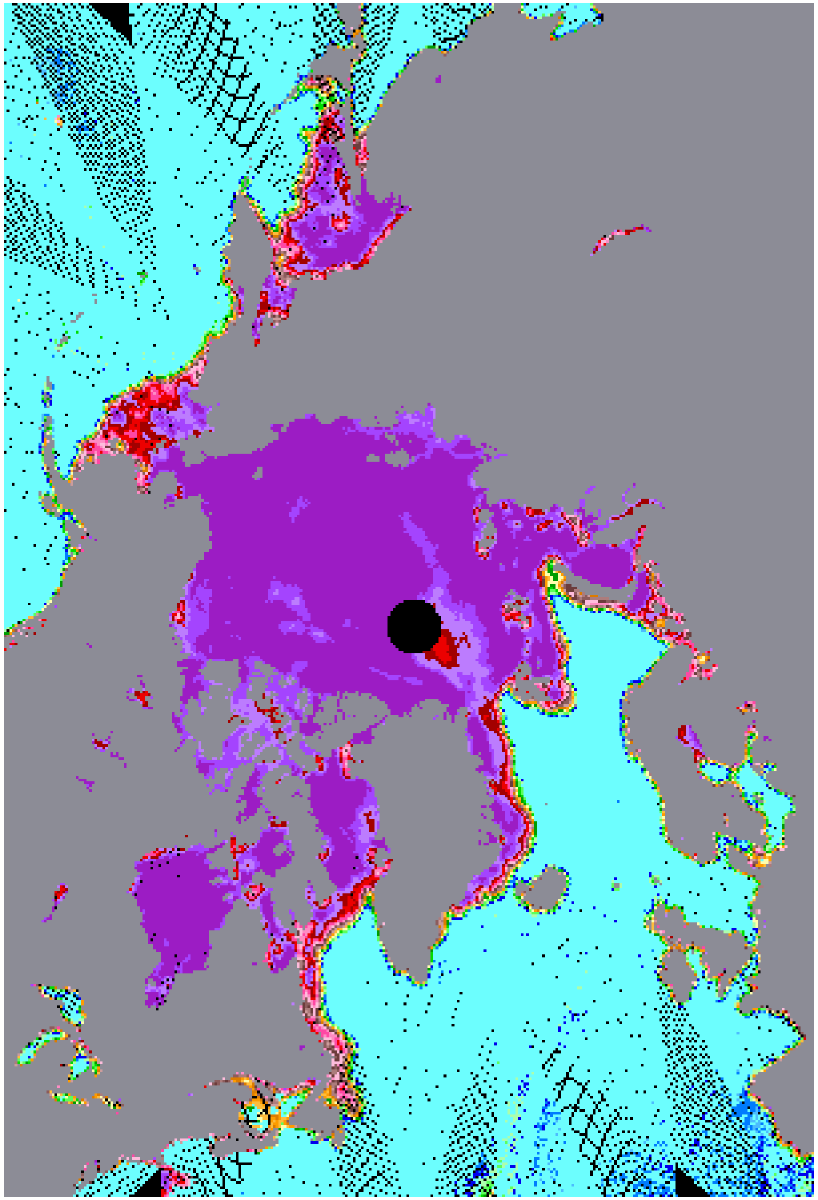

Sea Ice Concentration from SSM/I Temperature Data

October 27, 2002 Antarctica

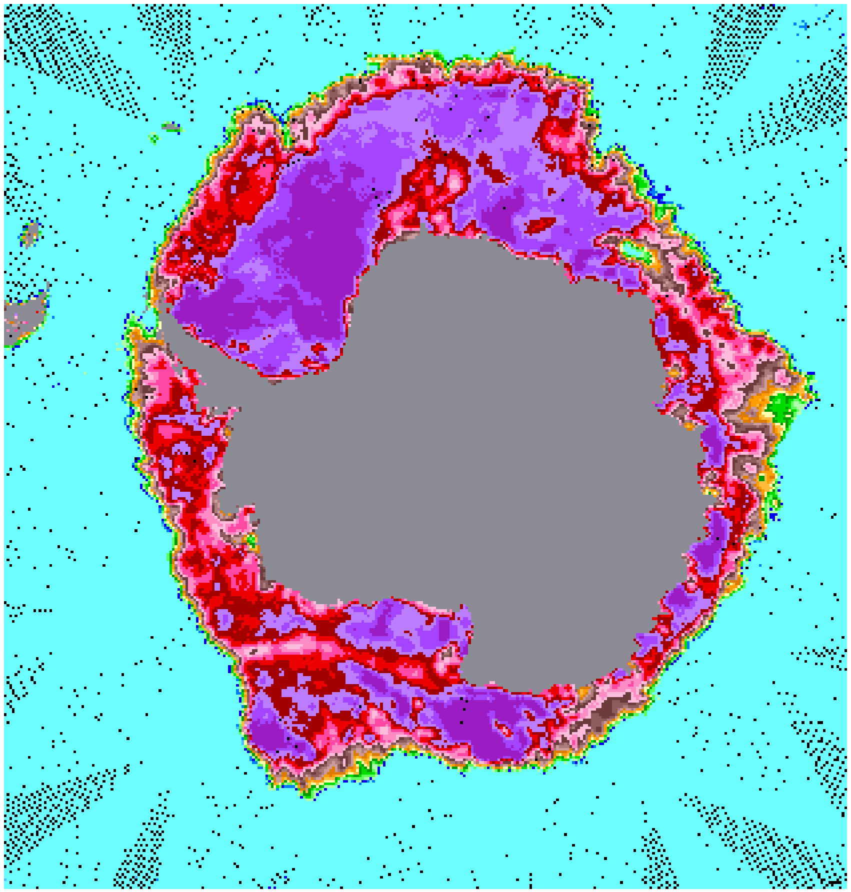

0% 50% 100%

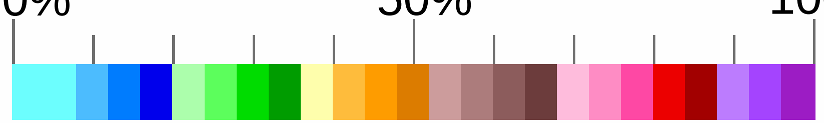

Arctica

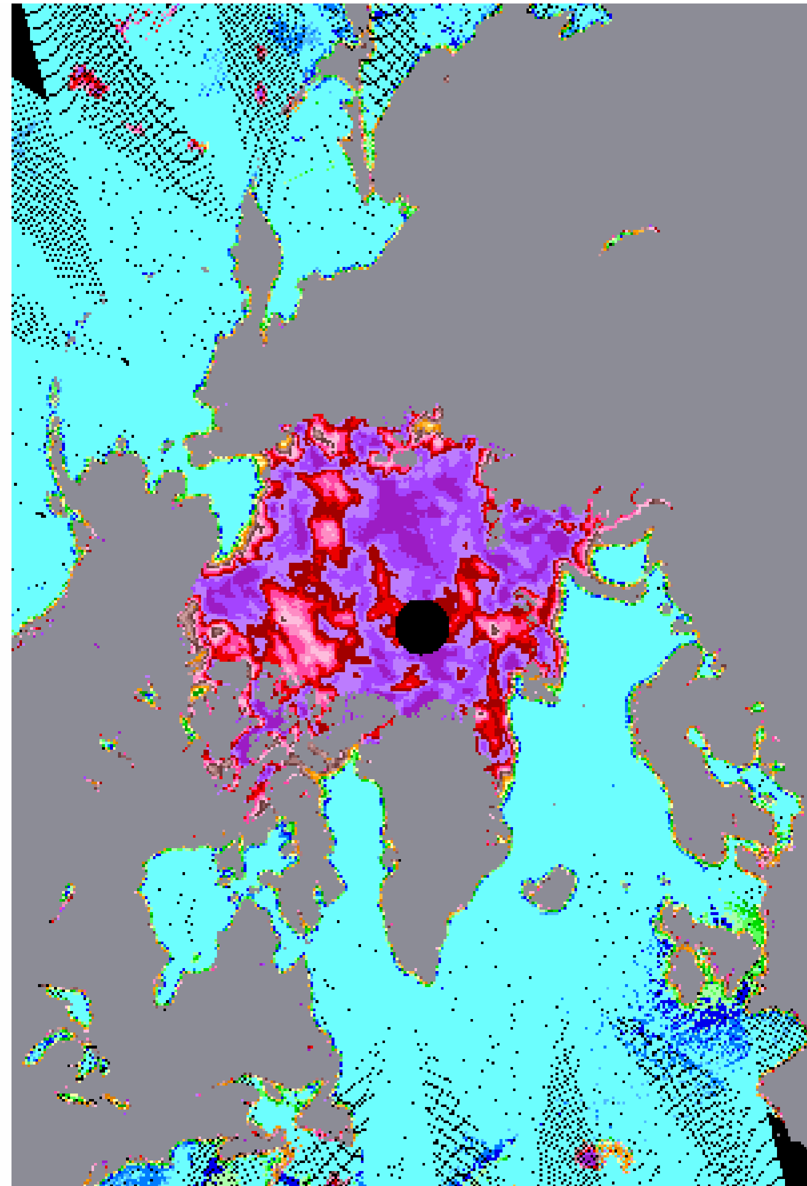

Arctic

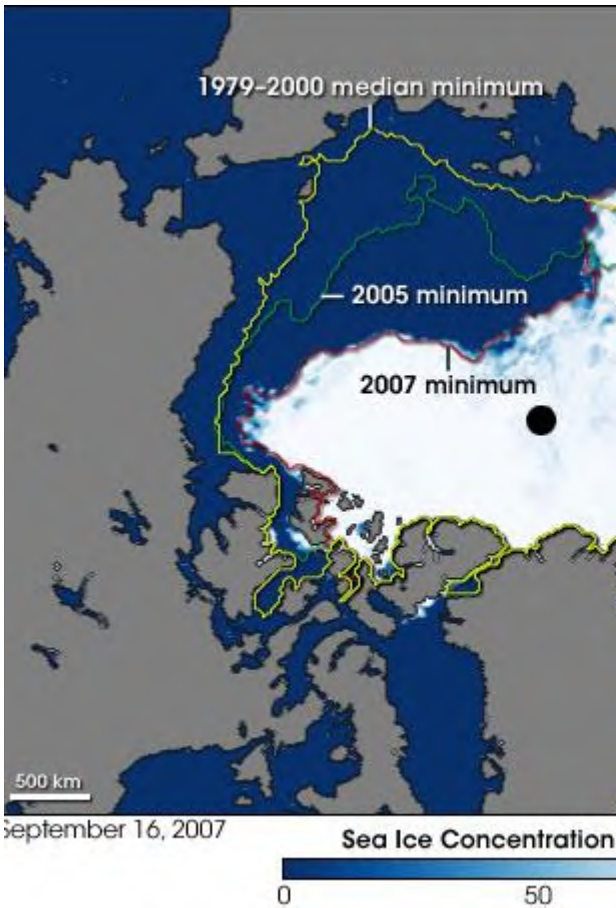

Fetterer, F., K. Knowles, W. Meier, and M. Savoie. 200

Sea Ic
Dec 20

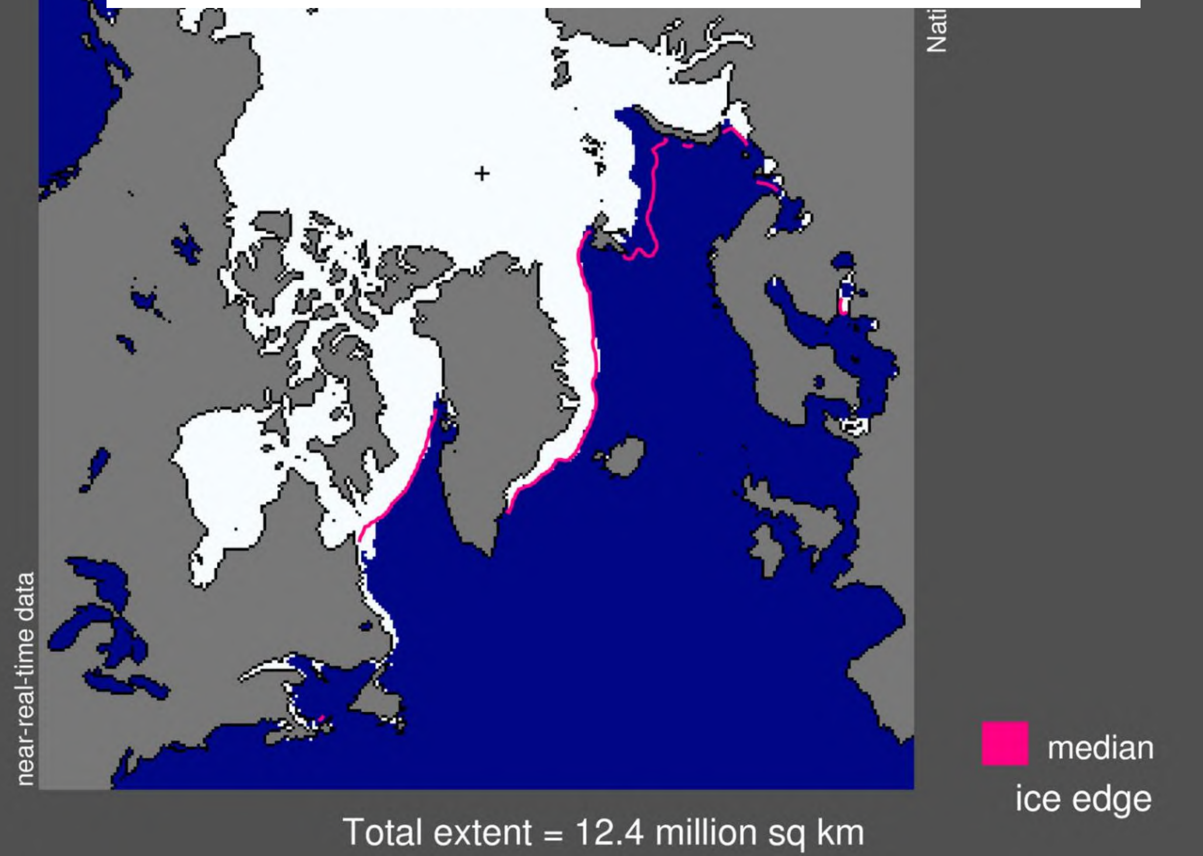

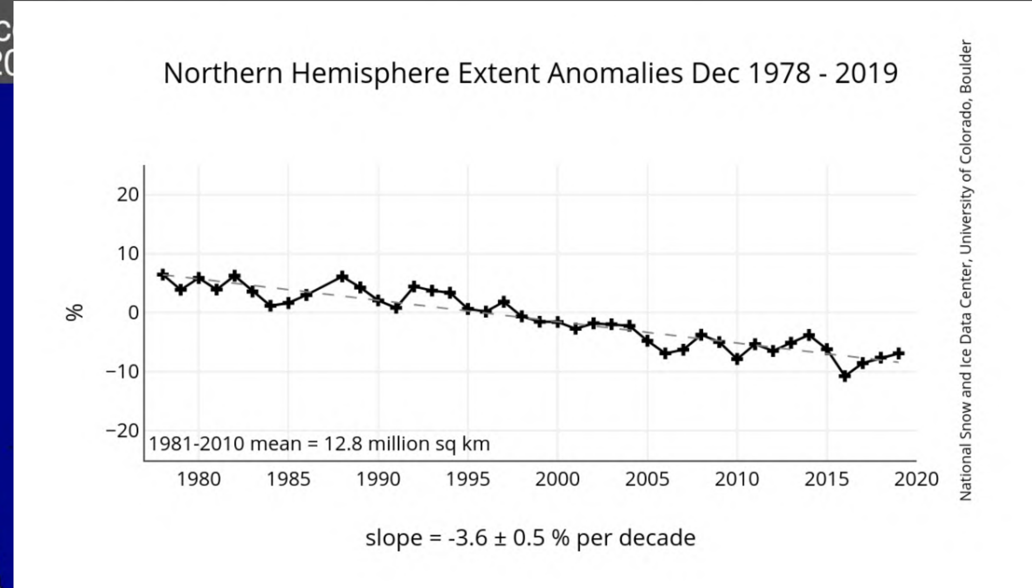

Methodik der Fernerkundung

Microwave Satellite Remote Sensing

Goal: Measurement of Sea Level Topography

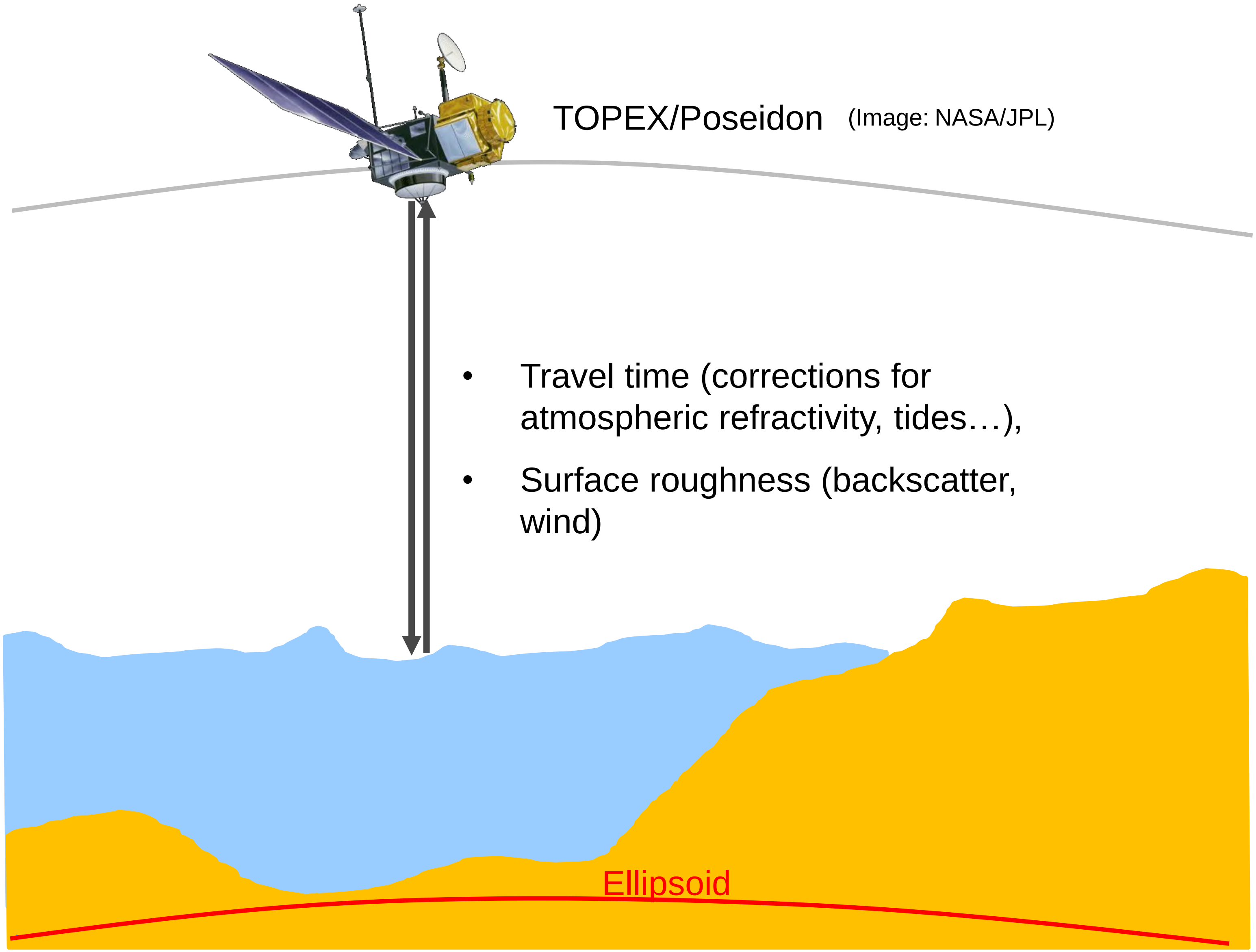

- Travel time (corrections for atmospheric refractivity, tides…),
- Surface roughness (backscatter, wind)

Some Radar Altimeters

TOPEX/Poseidon (´92), Jason 1/2 (´01)

Sentinel-3A/B (‘16,‘18)

Radar Altimeter: Brown Waveform Model

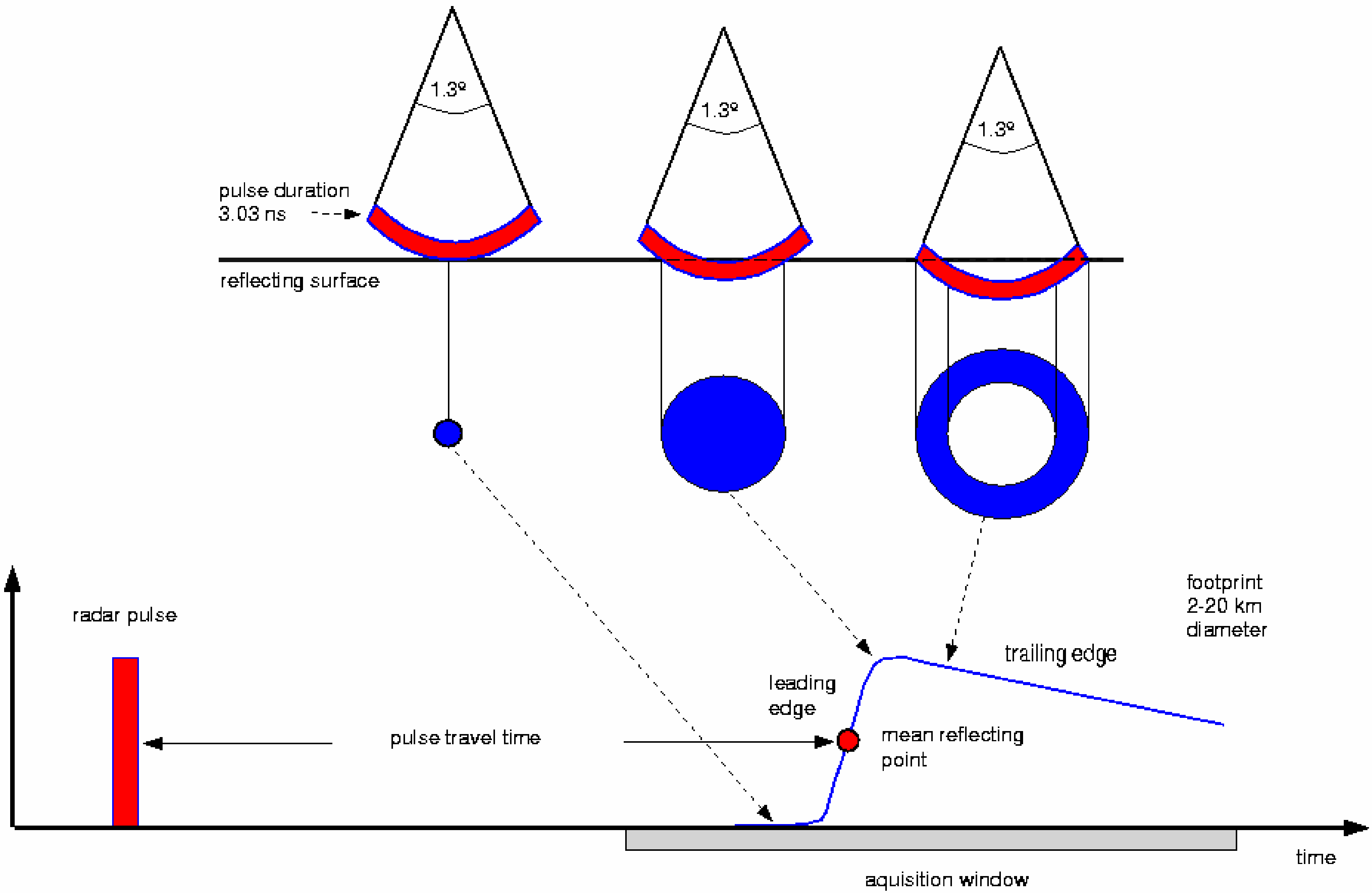

Radar Altimeter: Ocean Wave Height, Signal Waveform

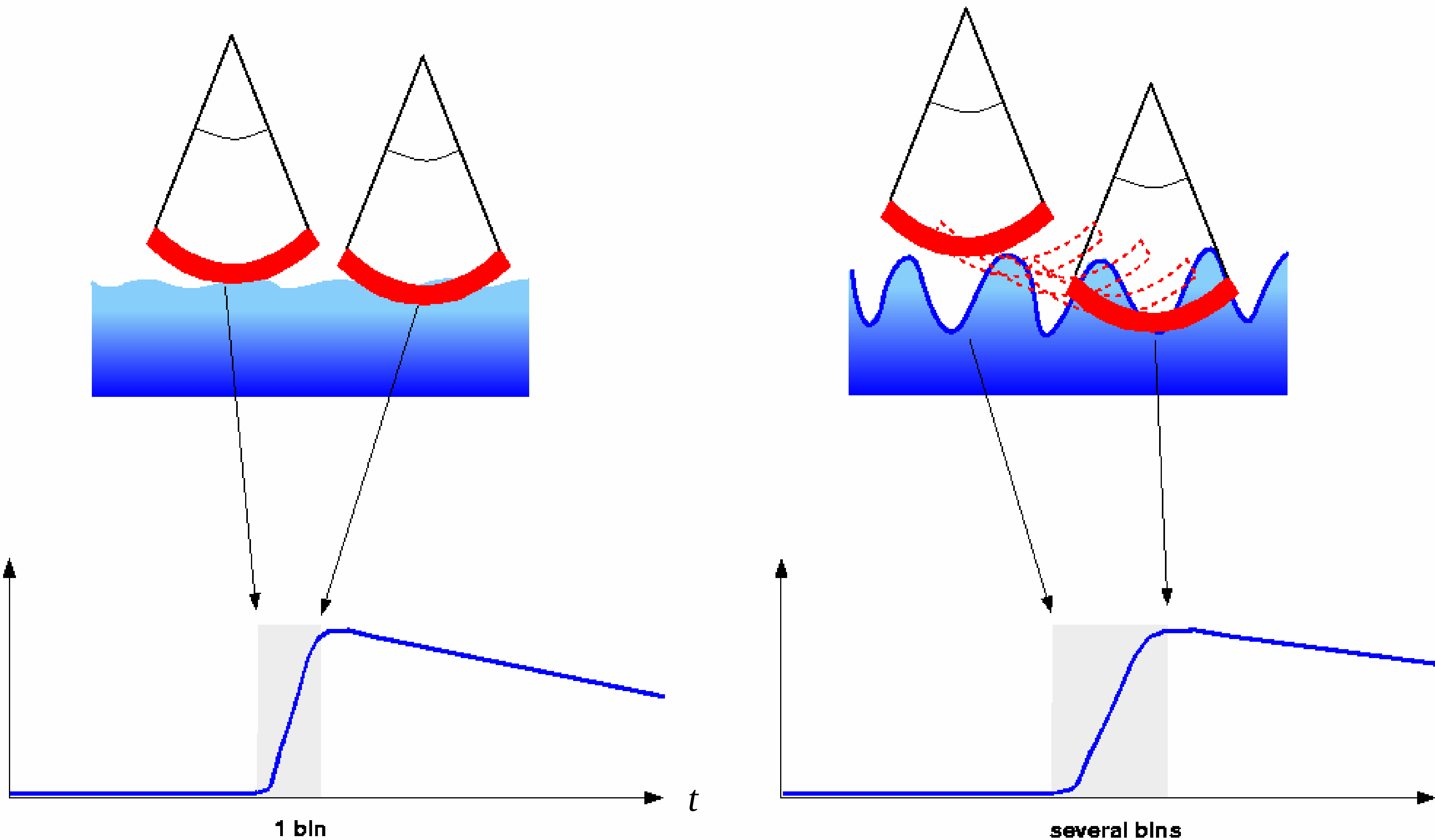

Some Radar Altimeters (ca. 13.5 GHz, Ku)

	Skylab	GEOS 3	SeaSat	Geosat	ERS- 1/2	TOPEX/ Poseidon	Envisat	Jason	Cryosat	Sentinel-3
Launch	1973	1974	1978	1985	1991	1992	2002	2001	2010	2016
Altitude (km)	435	840	800	800	800	1300	800	1300	717	811
RF power (W)	2000	2000	2000	20	50	20/5	50	?	25	
Beam width (deg)	1.5	2.6	1.6	2.1	1.3	1.1	1.3	?		
Footprint (km)	8	3.6	1.7	1.7	1.7	2.3	1.7	?	15 .25 SAR	0.3 / 1.6
Pulse width (ns)	100	12.5	3	3	3	3	3	3	Equ. 3 (chirp)	
Second Freq. (GHZ)						5.3	3.2			5.41
PRF (Hz)	100	100	1020	1020	1020	4000/ 1700	1800	?	bursts	1.9 / 17.8
Noise (cm)	➢ 100	25	5	3	4	2 / 2	2	?	1.6	

CryoSAT-2 (ESA/AWI, launched April 2010)

- Payload

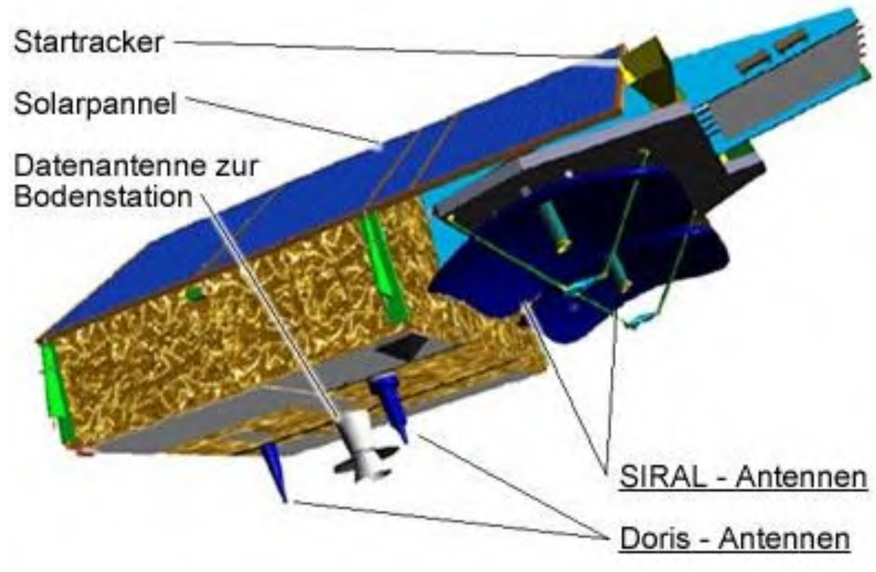

(Radar-Altimeter)

(Two frequencies for determining the ice radial velocity and influences of the ionosphere)

- Application: Monitoring of ice masses in the Arctic and Antarctic

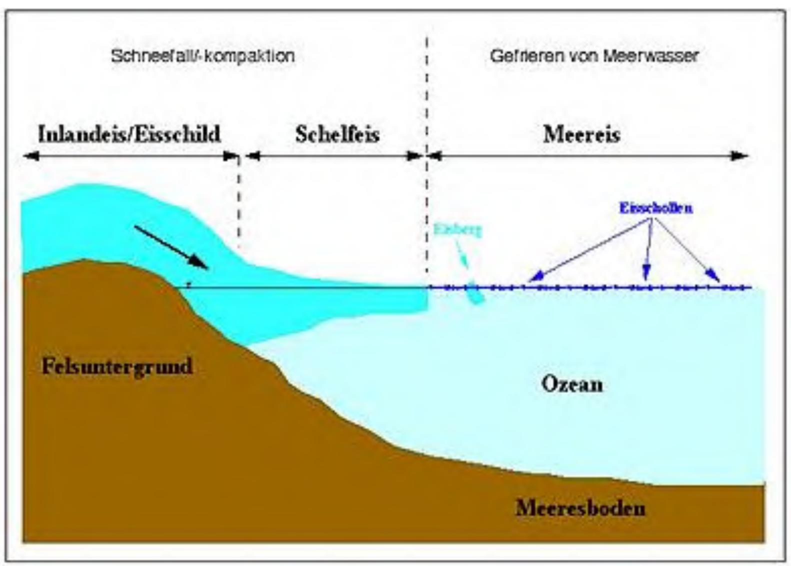

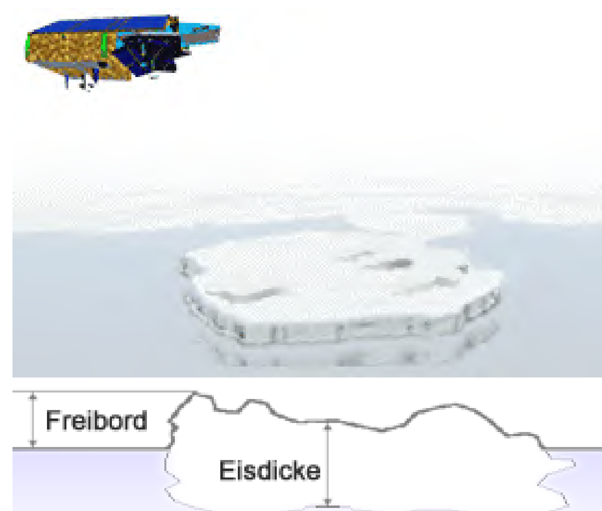

- SIRAL

  => three modes of operation:

  1) conventional pulse-limited mode
     - Operated over ocean areas and central areas of ice masses

  2) SAR-mode (SAR = Synthetic Aperture Radar)
     - Enhancement of azimuth resolution
     - Operated over sea ice for better discrimination of ice and water

  ⇒ SAR: See following lectures

  3) Two-channel SAR-interferometry mode:
     - Operated over sea-/land-ice boundaries for determination of slope and hight of ice masses

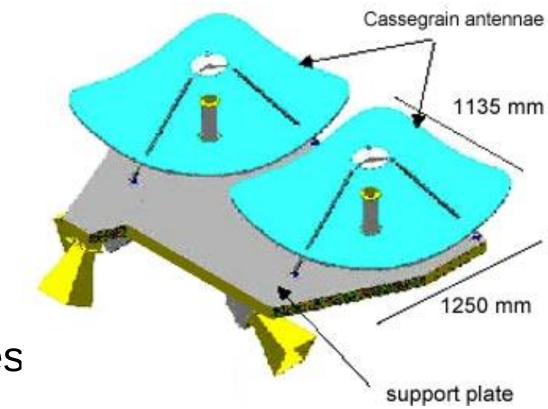

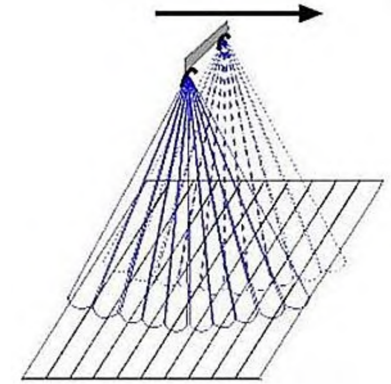

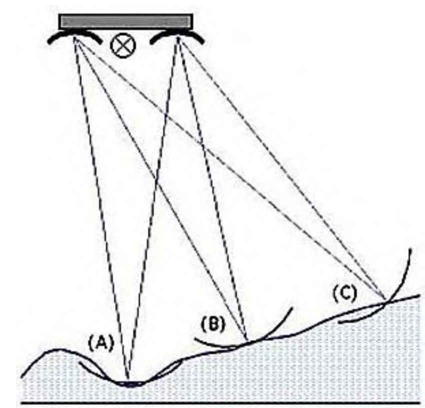

Radar-Altimeter: Error sources and accuracy potential

- Ionosphere: total electron content (TEC) influences signal travelling time:

  $$\Delta t \propto \frac{TEC_{LOS}}{f_0^2}$$

  => Can be corrected using 2 frequencies

- Troposphere: water vapor delays signal travelling time

  => Can be corrected though direct measurement of water vapor e.g. Microwave Radiometers

- Accuracy potential over sea: 3 – 10 cm

CryoSat Results

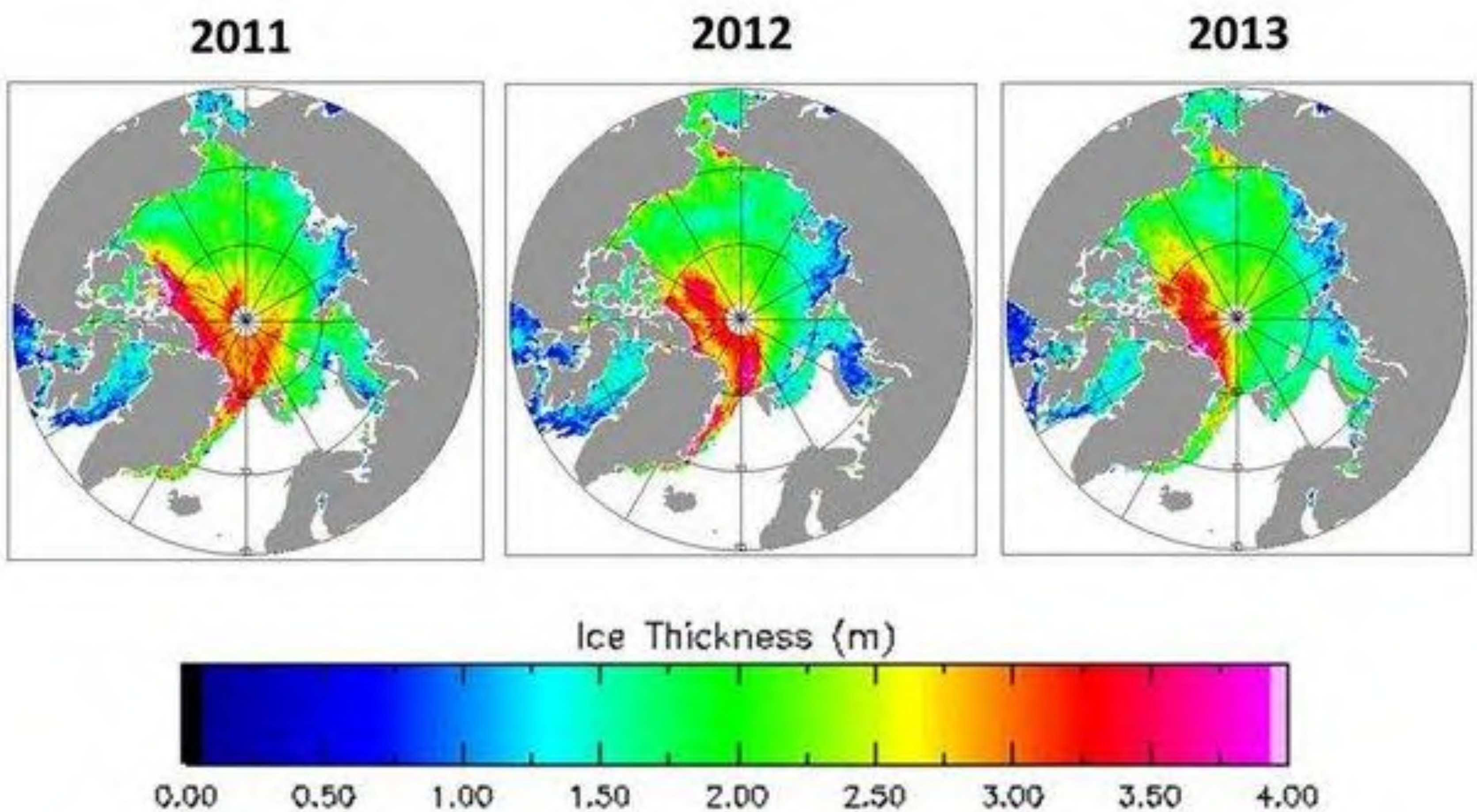

Changes in ice thickness for March/April 2011, 2012 and 2013 as measured by CryoSat. A. Ridout–UCL, Data© ESA

Mean Sea Level Accumulated from Altimetry Data

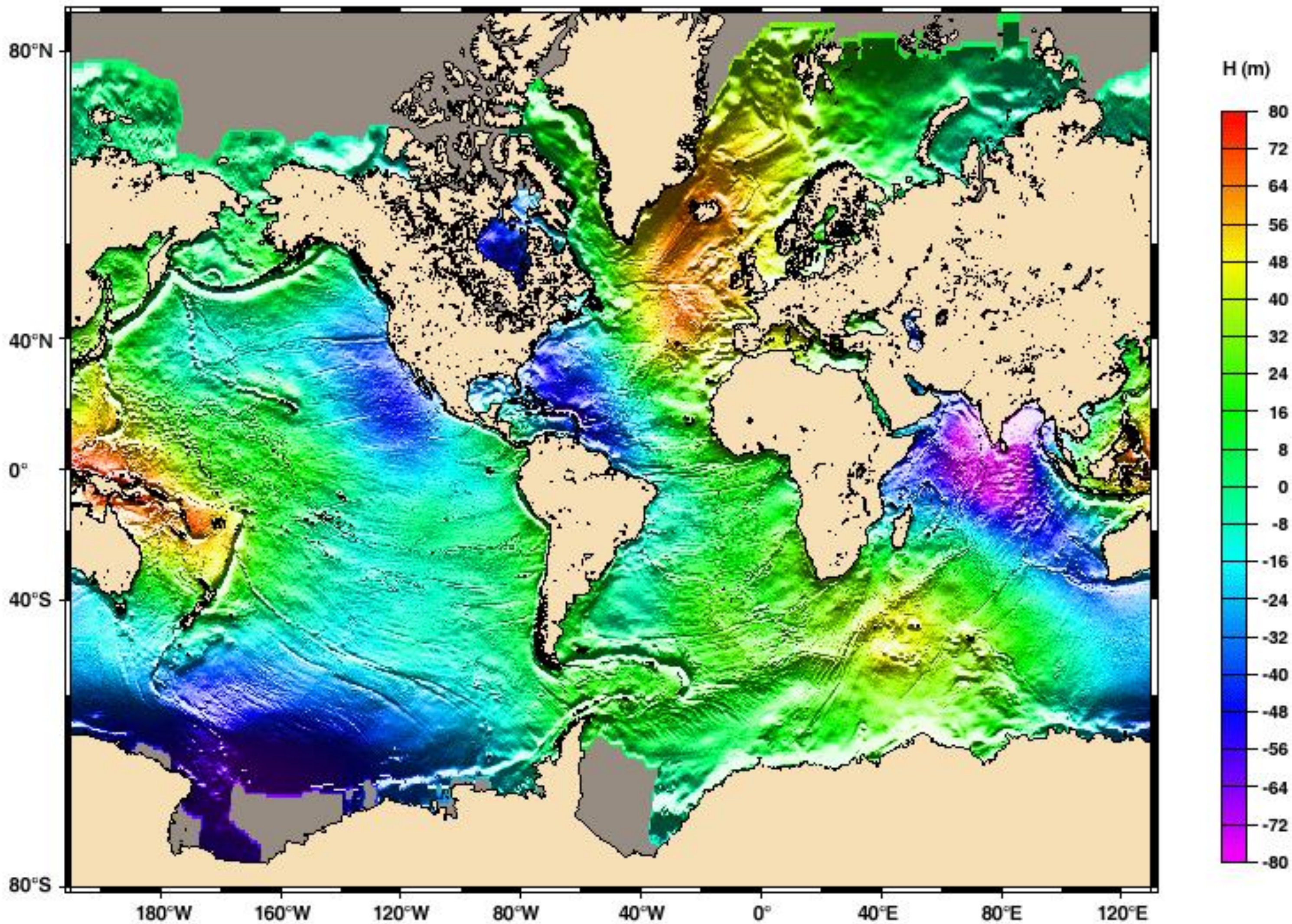

Image © ESA, Id 214973

Sea Level Anomalies (Jason-1 / Envisat)

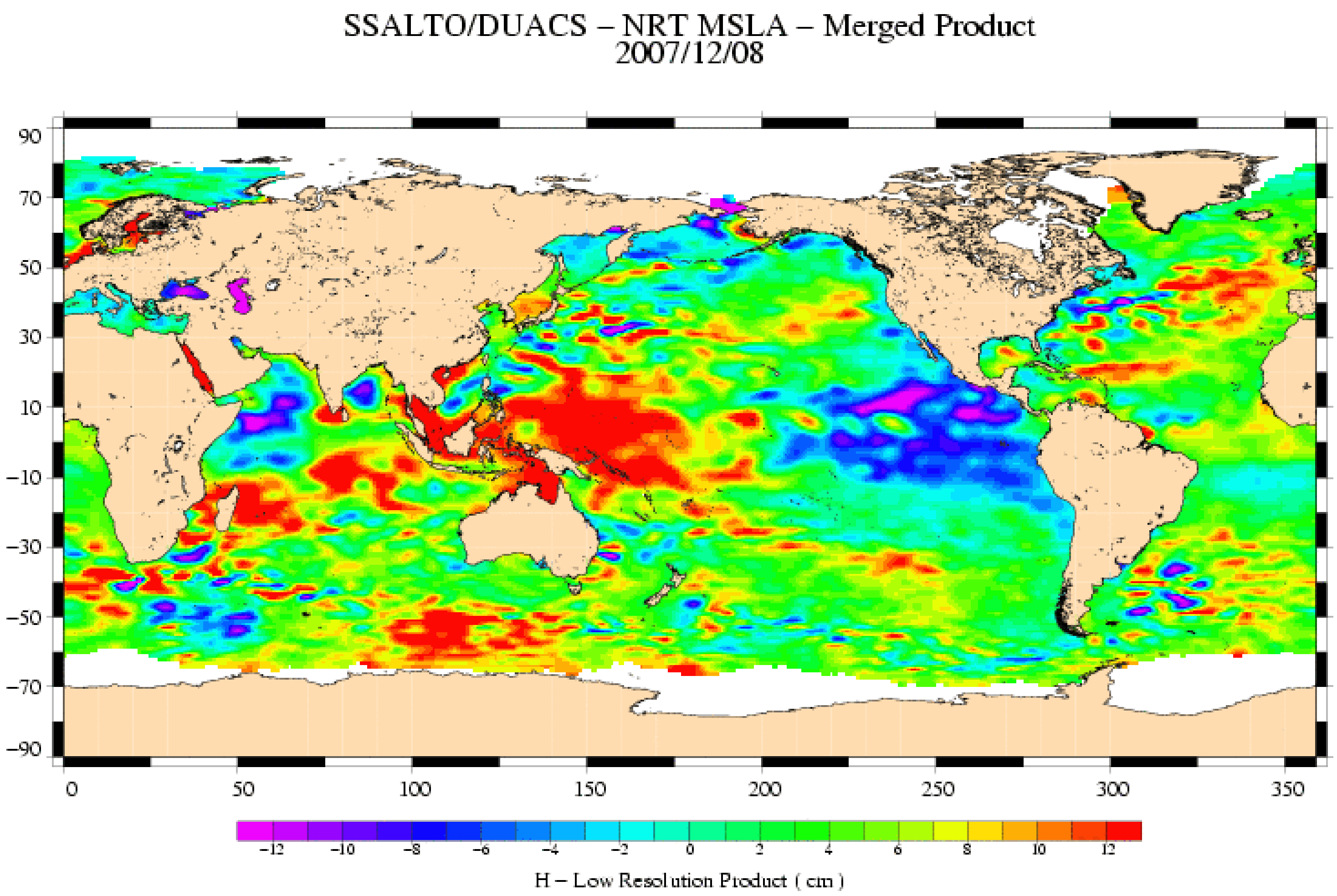

Source: CNES (Centre National d'Etudes Spatiales); CLS (Collecte Localisation Satellites)

Active Instruments!

Goal: measurement of wind speed and direction over ocean

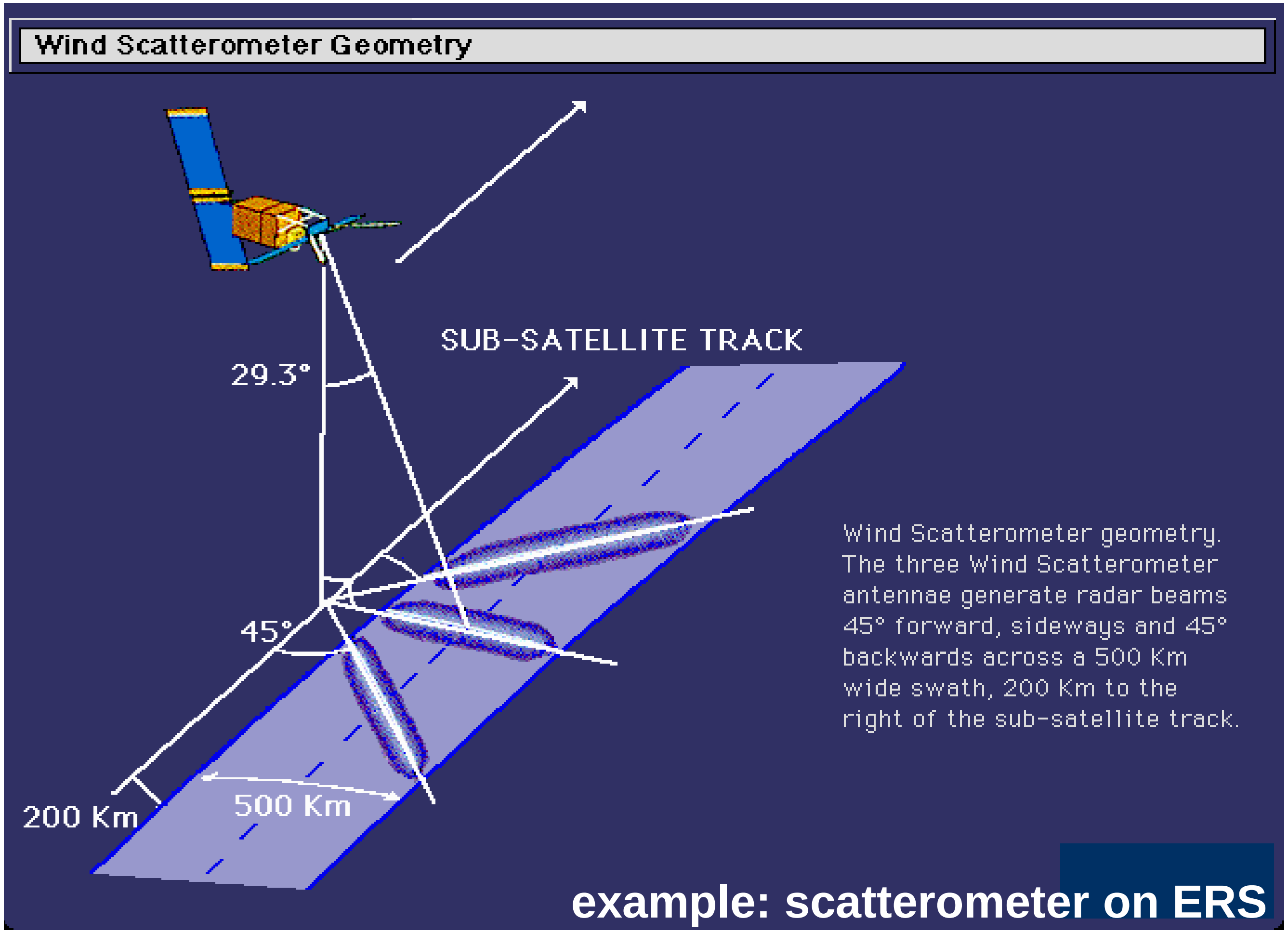

example: scatterometer on ERS

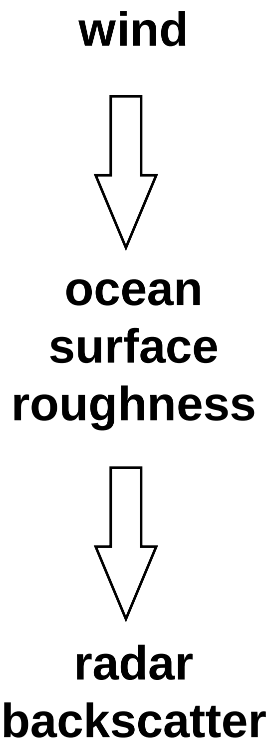

Microwave Scatterometers

Instrument		Satellite	
SASS	SEASAT-A Scatterometer System	SEASAT	‘78
AMI/WNS	AMI Wind Scatterometer	ERS-1&2	’91-
NSCAT	NASA Scatterometer	ADEOS	’96-’00
SeaWinds	SeaWinds Scatterometer	QuikSCAT, ADEOS-II	’99-
ASCAT	Advanced Scatterometer	METOP	’05-

QuickSCAT Windfield (NASA)

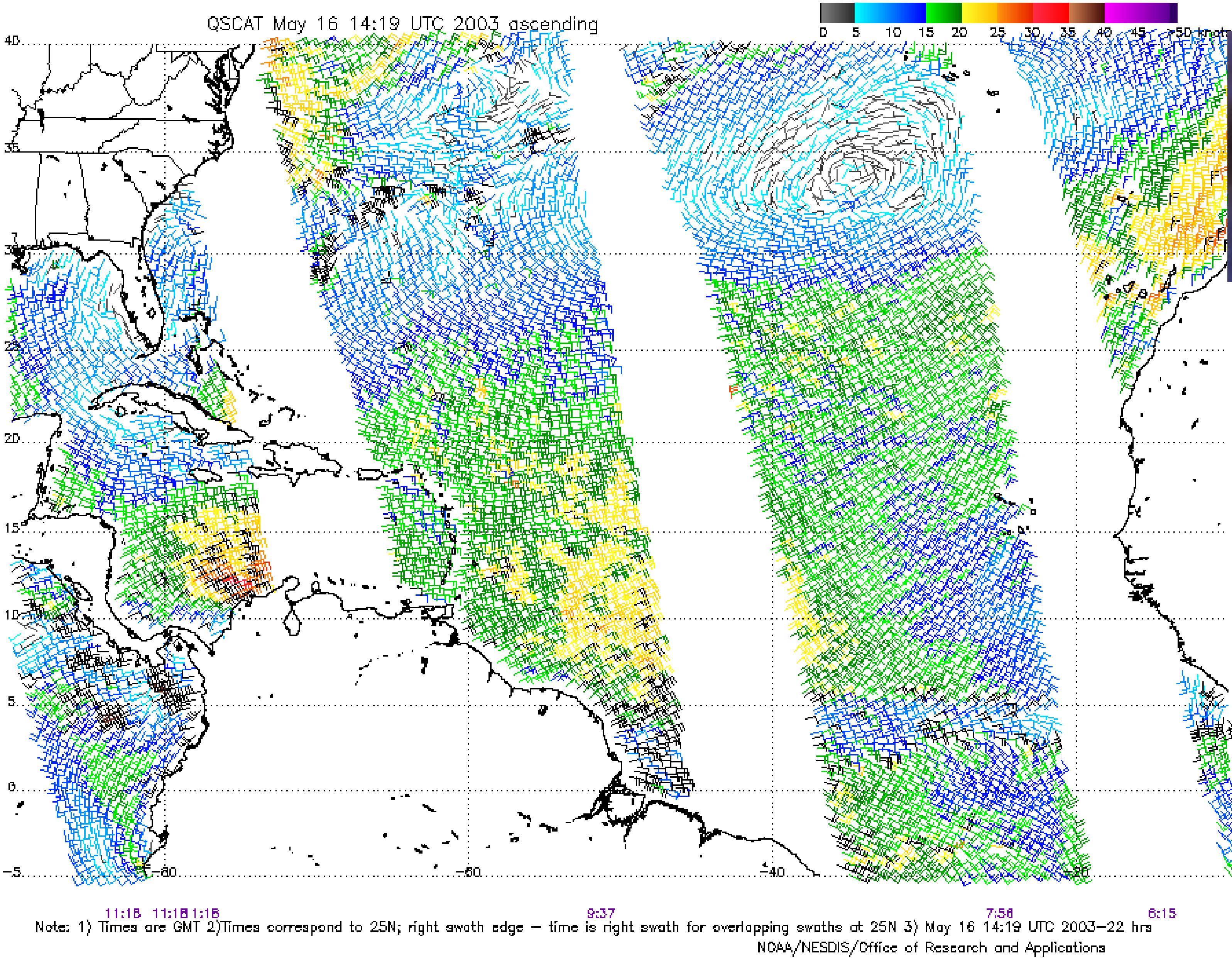

QucikSCAT: Hurricane Katrina (2005)

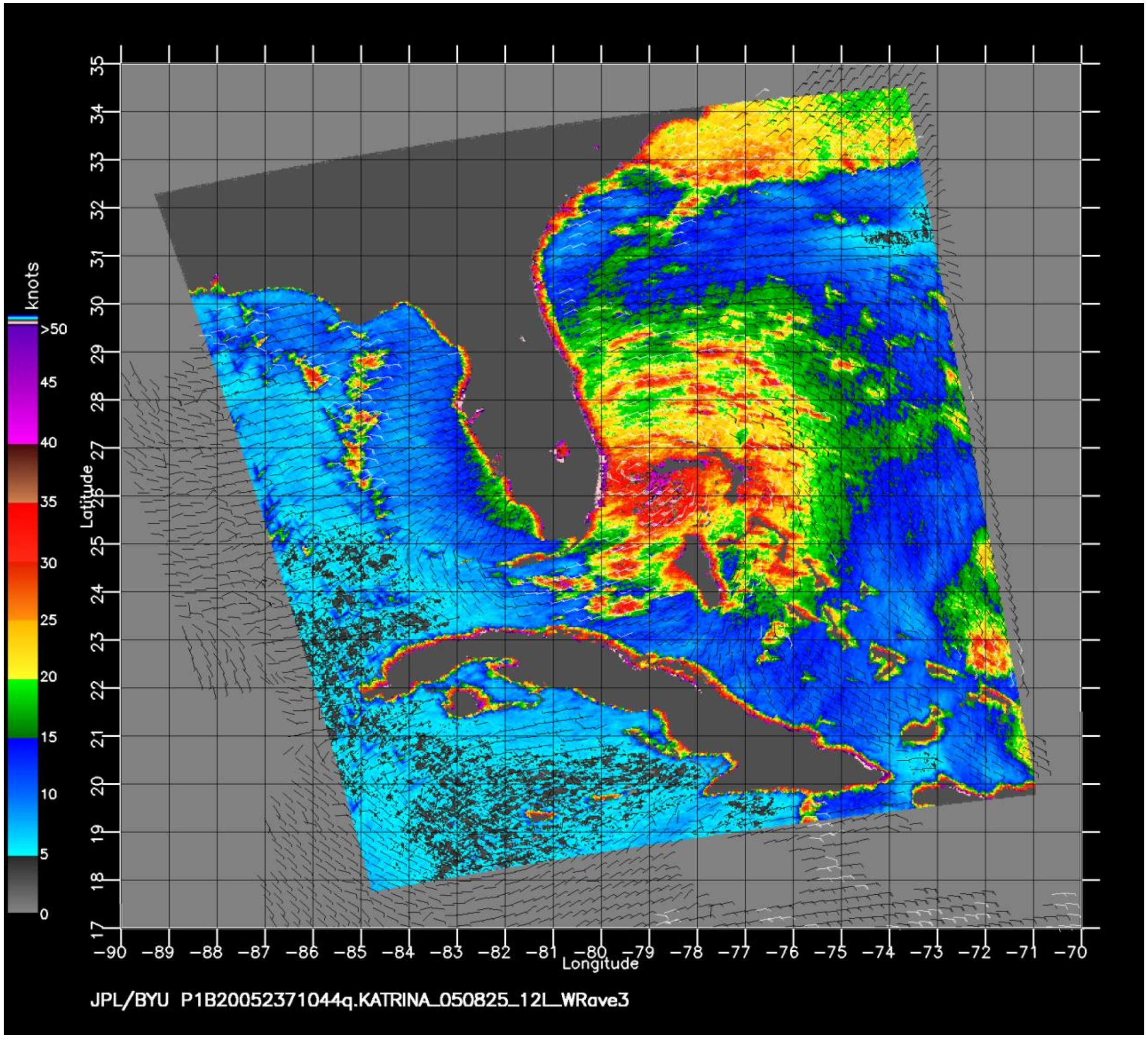

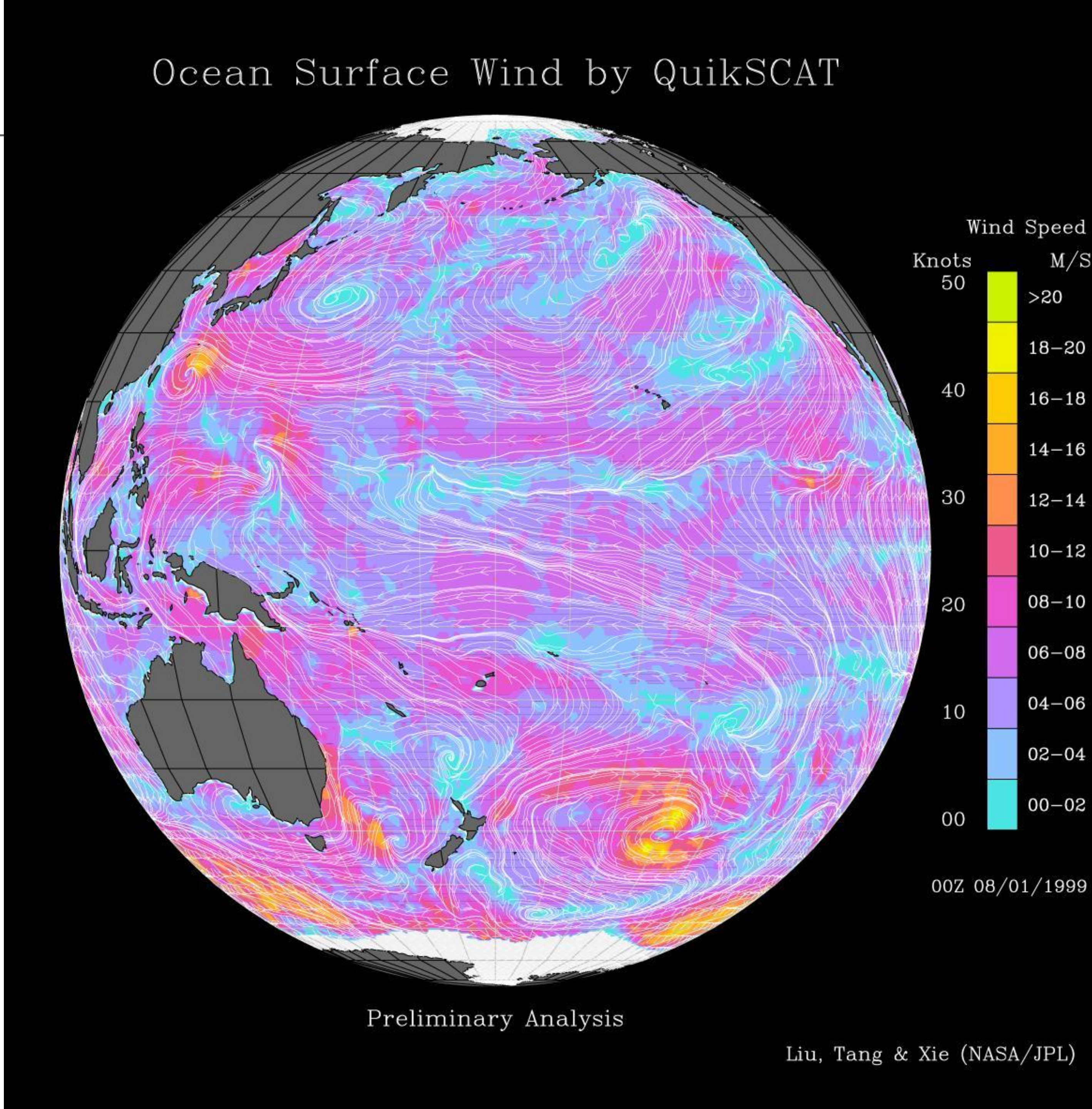
Ocean Surface Wind by QuikSCAT
Wind Speed
Knots
M/S
50
40
30
20
10
00
>20
18–20
16–18
14–16
12–14
10–12
08–10
06–08
04–06
02–04
00–02
00Z 08/01/1999
Preliminary Analysis
Liu, Tang & Xie (NASA/JPL)

DLR

More interesting …

http://www.scp.byu.edu/movies/QuikSCAT_movies.html

Scatterometer

time series

Antarctica

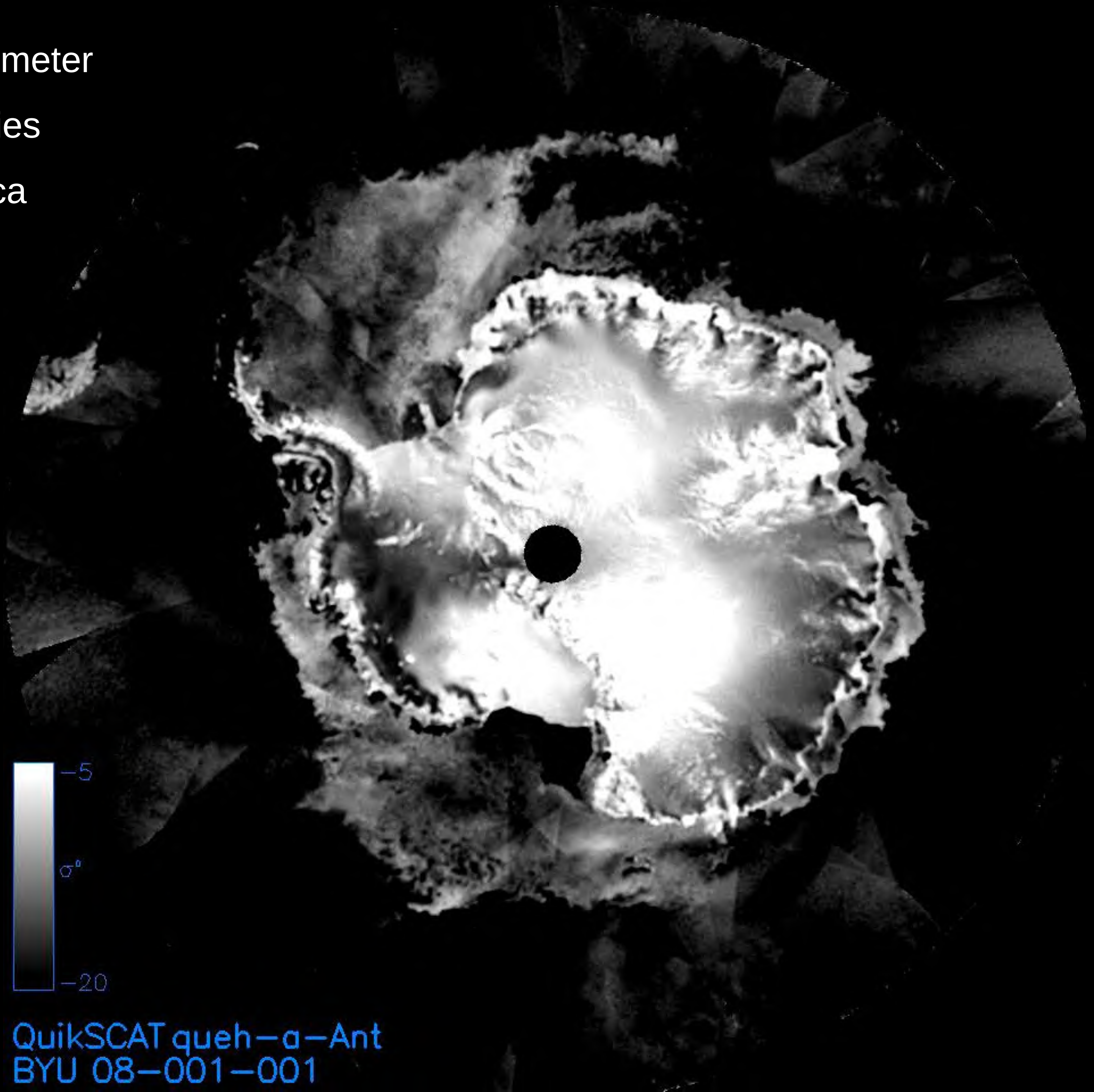

Scatterometer

time series

Greenland

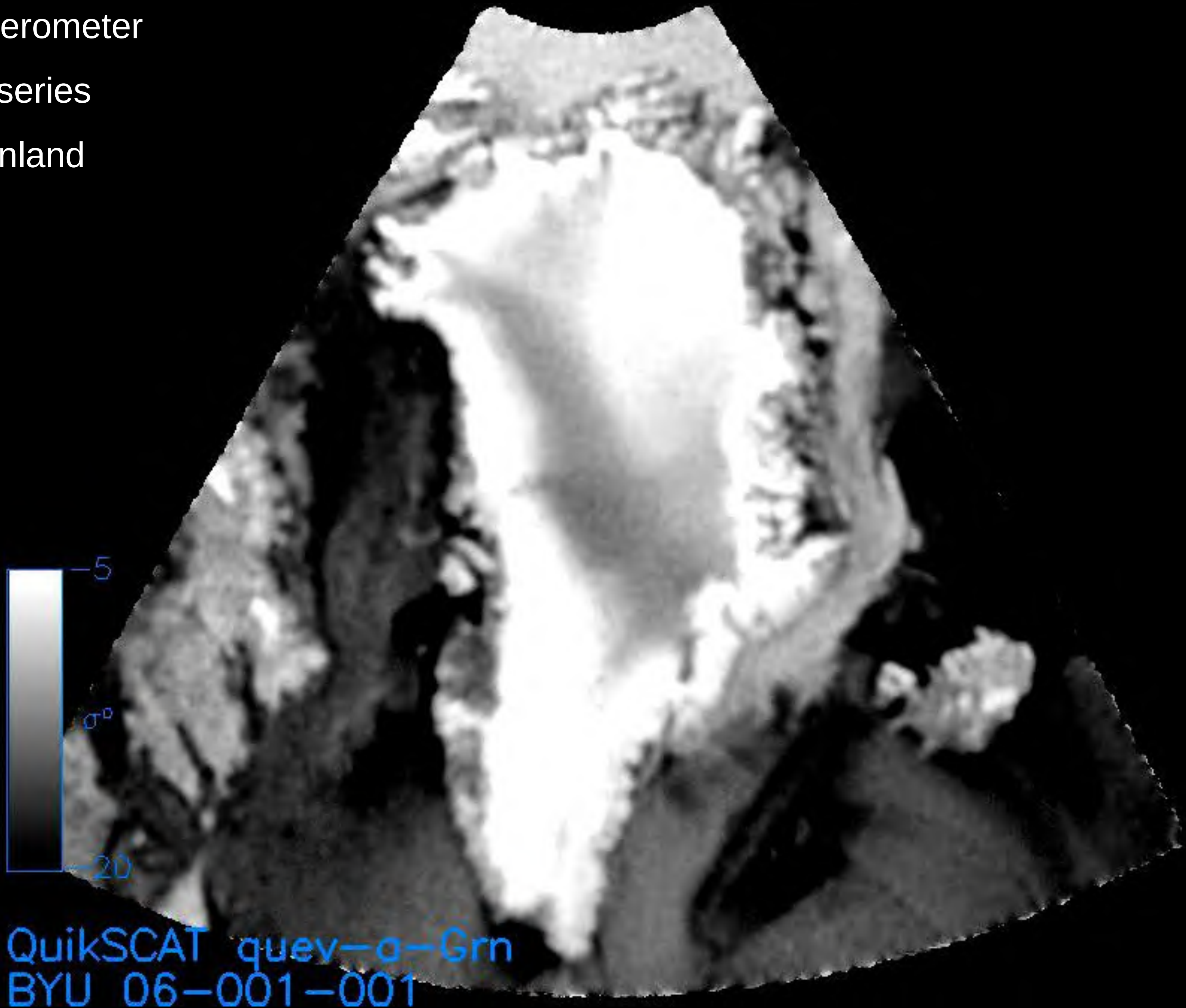

Signal Processing and Microwave Remote Sensing WS 19/20

II. Synthetic Aperture Radar (SAR)

Prof. Dr. Michael Eineder

Institut für Methodik der Fernerkundung
Deutsches Zentrum für Luft- und Raumfahrt DLR

Microwave Satellite Remote Sensing

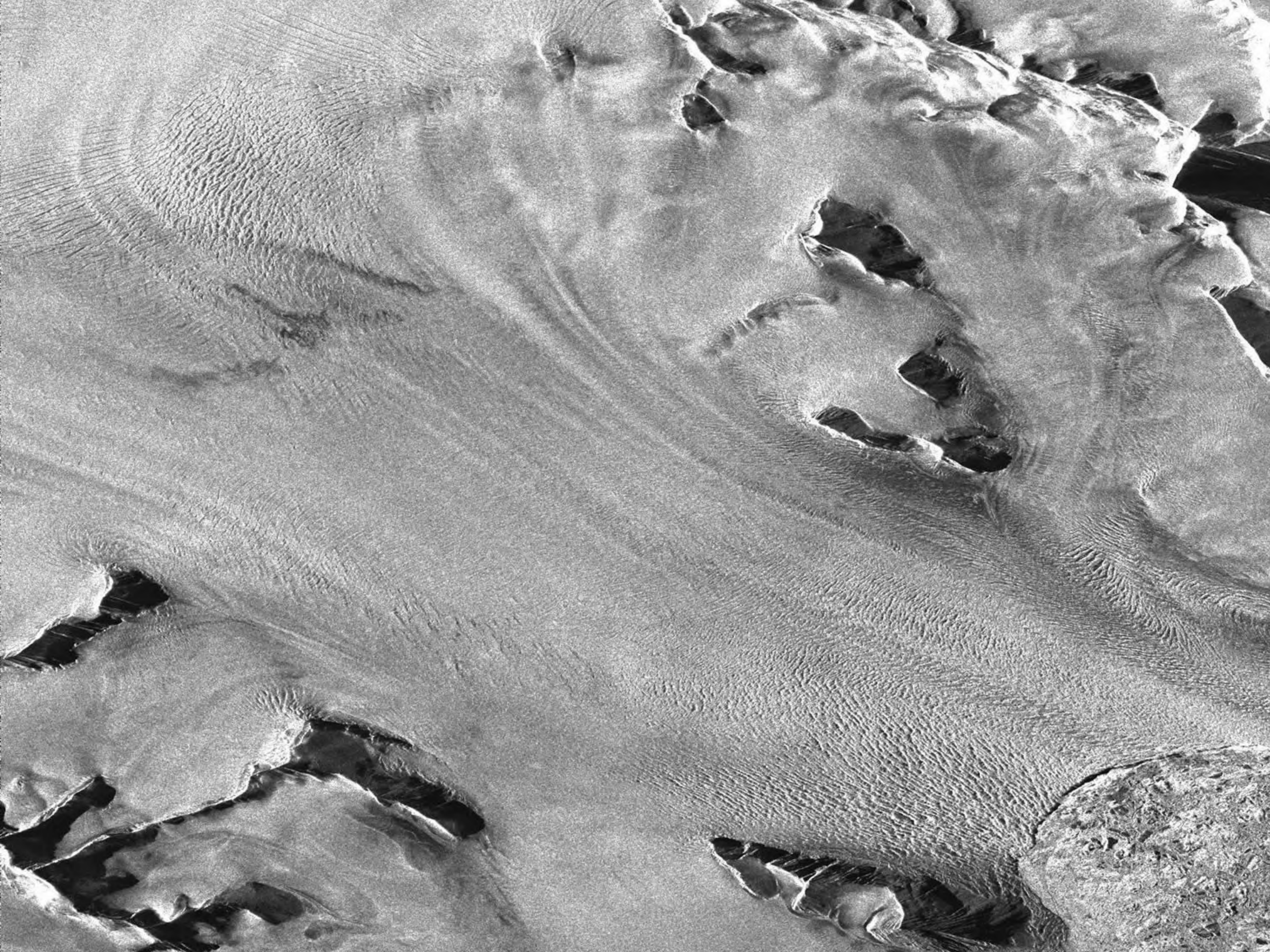

Remote Sensing Technology

Synthetic Aperture Radar (SAR)

5.1 Introduction

5.2 Radar Distance Measurement (Range-Component)

5.3 Formation of Synthetic Aperture (Azimuth-Component)

5.4 Characteristics of SAR Images

Synthetic Aperture Radar - SAR

- active $\Rightarrow$ independent of sun illumination
- microwave $\Rightarrow$ penetrates clouds and (partially) canopy, soil, snow

  wavelengths: X-band: 3 cm
  C-band: 6 cm
  L-band: 24 cm
- coherent $\Rightarrow$ interferometry, speckle
- polarization can be exploited
- spatial resolution: space-borne: 5 m - 100 m (TerraSAR-X: 1 m)
  air-borne: > 0.2 m

SAR Imaging Geometry

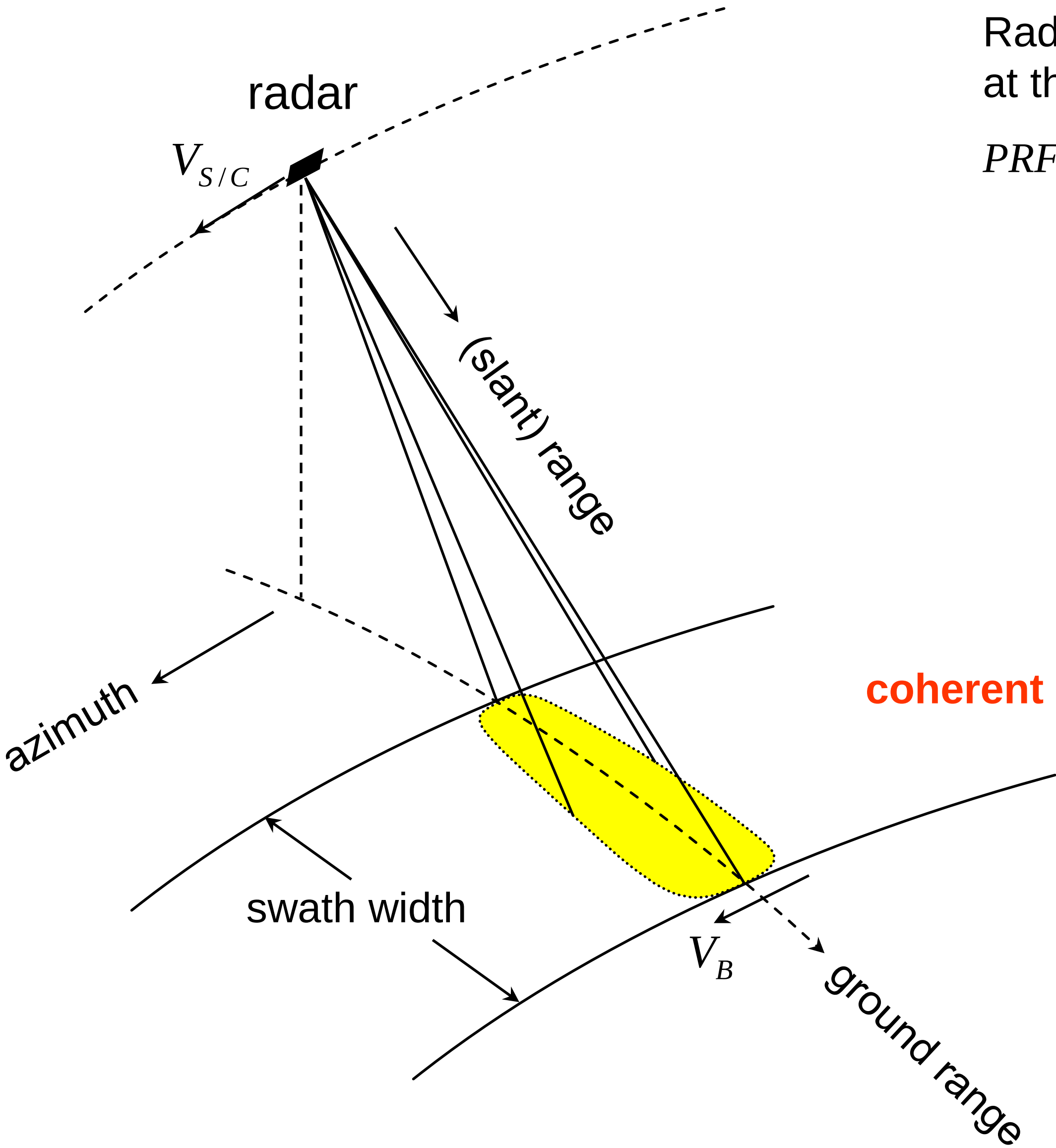

Radar transmits pulses and receives echoes at the rate of the pulse repetition frequency:

$PRF \approx 1000 - 4000$ Hz

range: radar principle = scanning at speed of light

azimuth: scanning in flight direction at V_B plus aperture synthesis (holography)

coherent imaging: complex-valued pixels contain amplitude (brightness) and **phase** information

for this lecture: straight flight path

$$\Rightarrow \quad V_{S/C} = V_B = V$$

SAR – A Two-Step Imaging Process

SAR is a two-step imaging process:

1. data acquisition

Illumination of a scattering **object** and collection of received echoes

$\Rightarrow$ **raw data**

contribution of a single point is dispersed over $10^4 \dots 10^7$ samples

2. processing

raw data focusing $\Rightarrow$ **image** of the object

Airborne X-band SAR image

1 m resolution

SAR Image of the Ocean

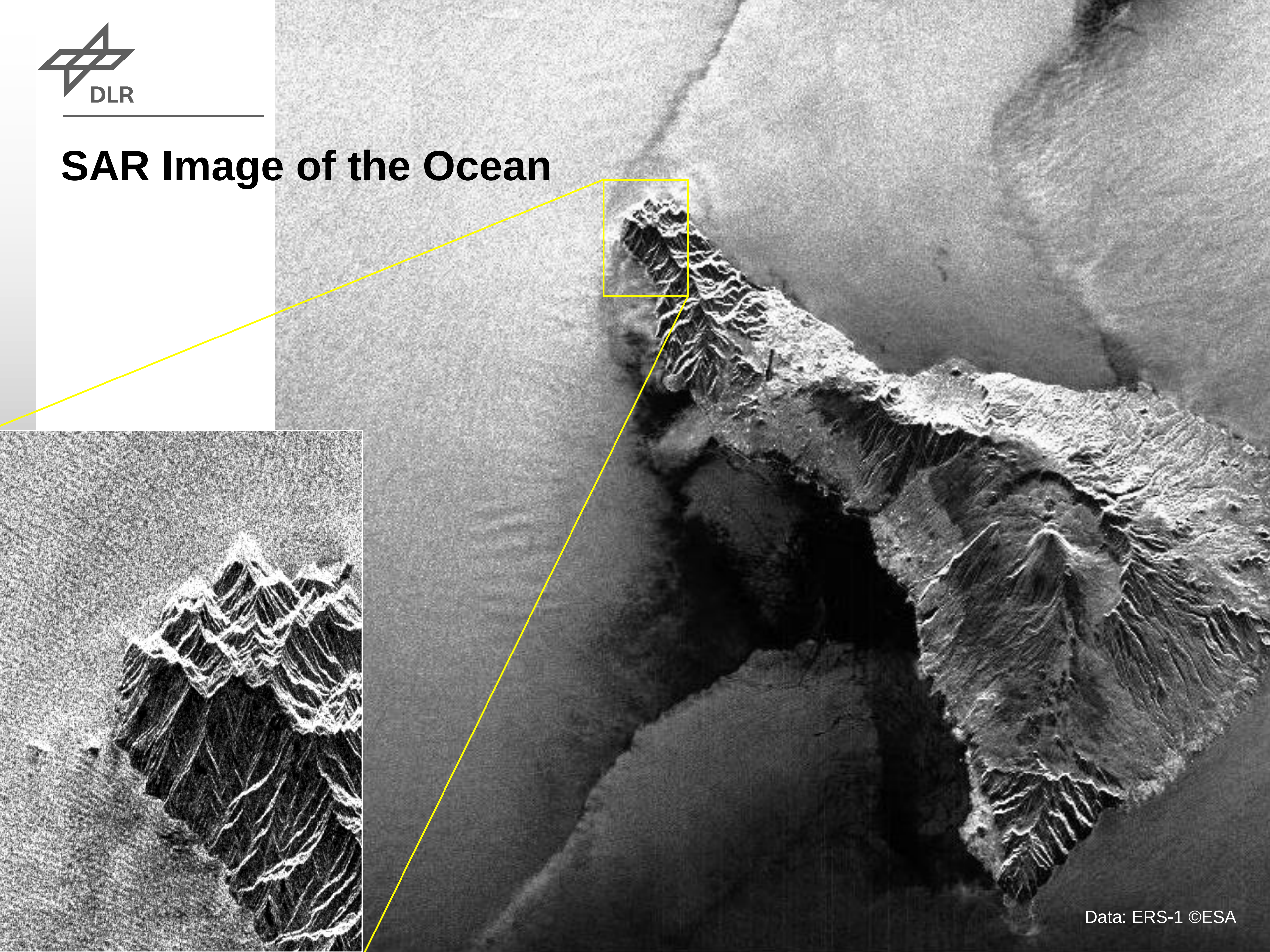

Data: ERS-1 ©ESA

“Prestige” Oil Tanker Disaster Off the Spanish Coast

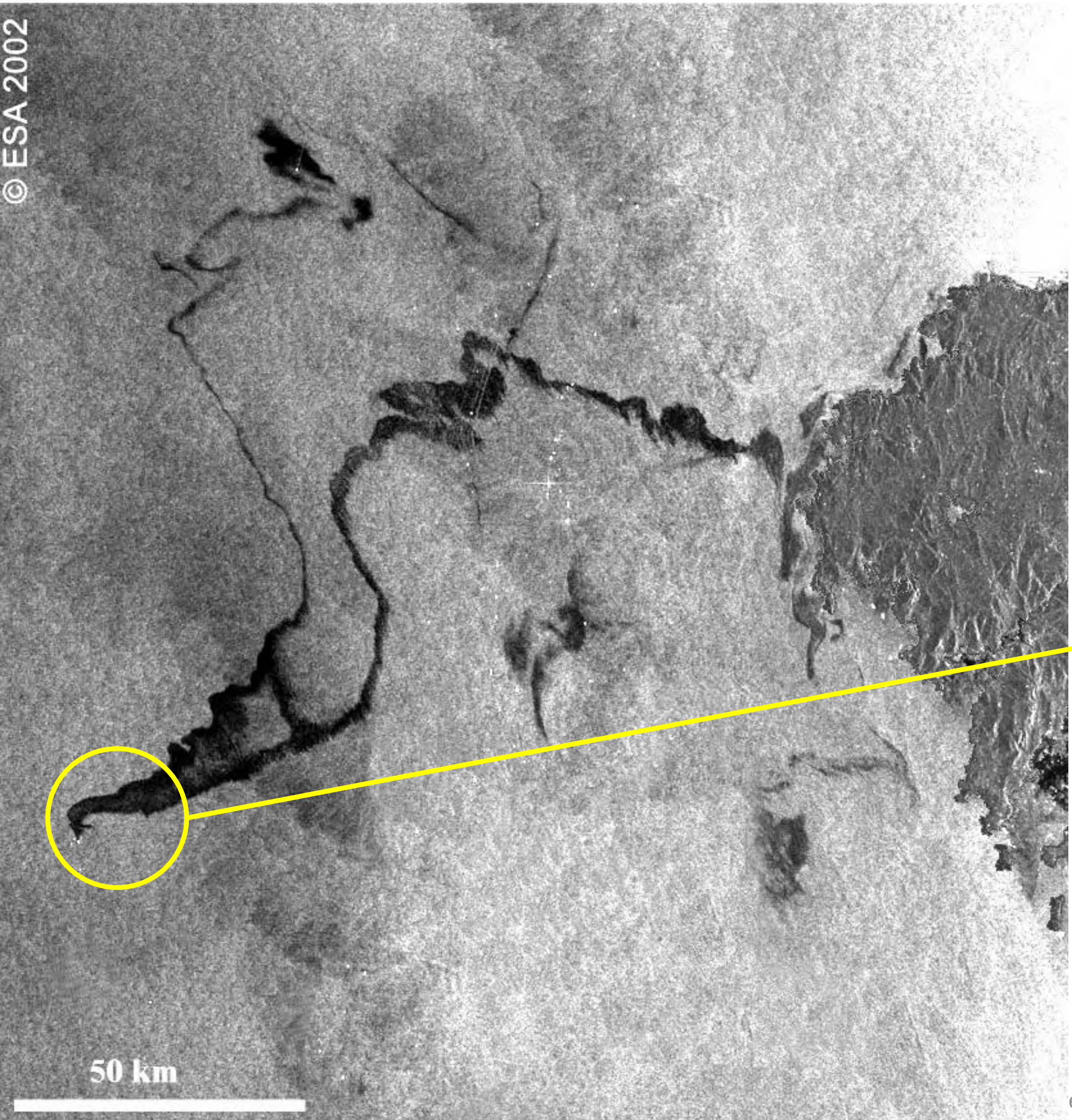

Envisat/ASAR
20 November 2002

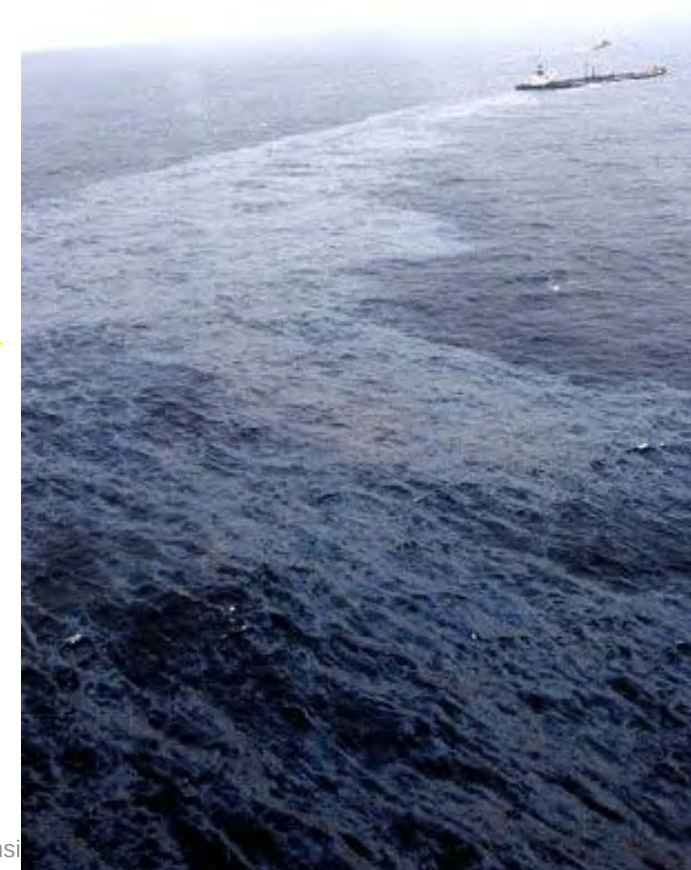

Synthetic Aperture Radar (SAR)

Radar Principle

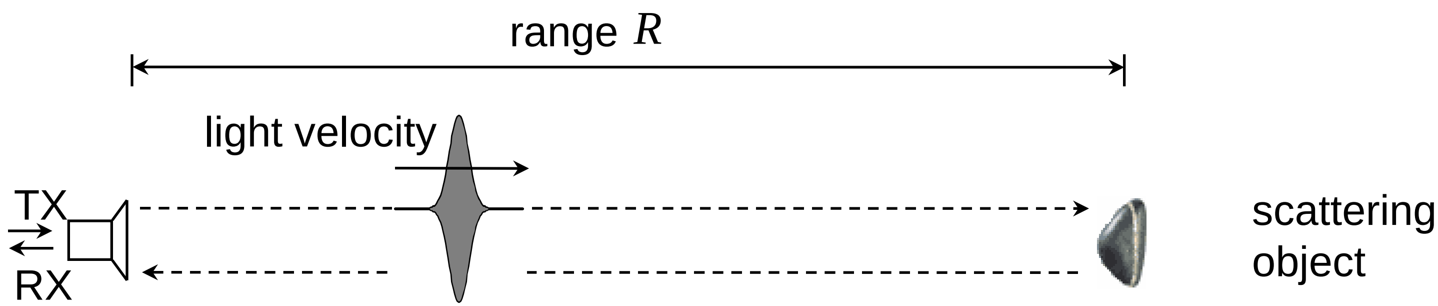

received echo:

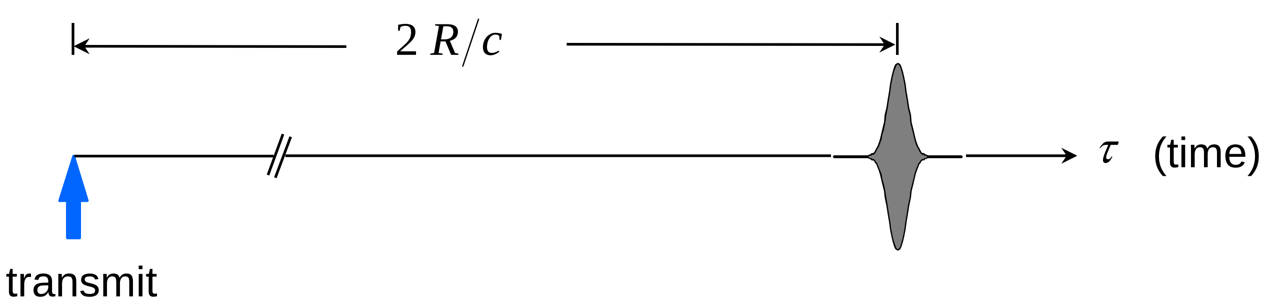

Range Imaging Principle

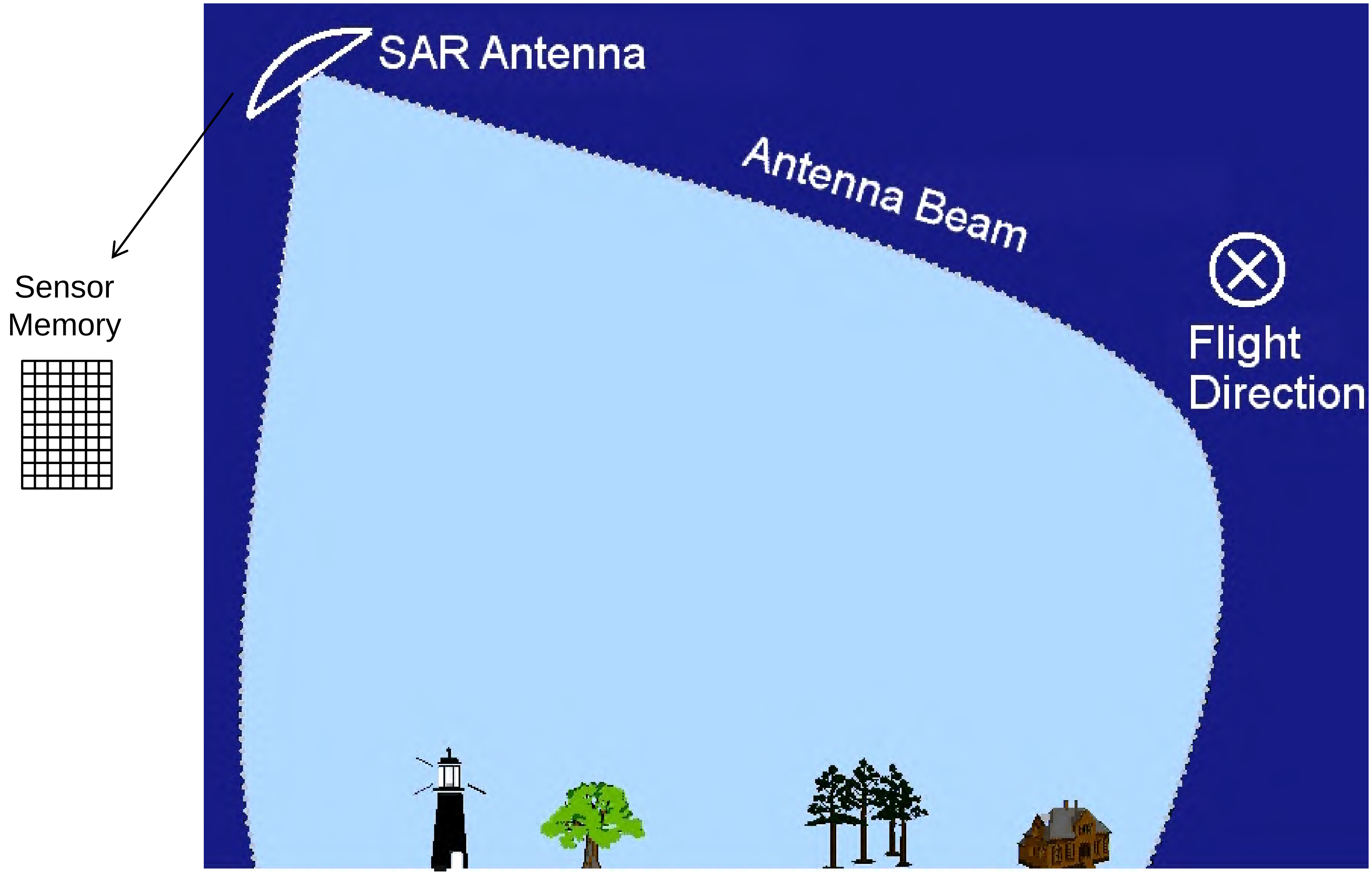

→ sampling and storing echoes of transmitted pulse

Real Timing of a Space-borne SAR

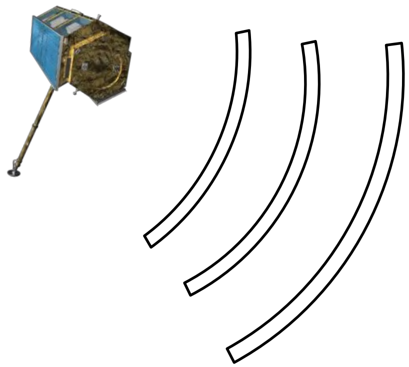

- SAR cannot receive during transmit
- Several pulses “in the air” simultaneously

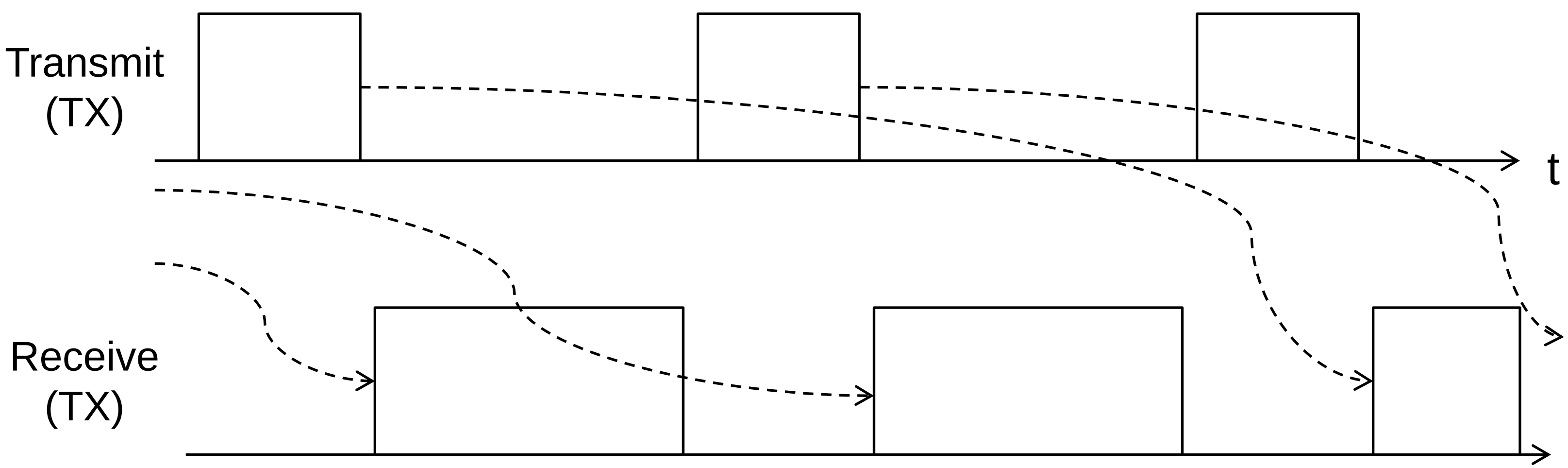

Coherently Received Echo of a Point Target

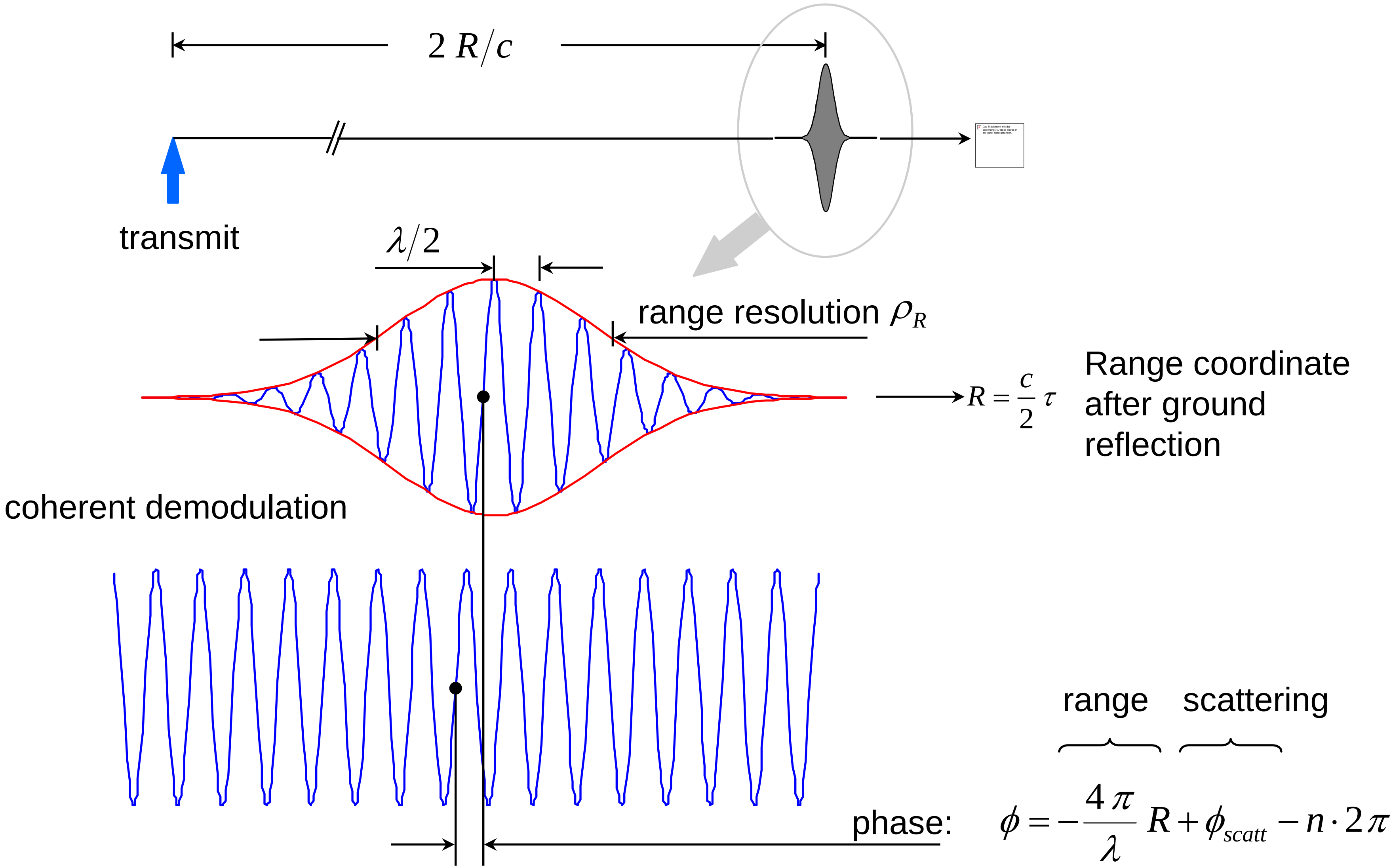

Phasor Representation of a Wave Signal

$$\left(\exp(j\,\alpha) = \cos(\alpha) + j\sin(\alpha)\right)$$

complex representation: $A \cdot \cos(2\pi\nu_0\tau + \phi) \quad \rightarrow \quad A \cdot \exp(j\,(2\pi\nu_0\tau + \phi))$

after demodulation: $u = A \cdot \exp(j \cdot \phi)$

amplitude: $A = |u|$

intensity, power: $A^2 = |u|^2$

phase: ϕ

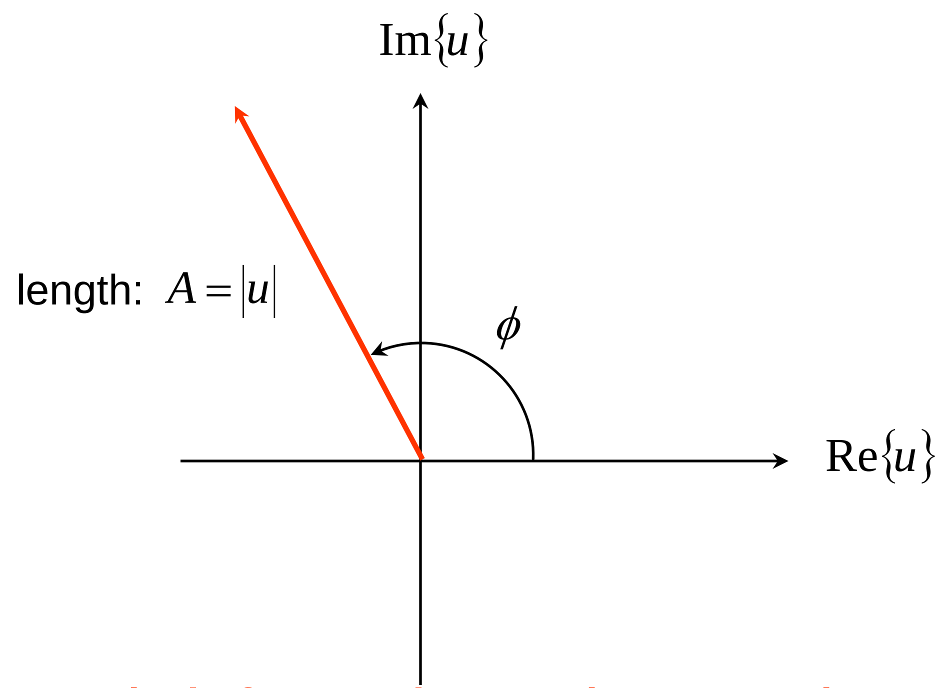

Every sample of a SAR raw data set and every pixel of a complex SAR image consists of a real and an imaginary part, i.e. it is a phasor and contains amplitude and phase information.

Pulse Waveform and Range Resolution

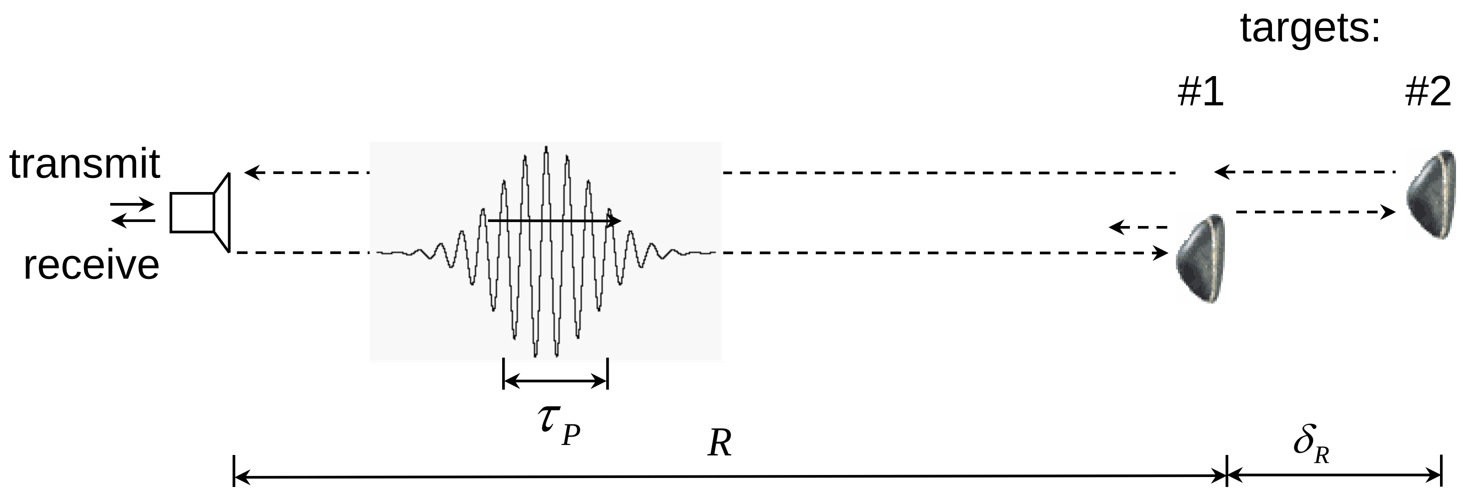

radar frequency : ν_0

transmitted pulse: $g(\tau)\cdot\exp(j\,2\pi\nu_0\tau)$

received echo from target #1: $g(\tau-2\,R/c)\cdot\exp(j\,2\pi\nu_0(\tau-2\,R/c))$

targets #1 and #2 easily separable, if $\delta_R \geq \rho_R = \tau_P\,c/2$ (range resolution)

for phase coded pulses, e.g. chirps, of bandwidth W_P : $\rho_R = \dfrac{c}{2\,W_P}$

Chirp Signal

$$u(\tau) = \exp\left(j\pi k \tau^2\right) = \underbrace{\cos\left(\pi k \tau^2\right)}_{\text{real part}} + \underbrace{j\sin\left(\pi k \tau^2\right)}_{\text{imaginary part}} \quad \text{for} \quad -\frac{\tau_P}{2} \le \tau \le \frac{\tau_P}{2}$$

k : chirp rate

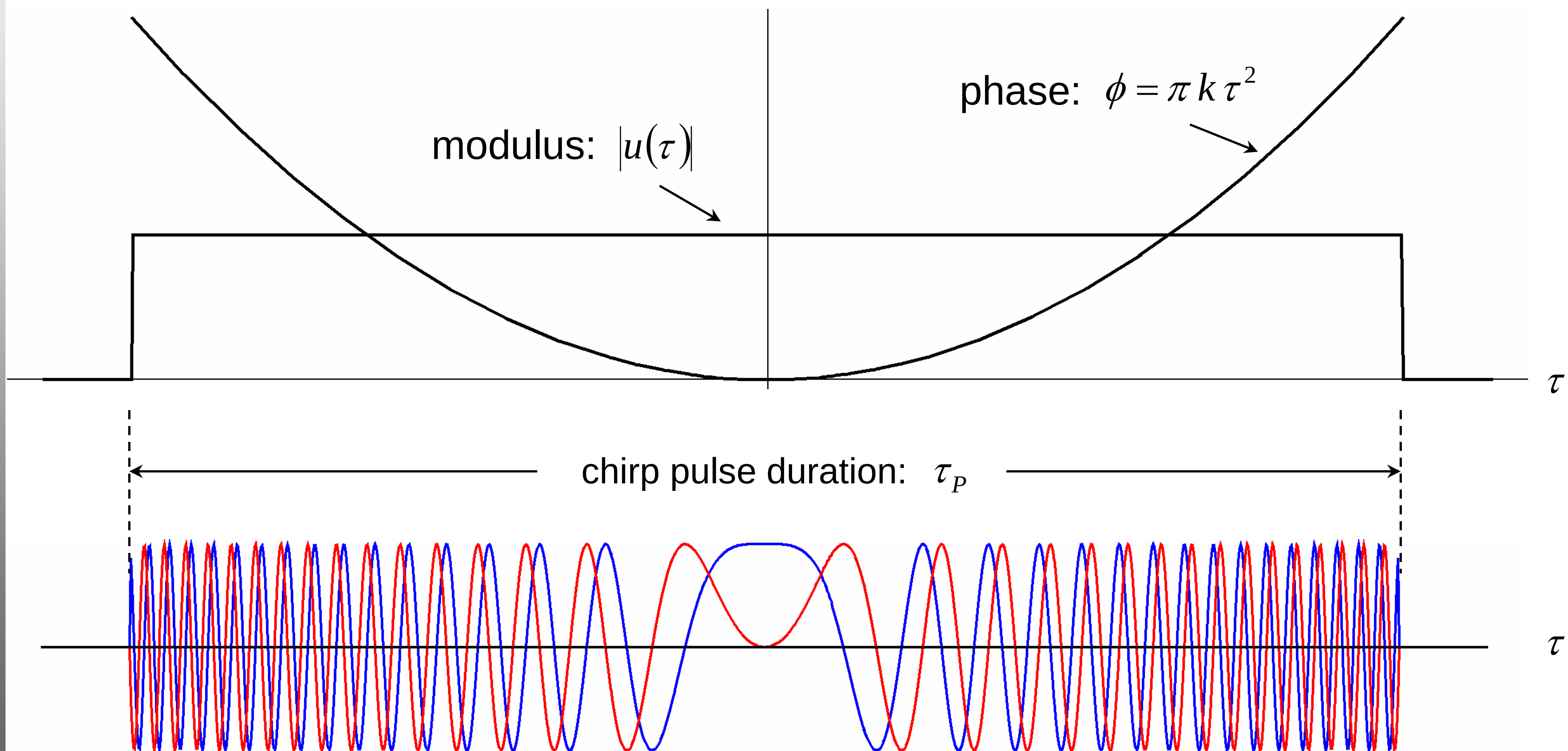

Range Compression

- transmit chirp instead of short pulse
- every point target will return chirp echo
- correlate received signal with replica of transmitted chirp
- final impulse response (approximation) with W_P chirp bandwidth: $\operatorname{sinc}(\tau \cdot W_P) = \dfrac{\sin(\pi \tau W_P)}{\pi \tau W_P}$
- final range resolution: $\rho_R \cong \dfrac{c}{2W_P}$ (exact value depends on definition)

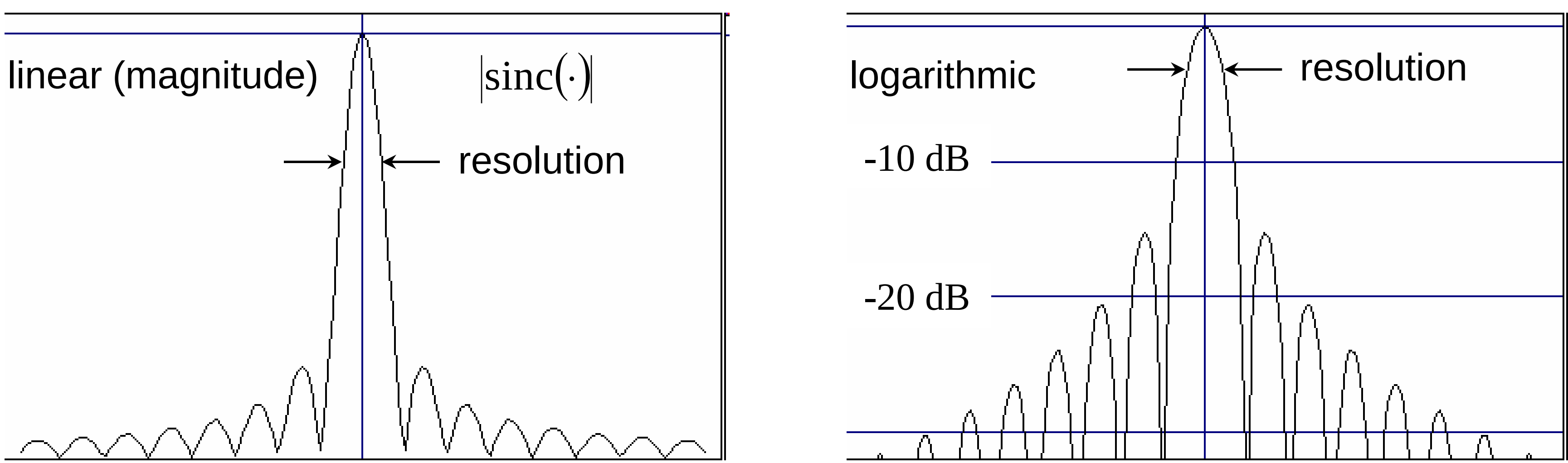

Range Compression by Matched Filtering

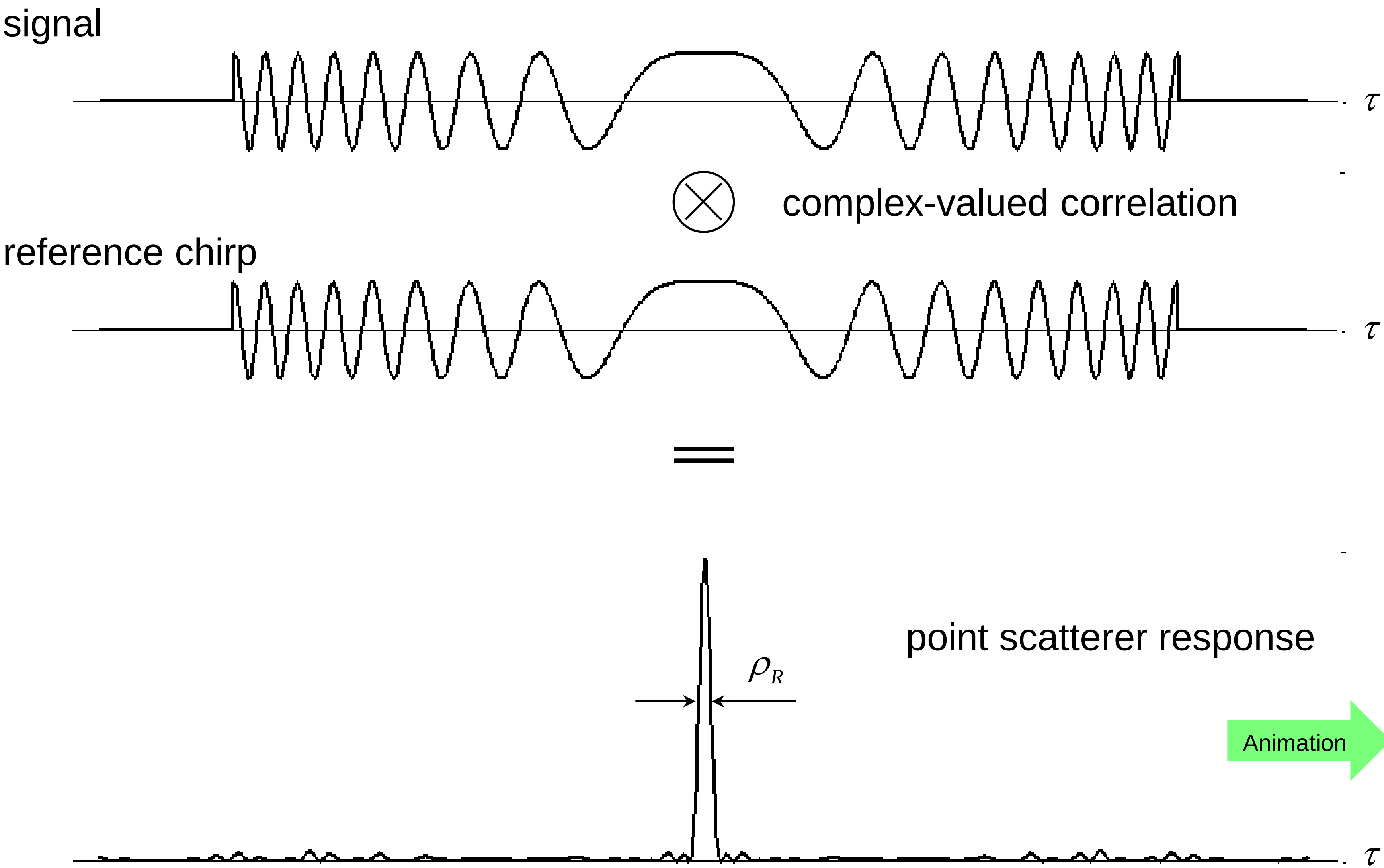

Animation

Synthetic Aperture Radar (SAR)

5.1 Introduction

5.2 Radar Distance Measurement (Range-Component)

5.3 Formation of Synthetic Aperture (Azimuth-Component)

5.4 Characteristics of SAR Images

Side-Looking Radar Geometry

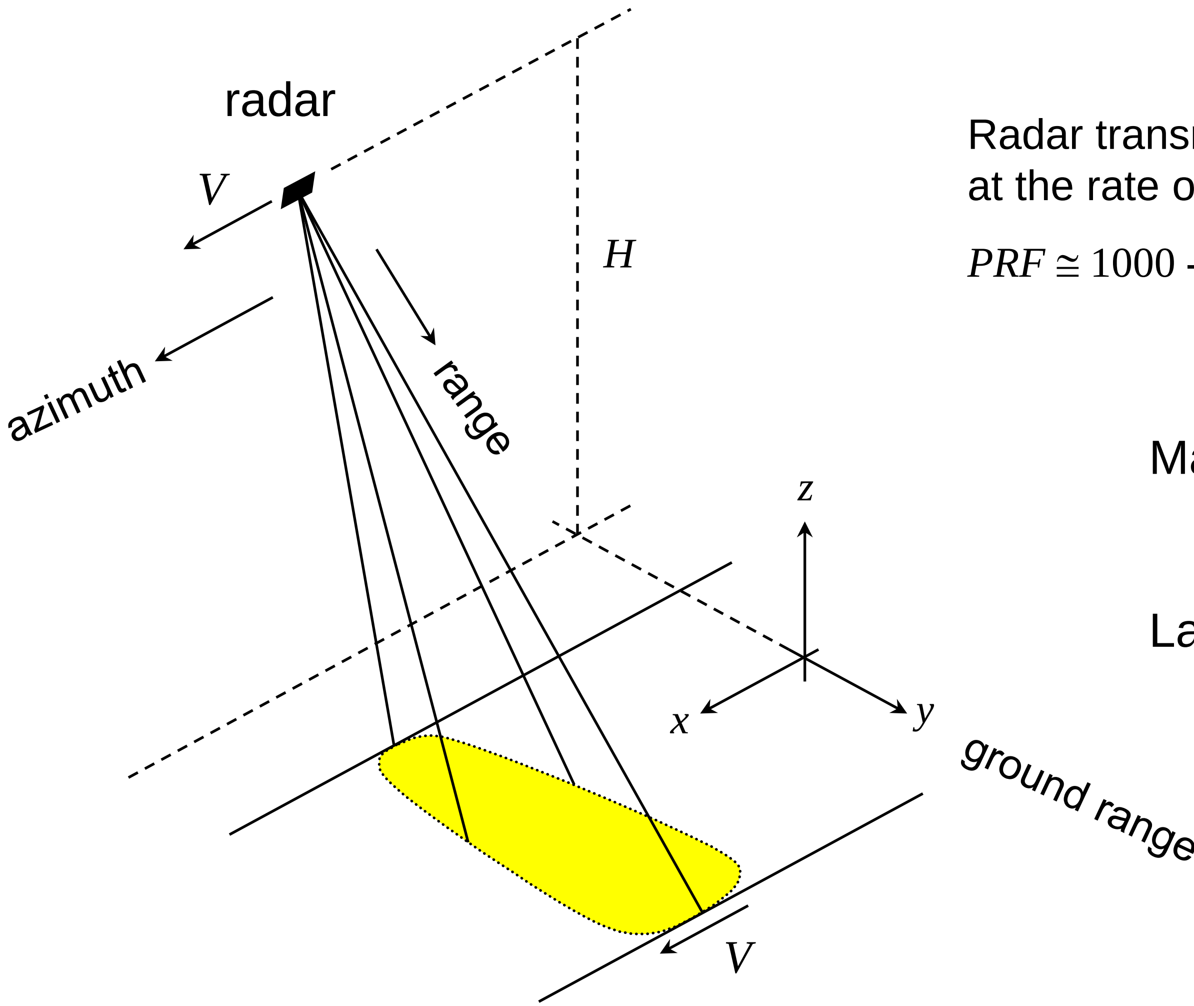

Radar transmits pulses and receives echoes at the rate of the pulse repetition frequency:

$PRF \cong 1000 \text{ - } 4000 \text{ Hz}$

Main topic in the following:

Stripmap-Mode SAR

Later:

Spotlight Mode SAR

ScanSAR

2-D Raw Data Matrix

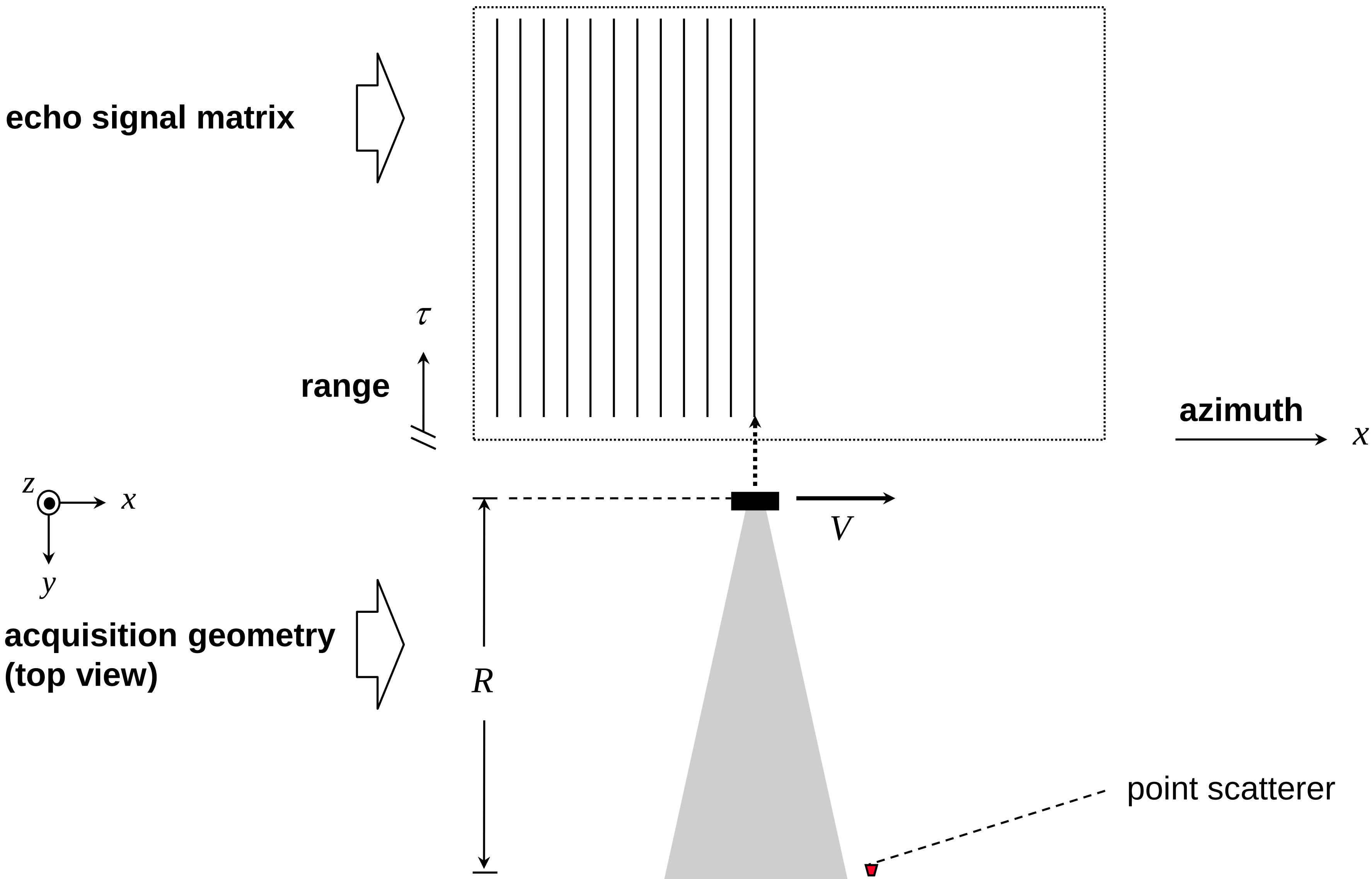

2-D Raw Data Matrix

echo signal matrix

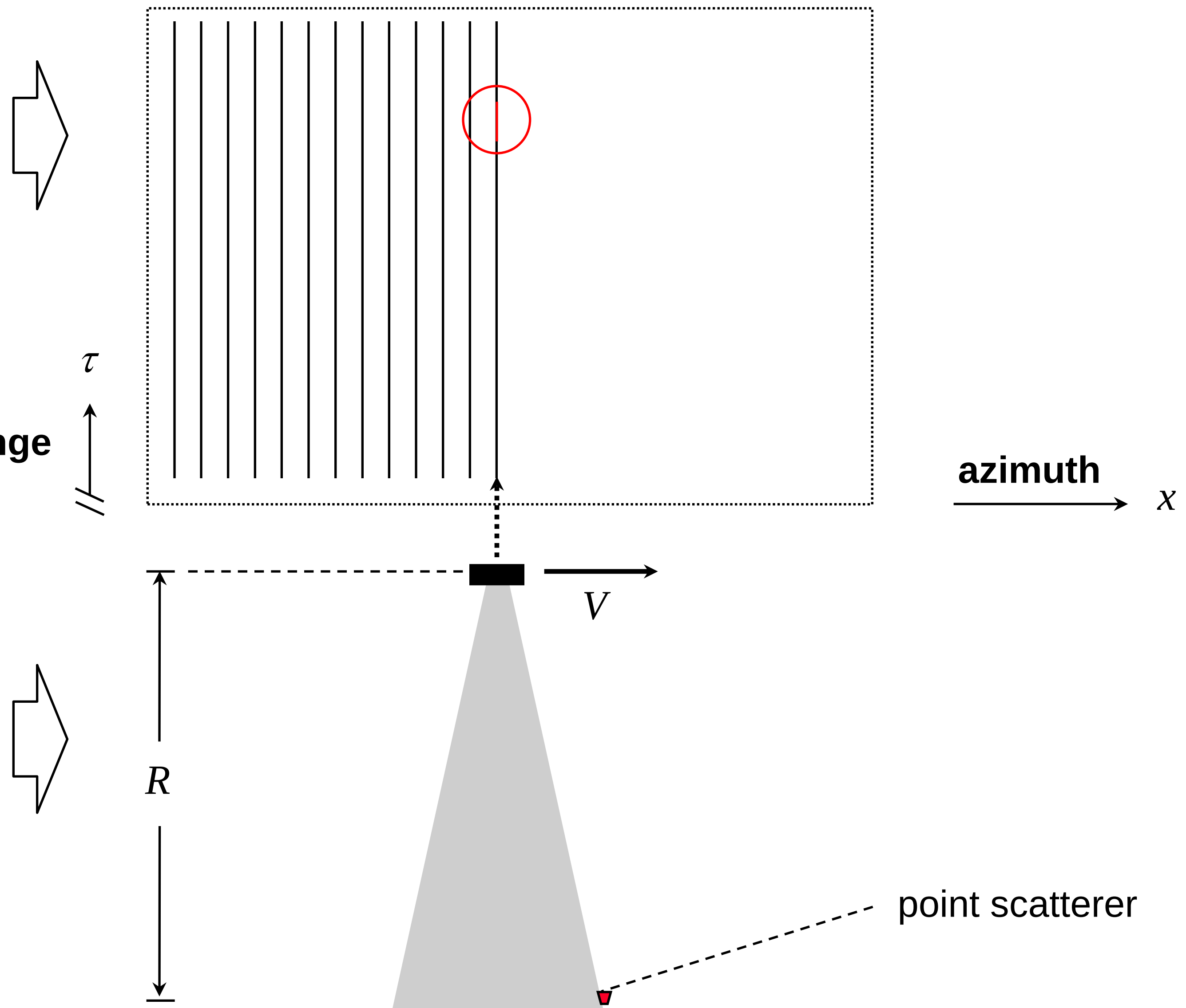

acquisition geometry
(top view)

2-D Raw Data Matrix

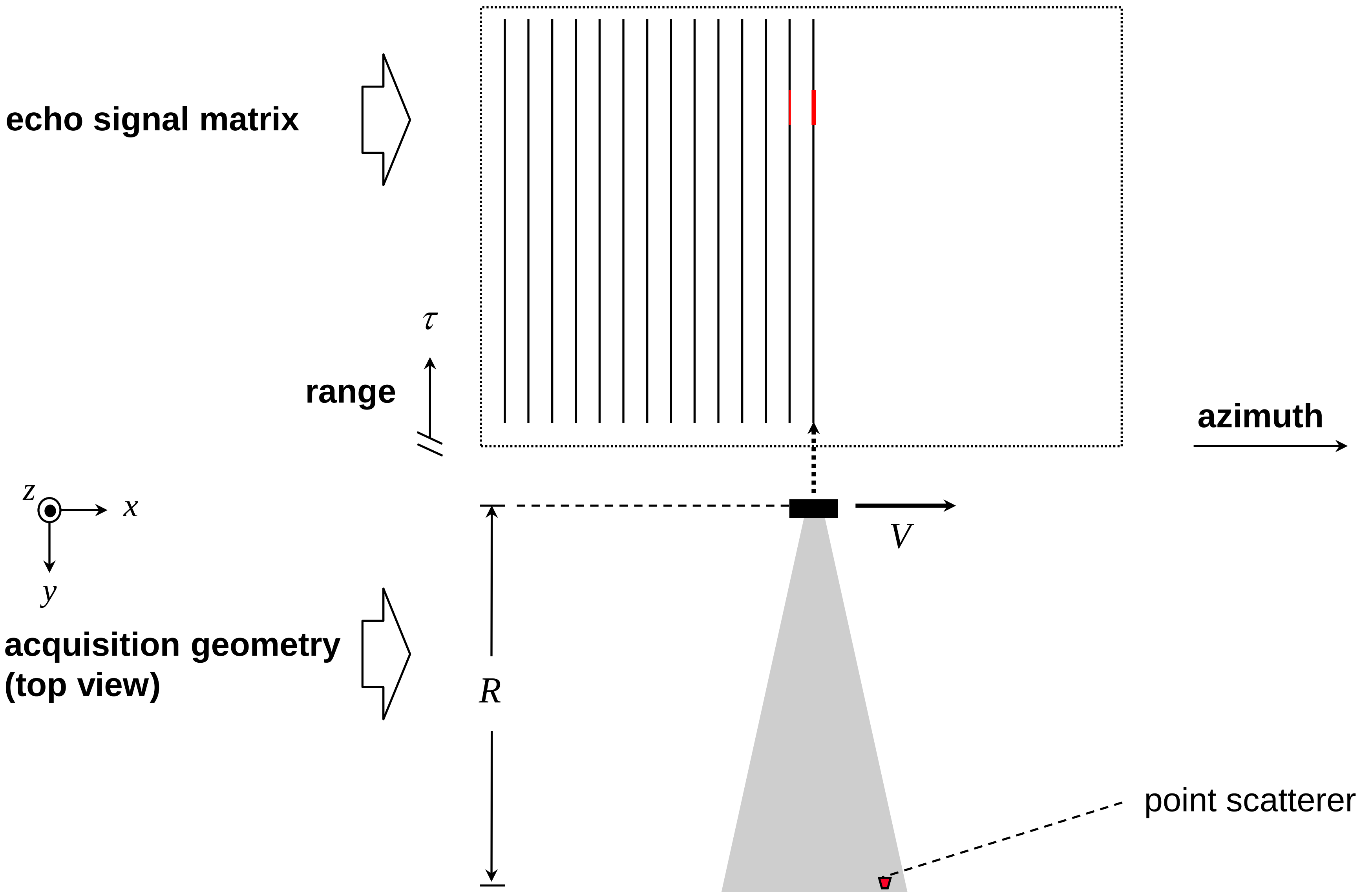

2-D Raw Data Matrix

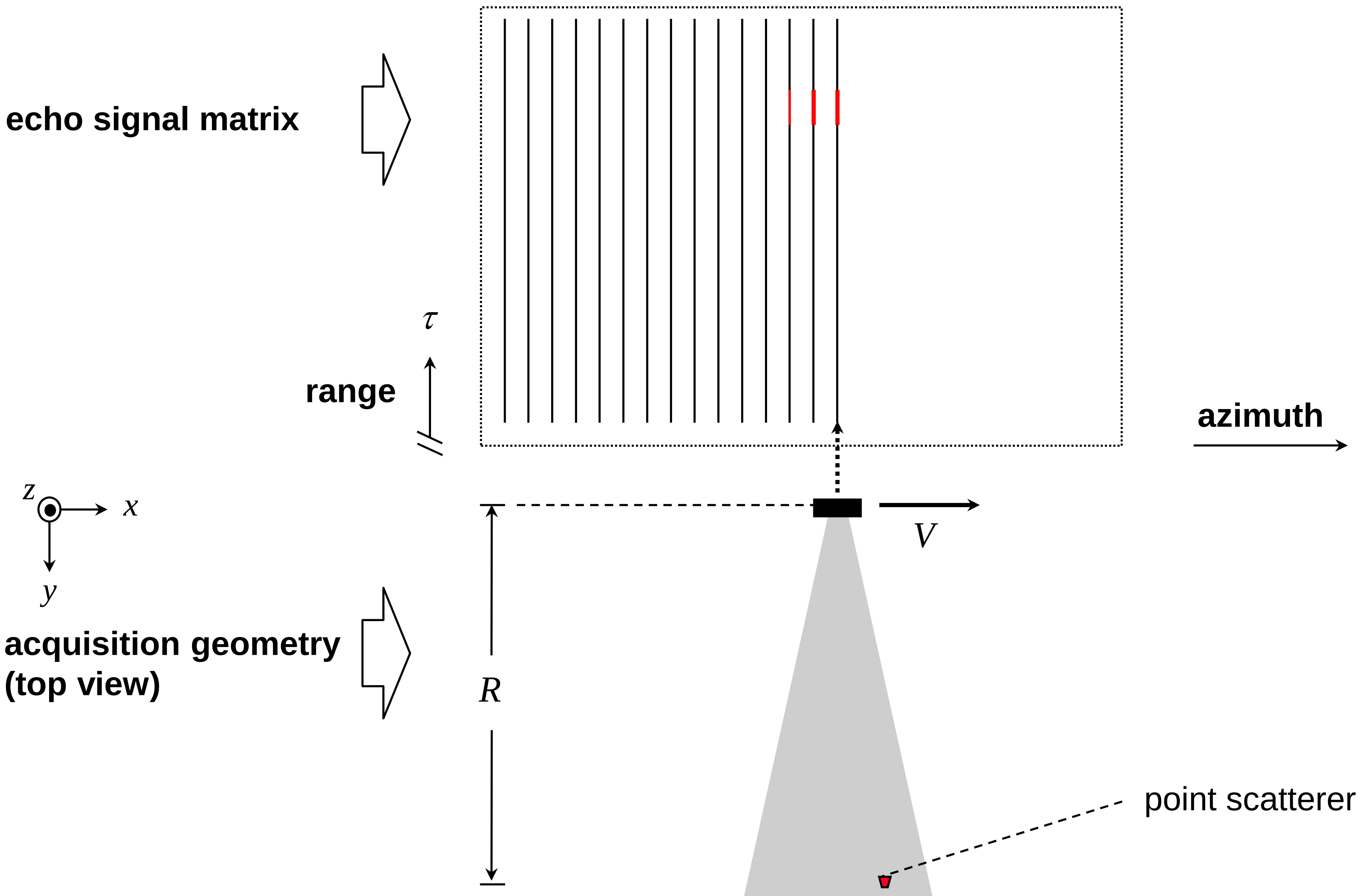

2-D Raw Data Matrix

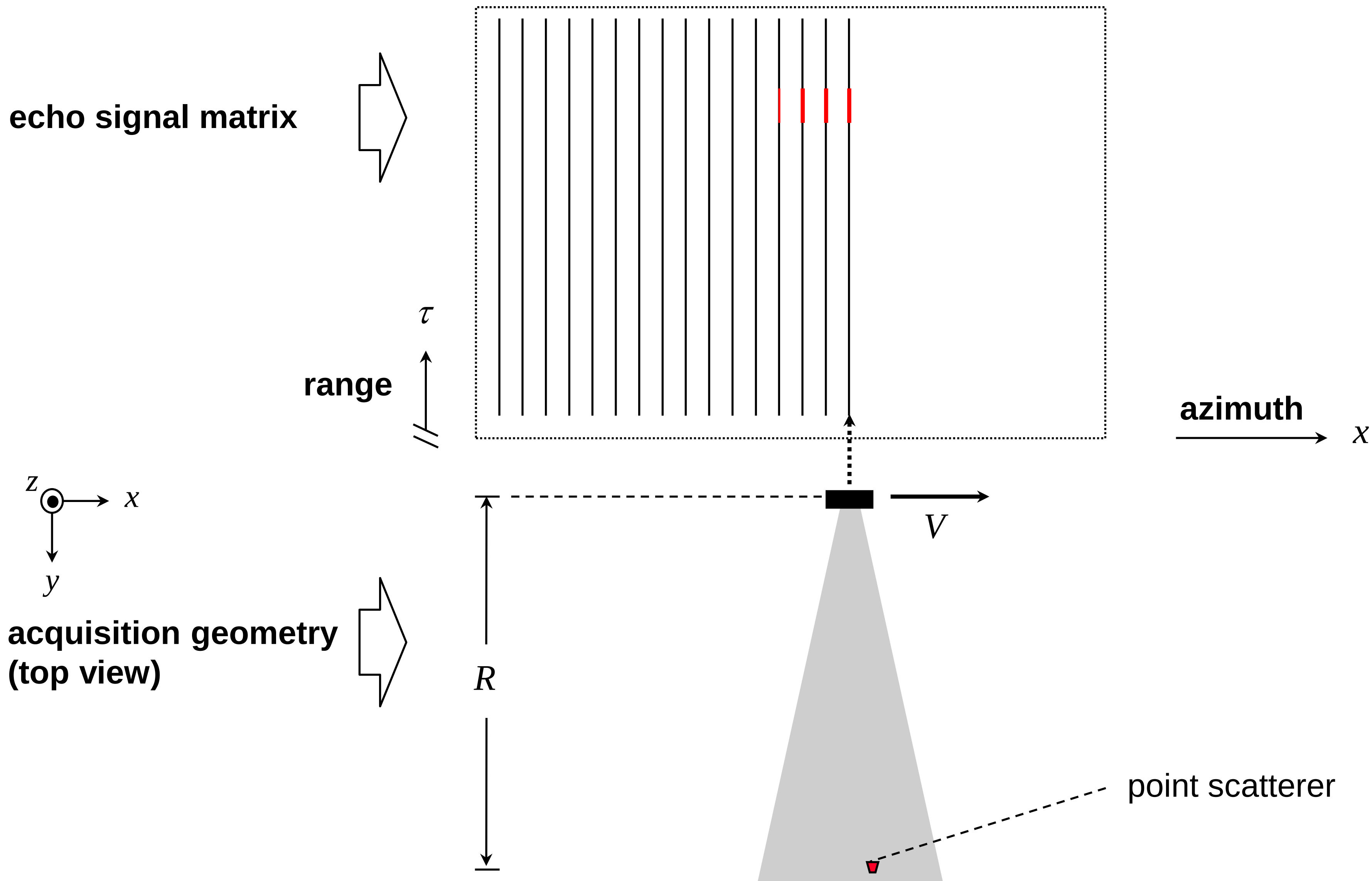

2-D Raw Data Matrix

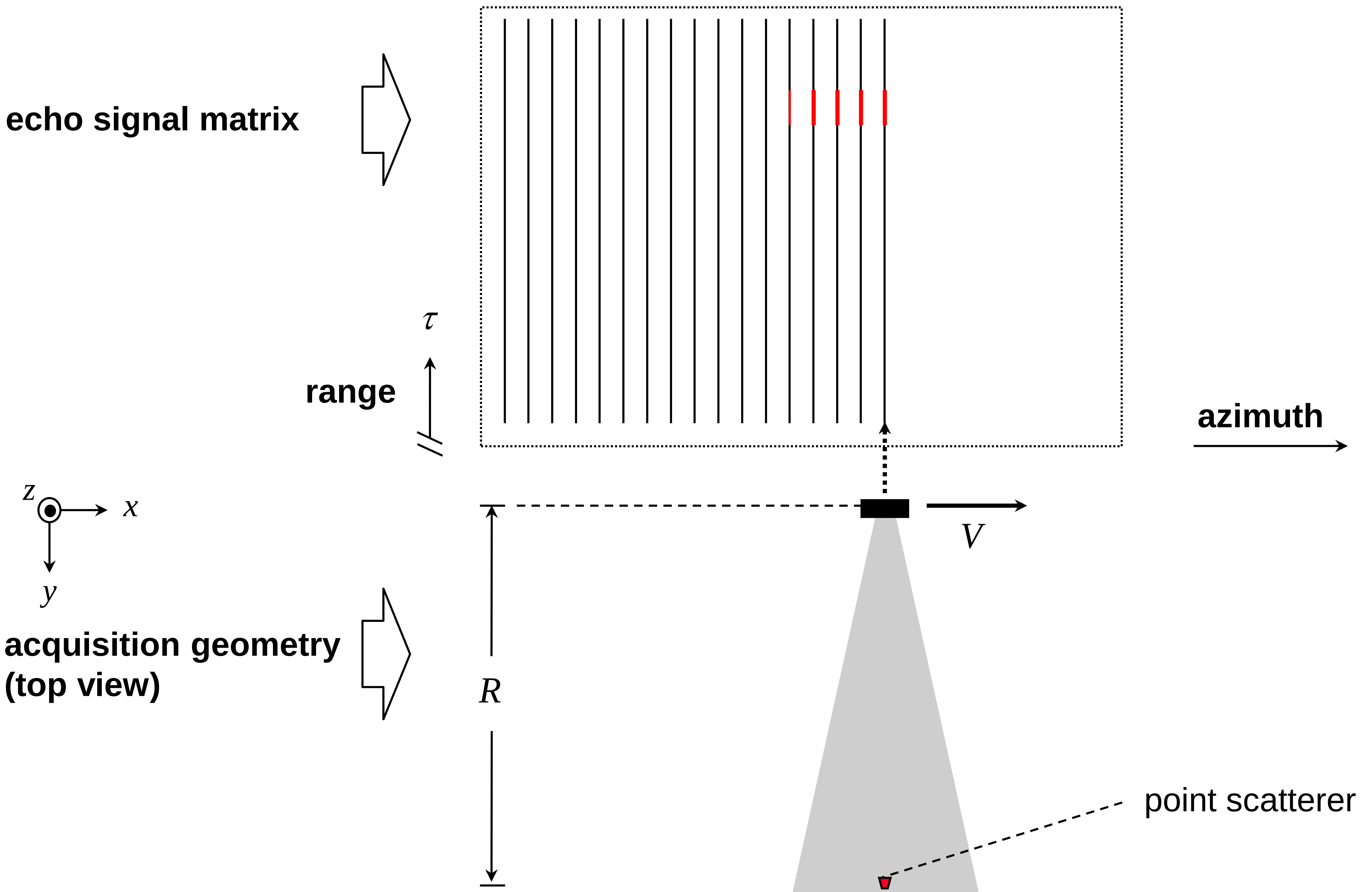

2-D Raw Data Matrix

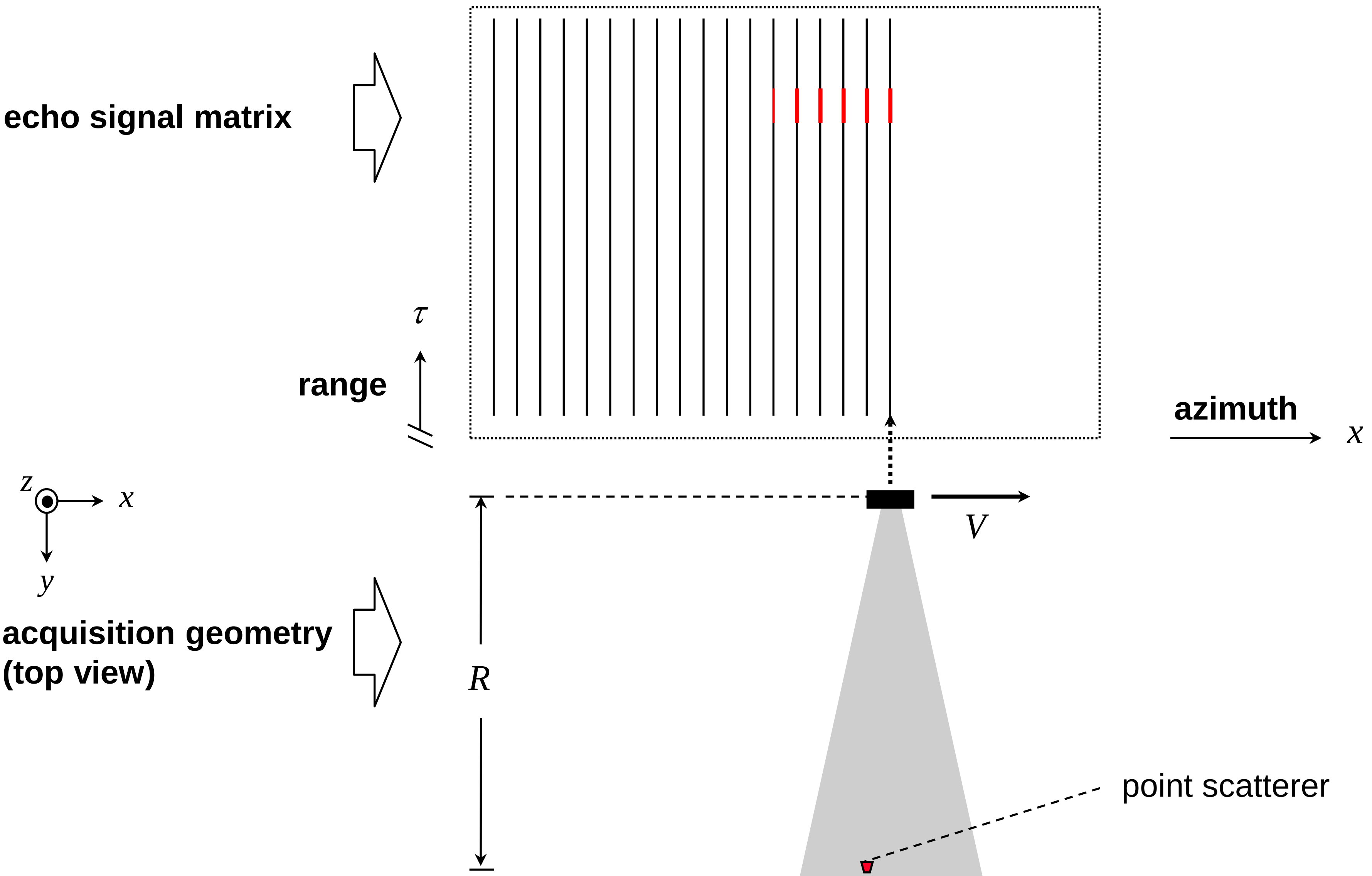

2-D Raw Data Matrix

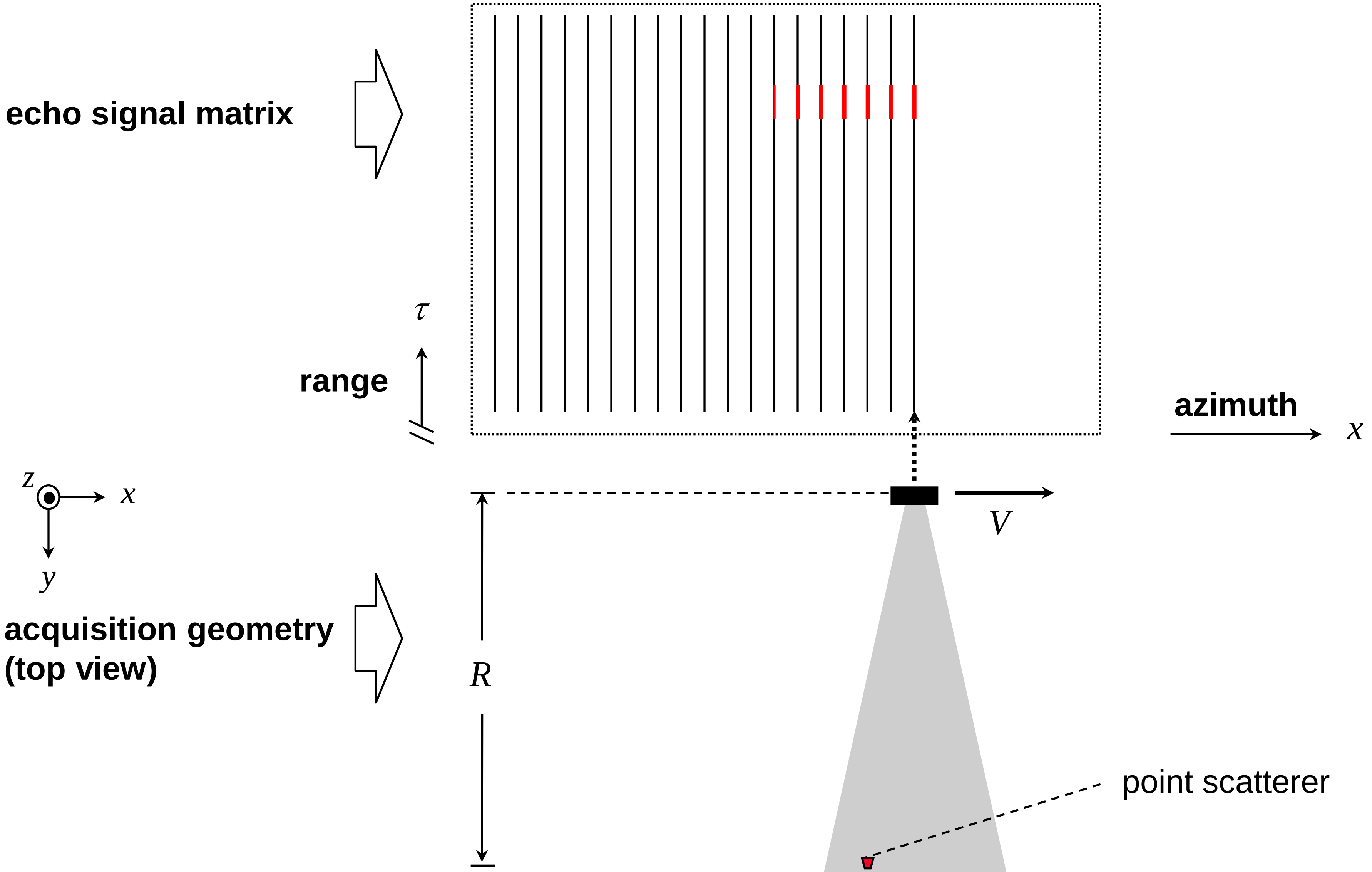

2-D Raw Data Matrix

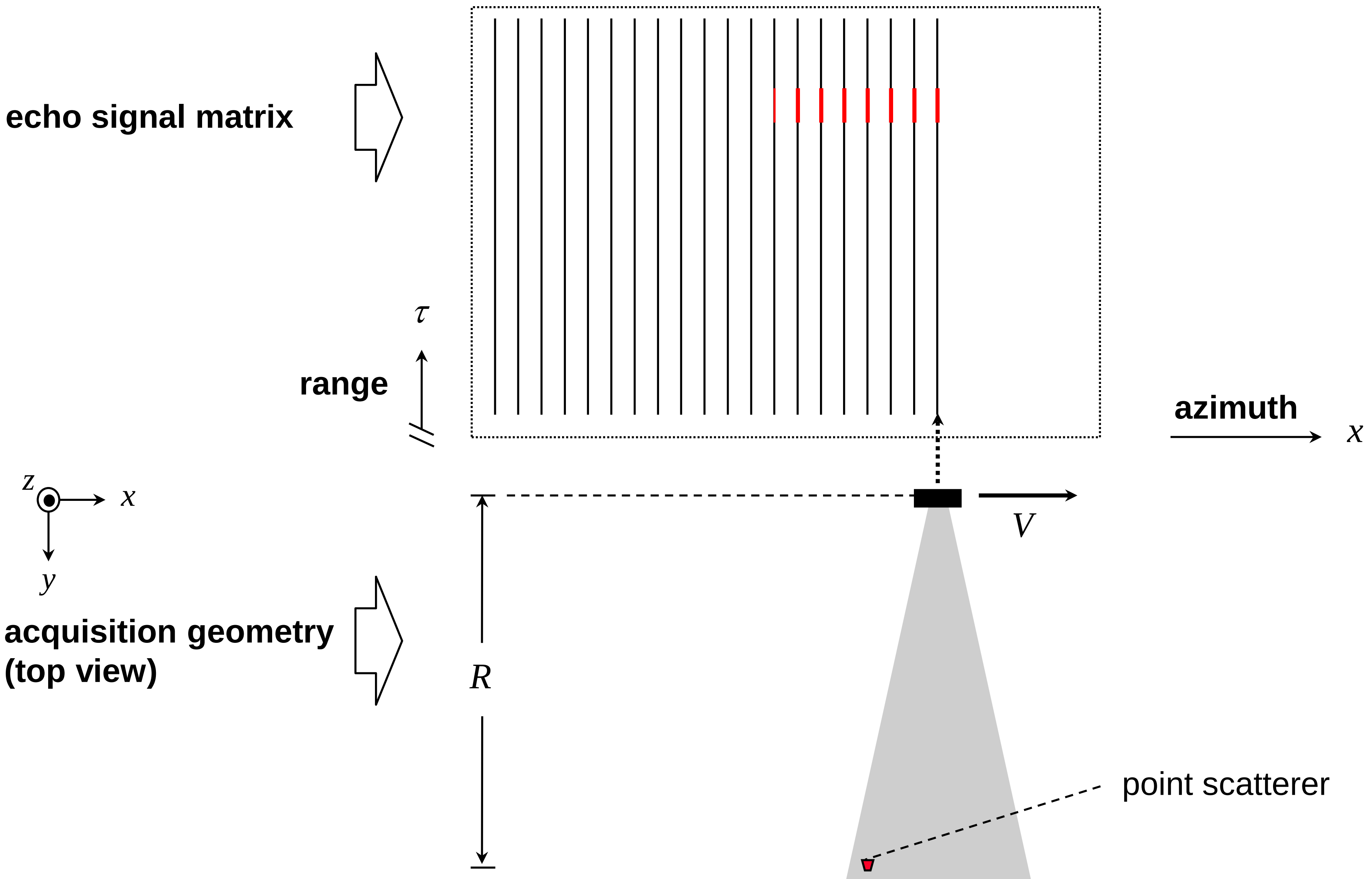

2-D Raw Data Matrix

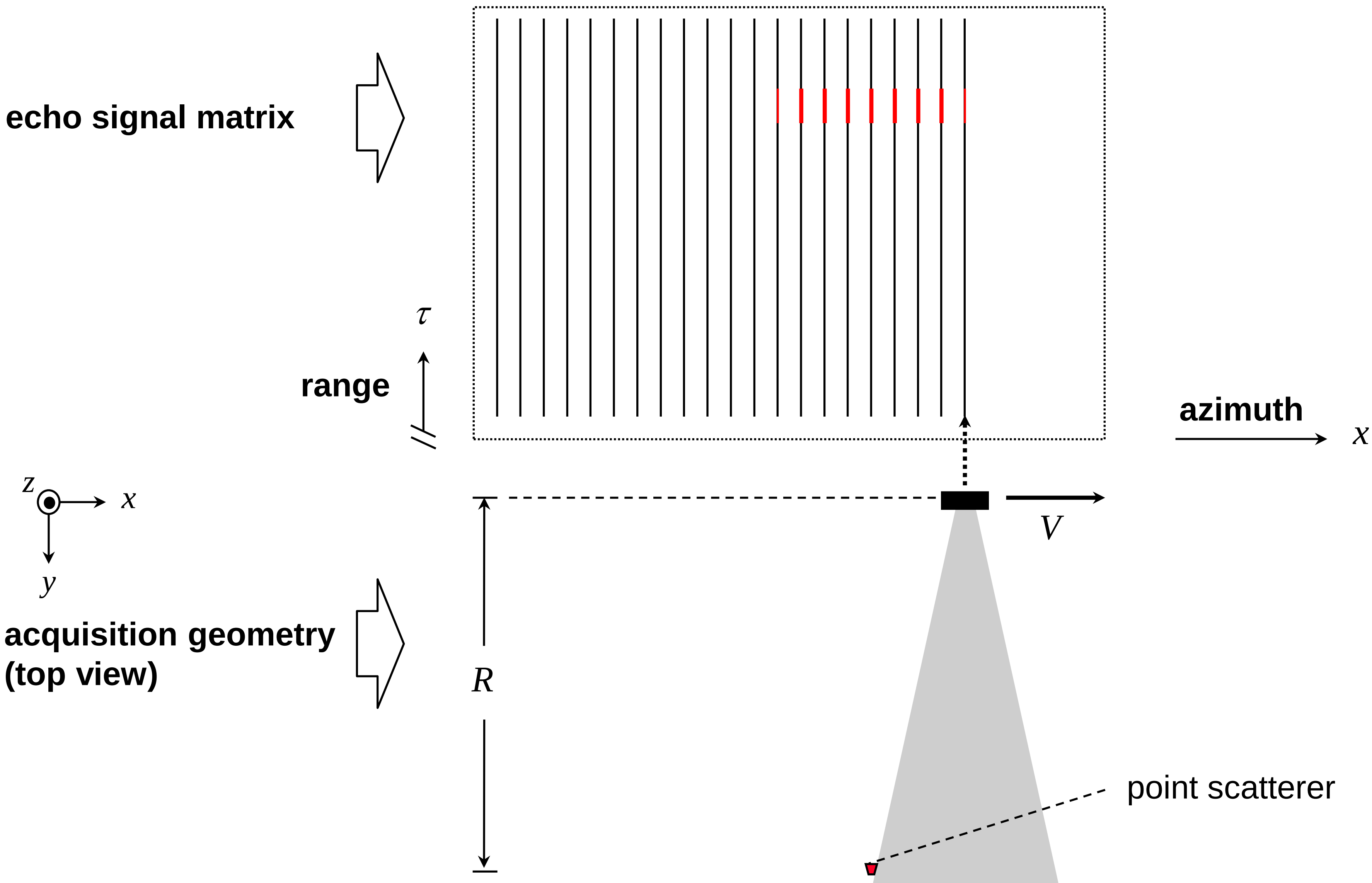

2-D Raw Data Matrix

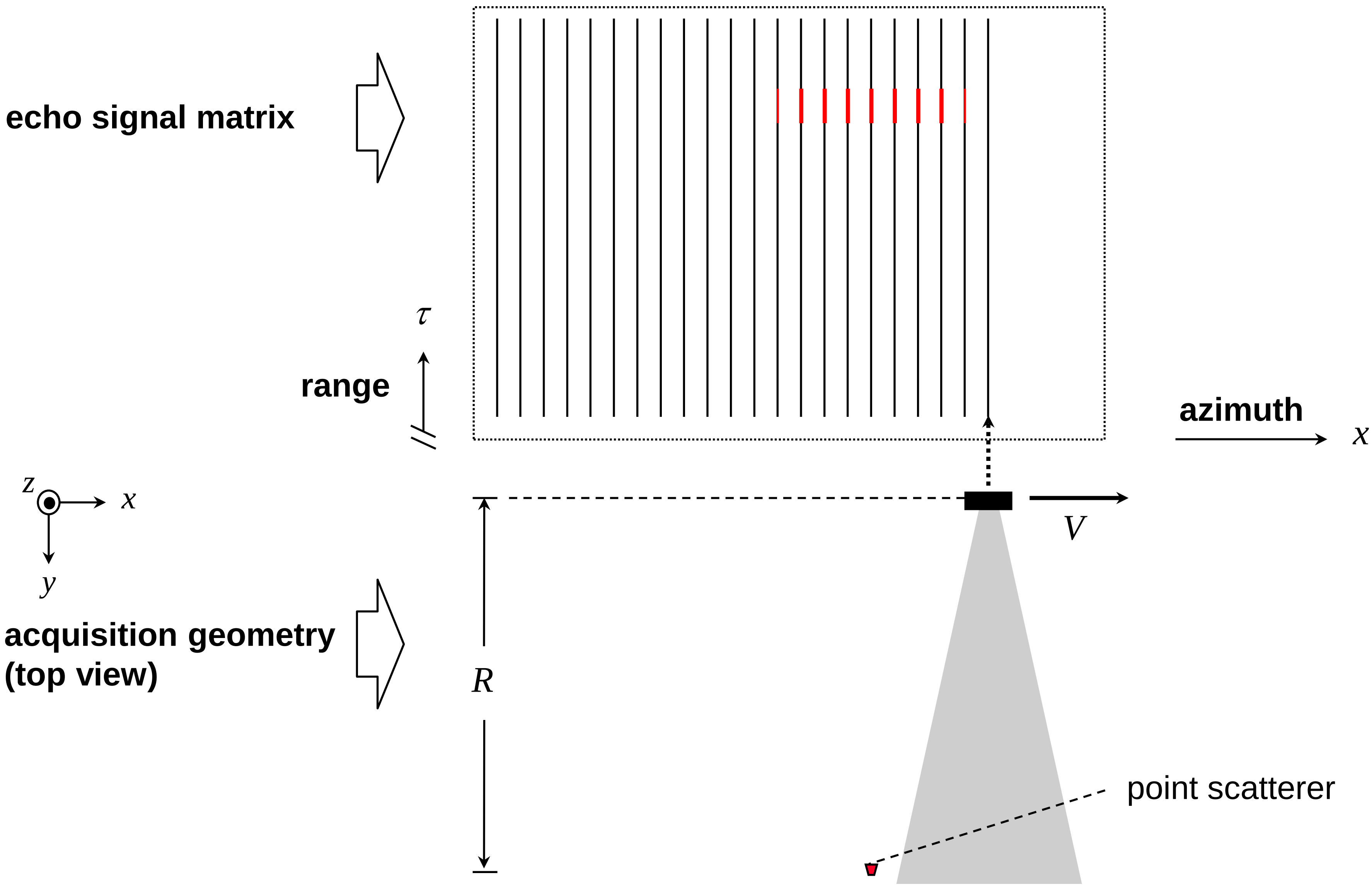

2-D Raw Data Matrix

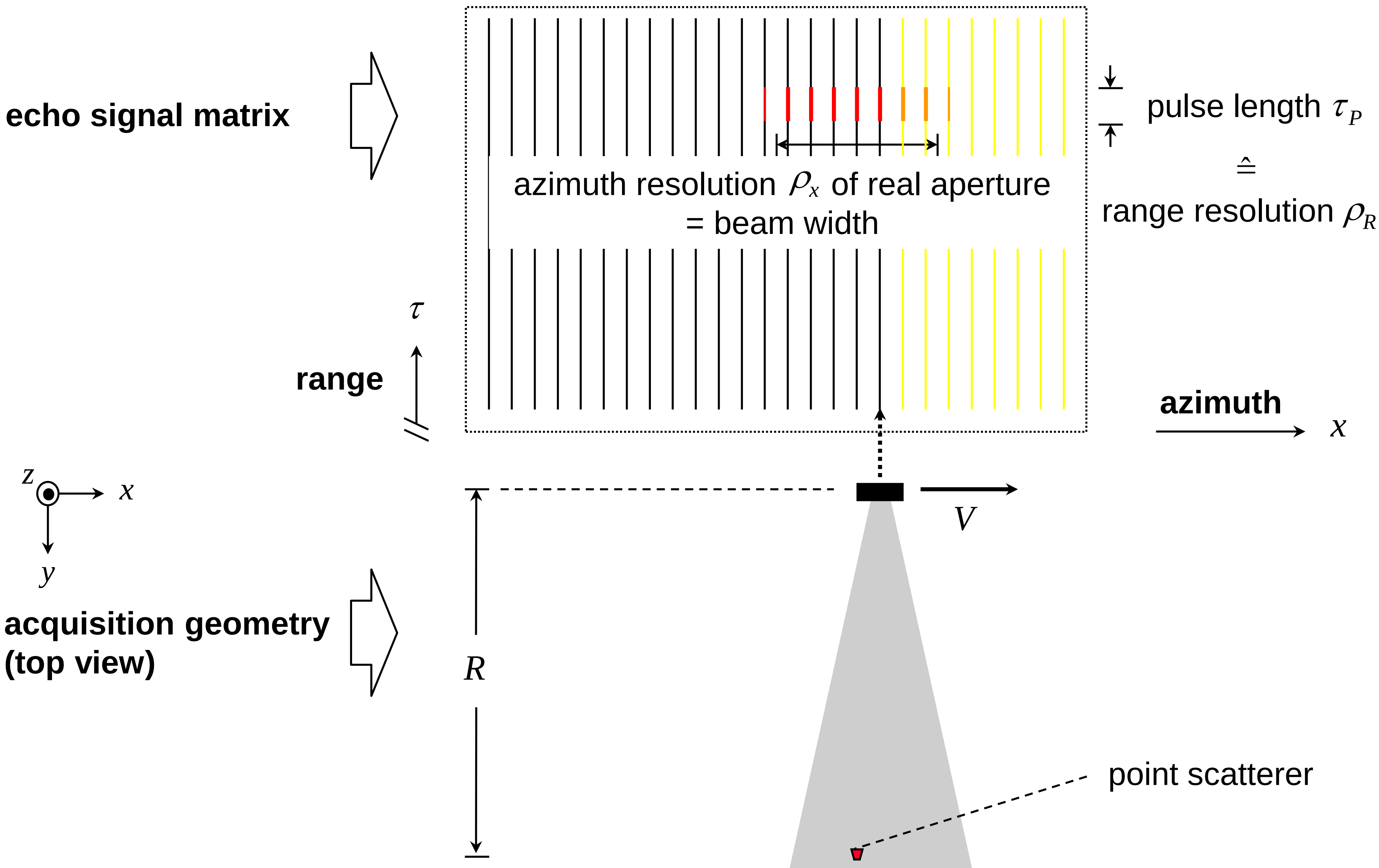

Antenna Size vs. Beam Width

short antenna

wide beam

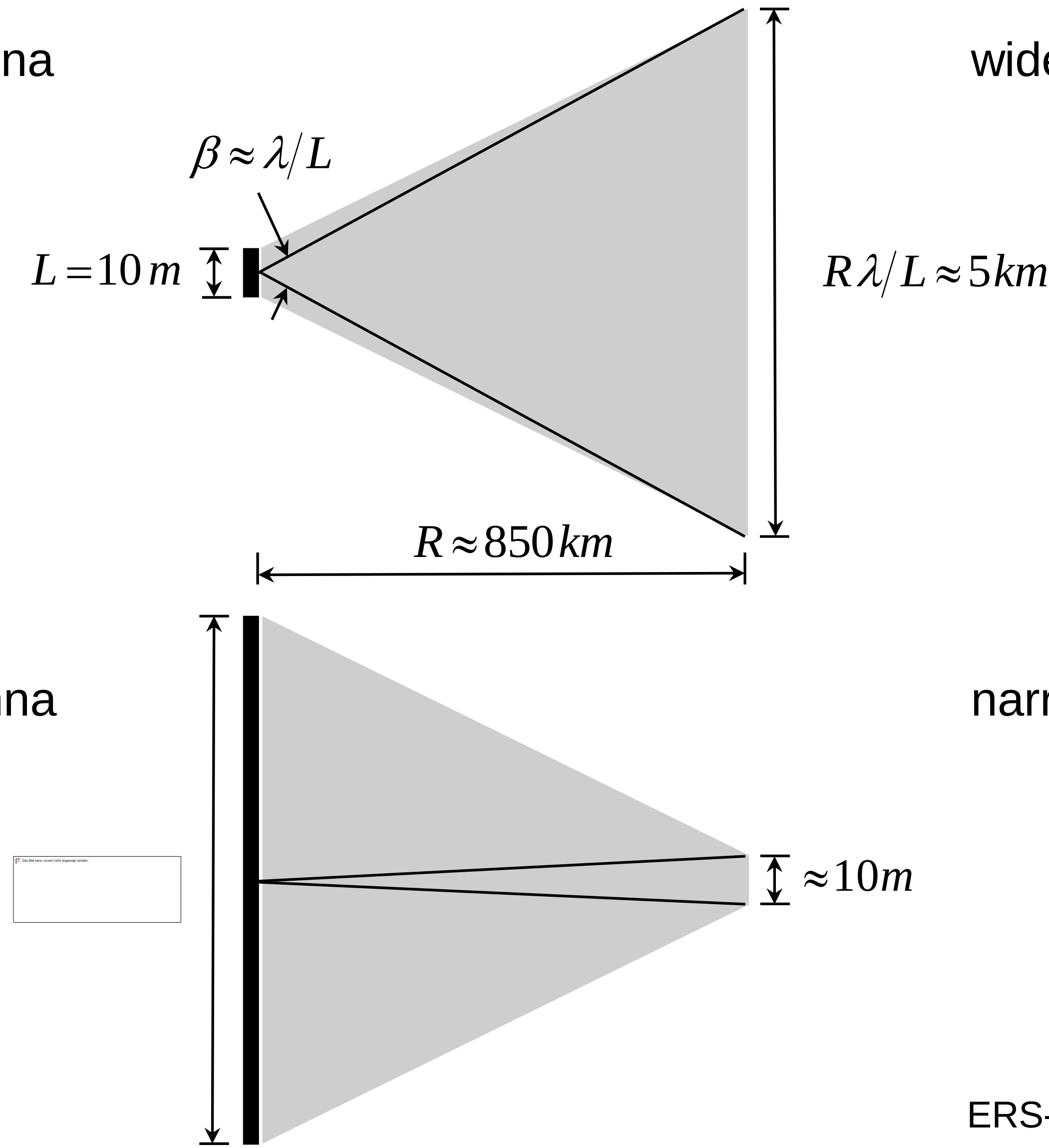

long antenna

narrow beam

ERS-1/2 parameters

Formation of a Synthetic Aperture - SAR Principle

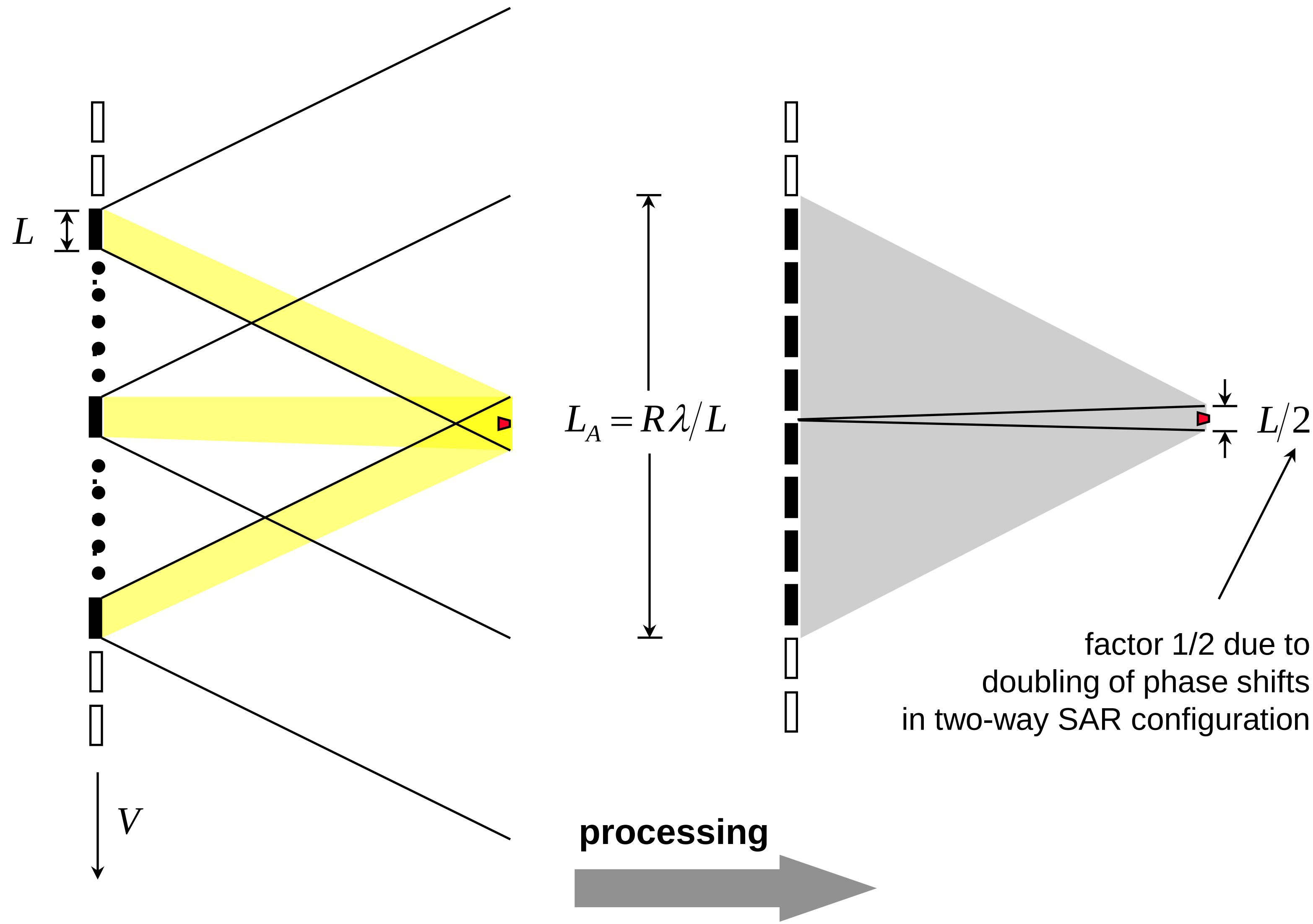

= phase corrected summation of echoes

Range History of a Single Point Scatterer

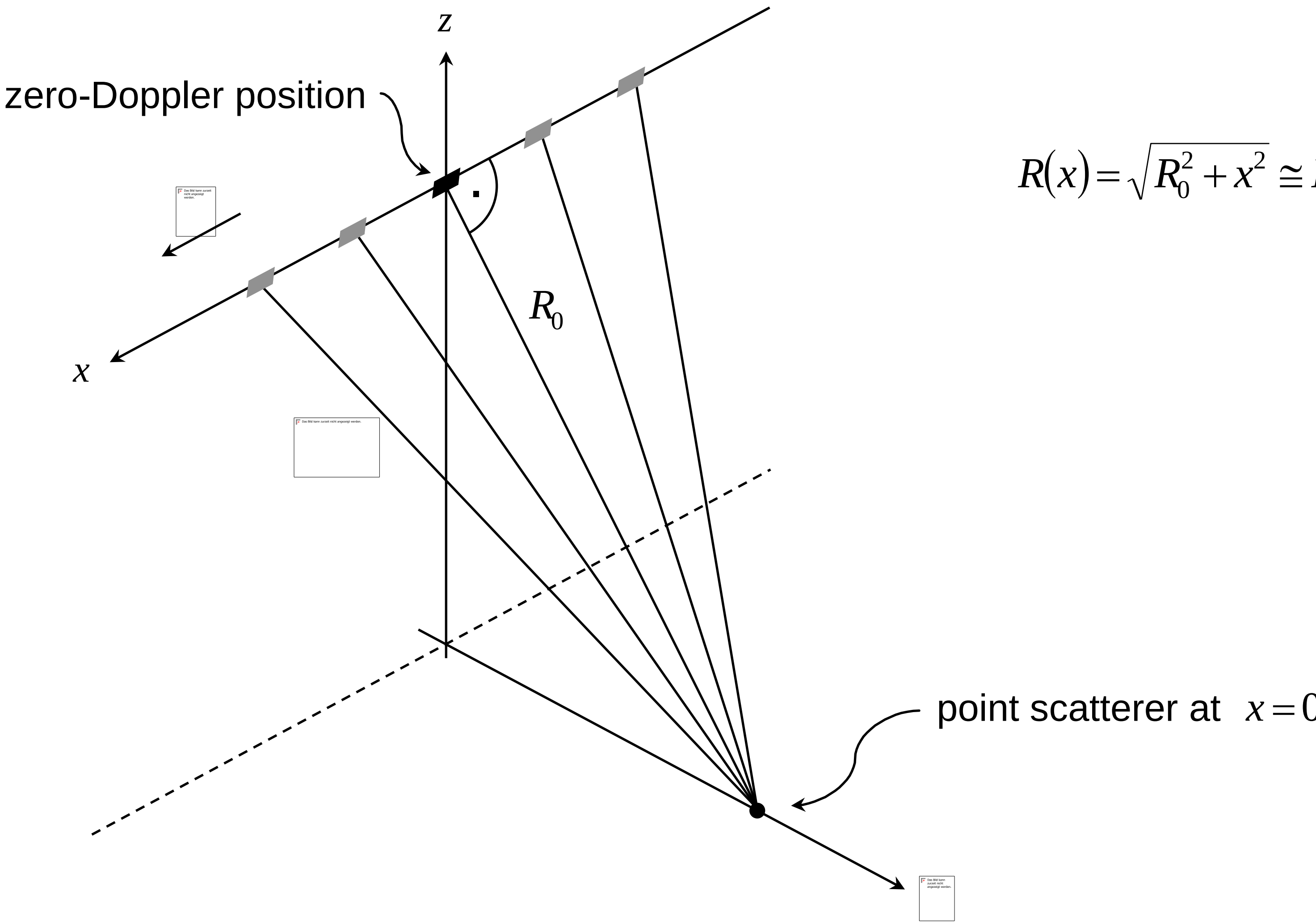

$$R(x) = \sqrt{R_0^2 + x^2} \cong R_0 + \frac{x^2}{2\,R_0}$$

2-D Raw Data Matrix

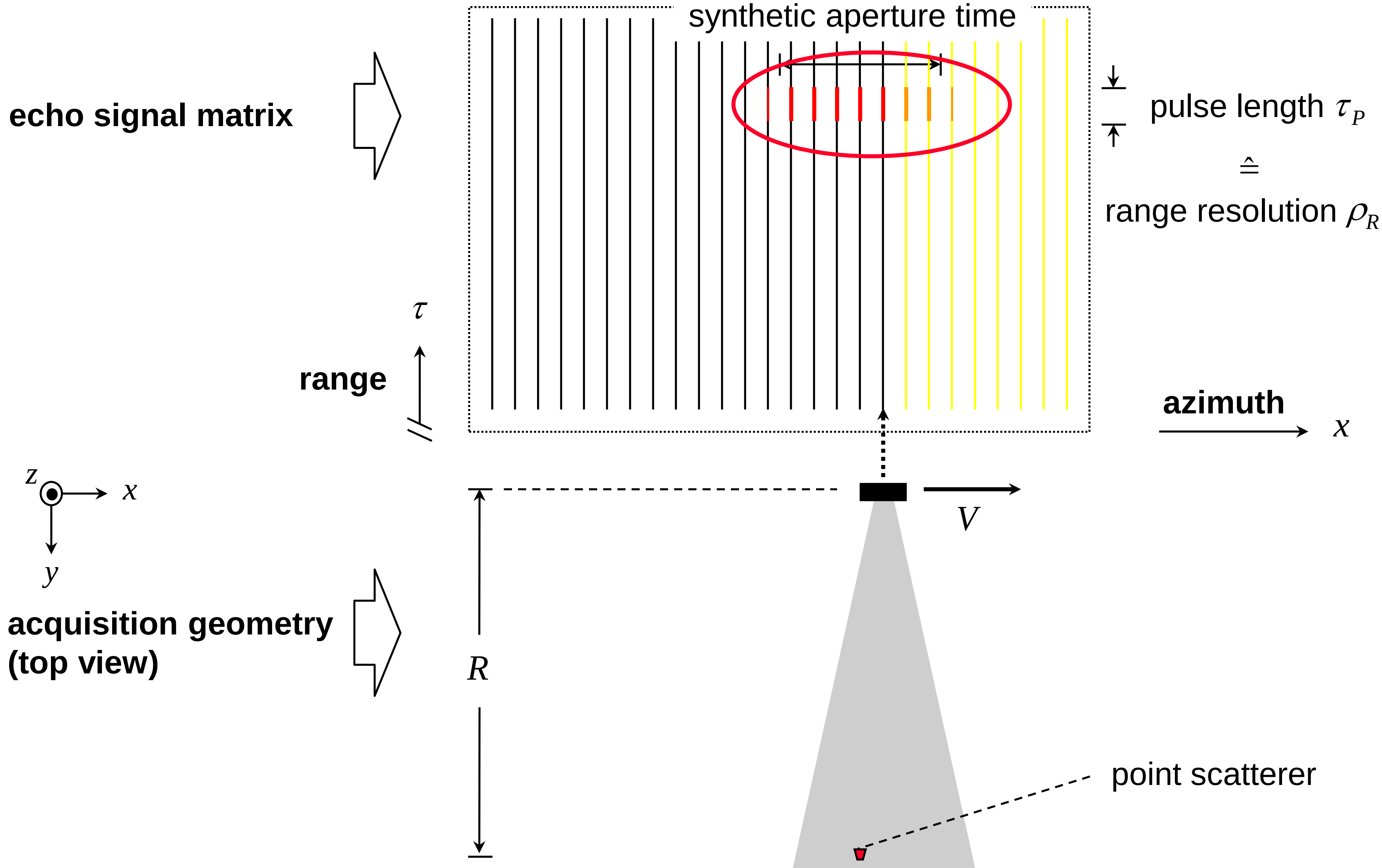

Remote Sensing Technology

Formation of the Azimuth Chirp Signal

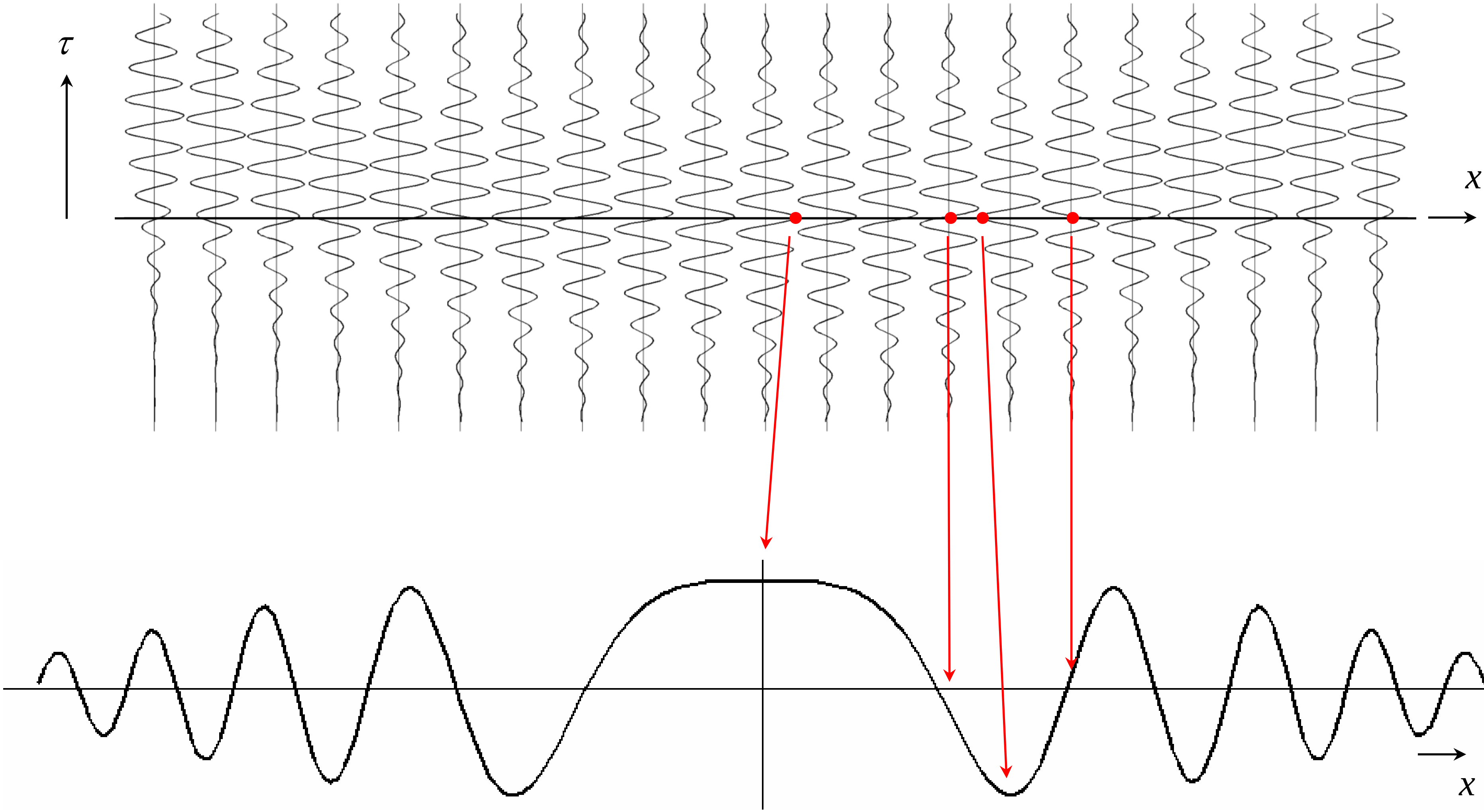

SAR Raw Data of a Point Scatterer (Simulation)

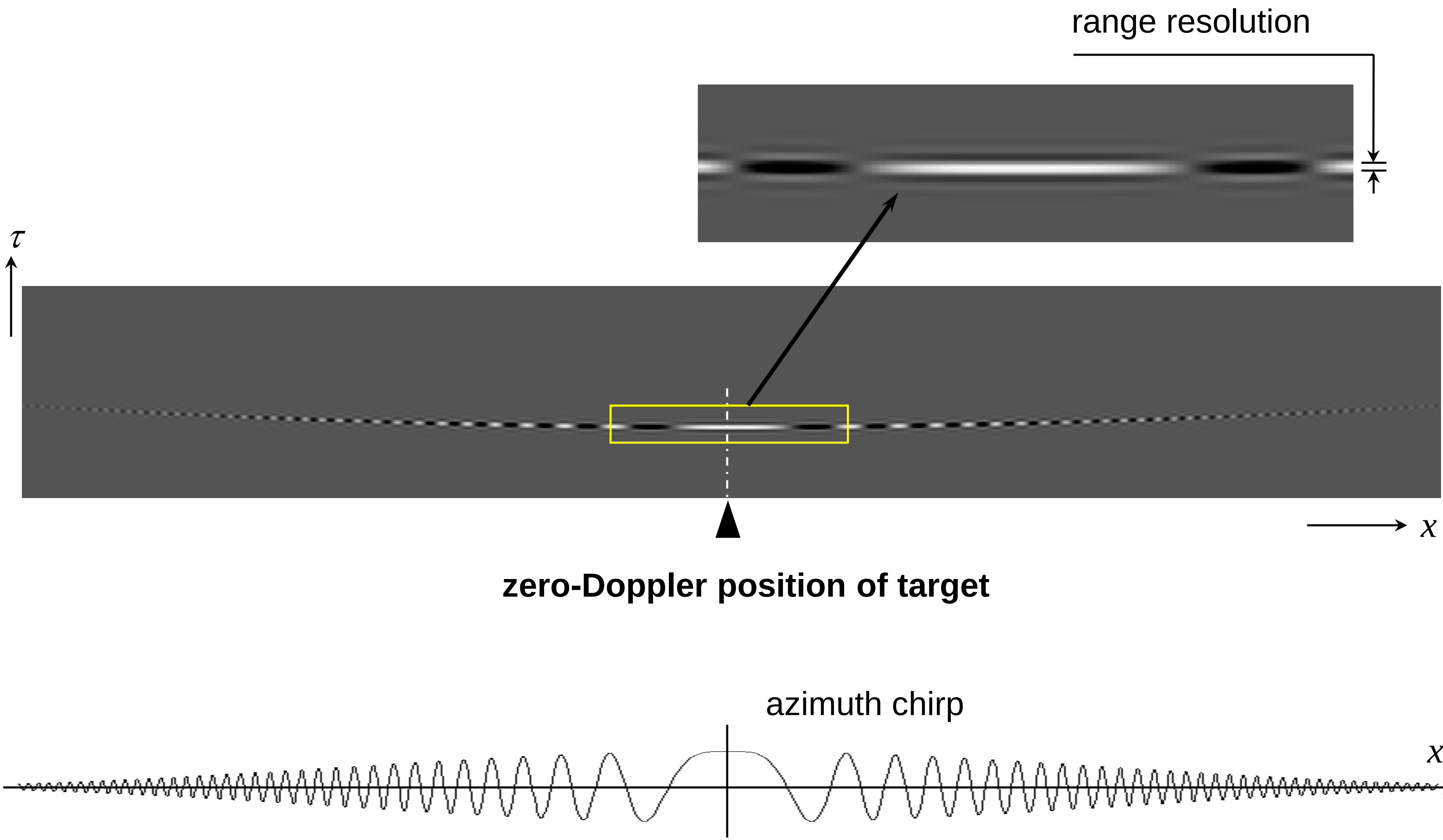

Azimuth SAR Processing by Correlation

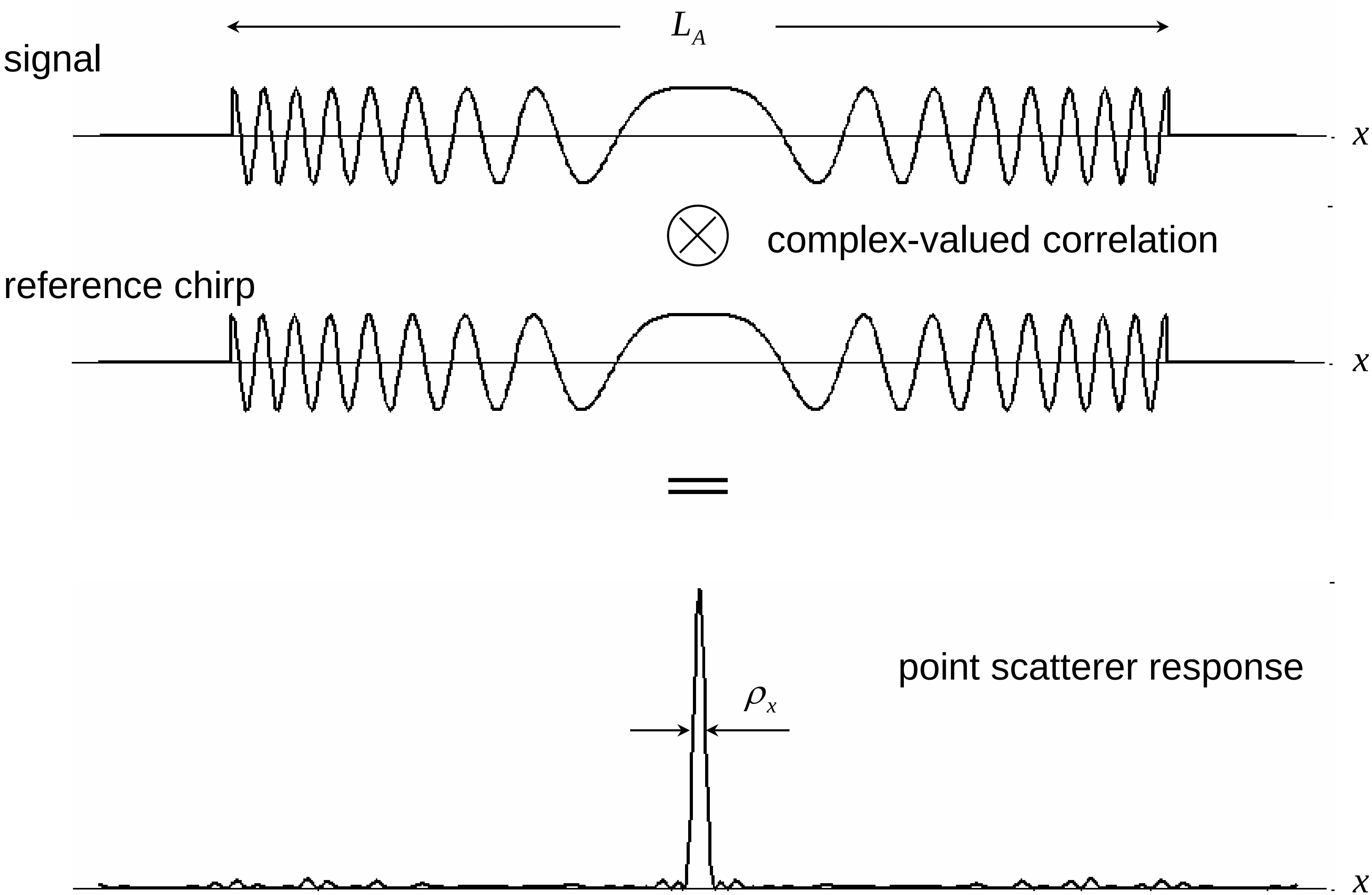

Linear Superposition of Chirps

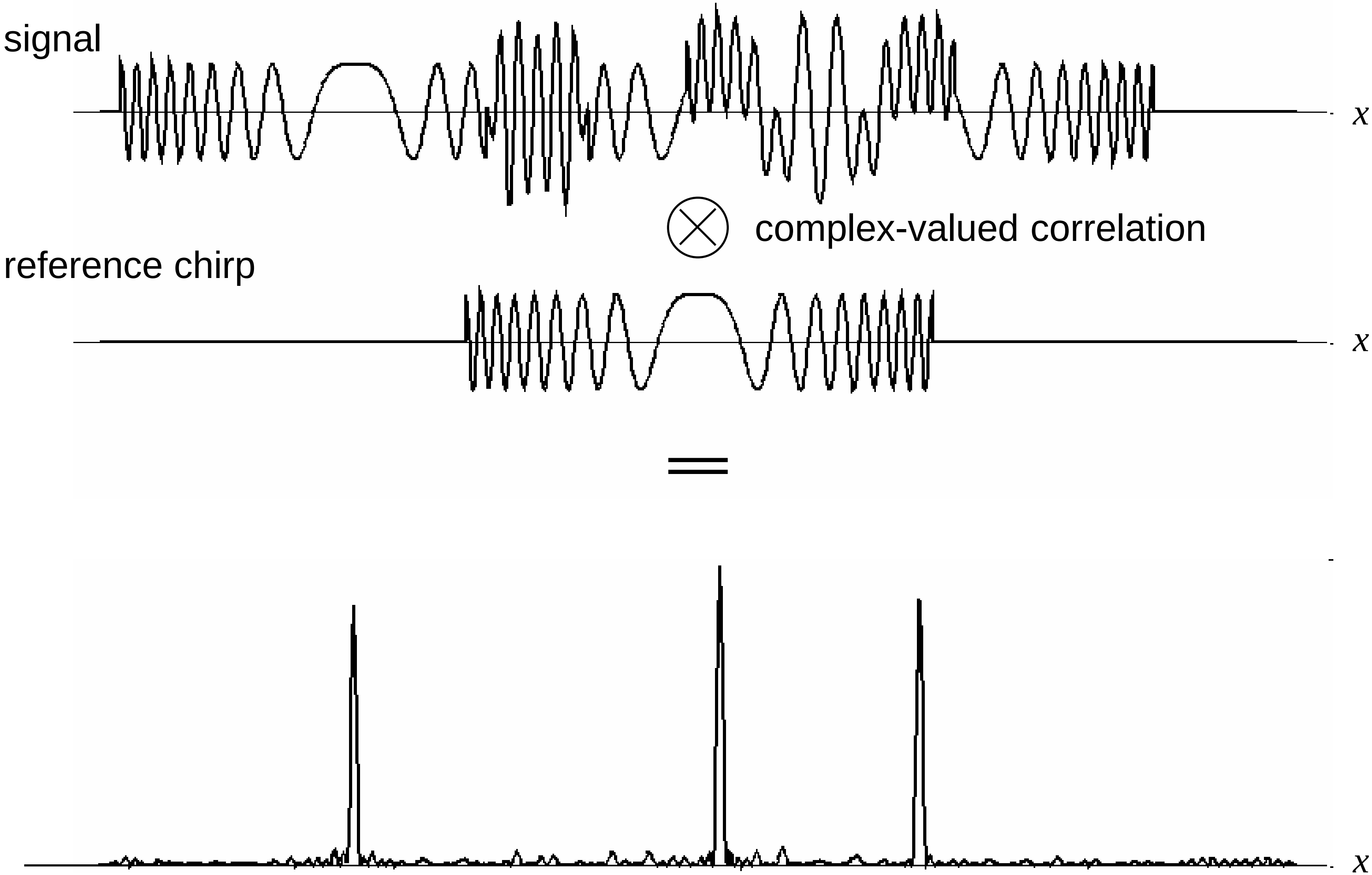

Unfocussed (Raw) 2D SAR Point Response

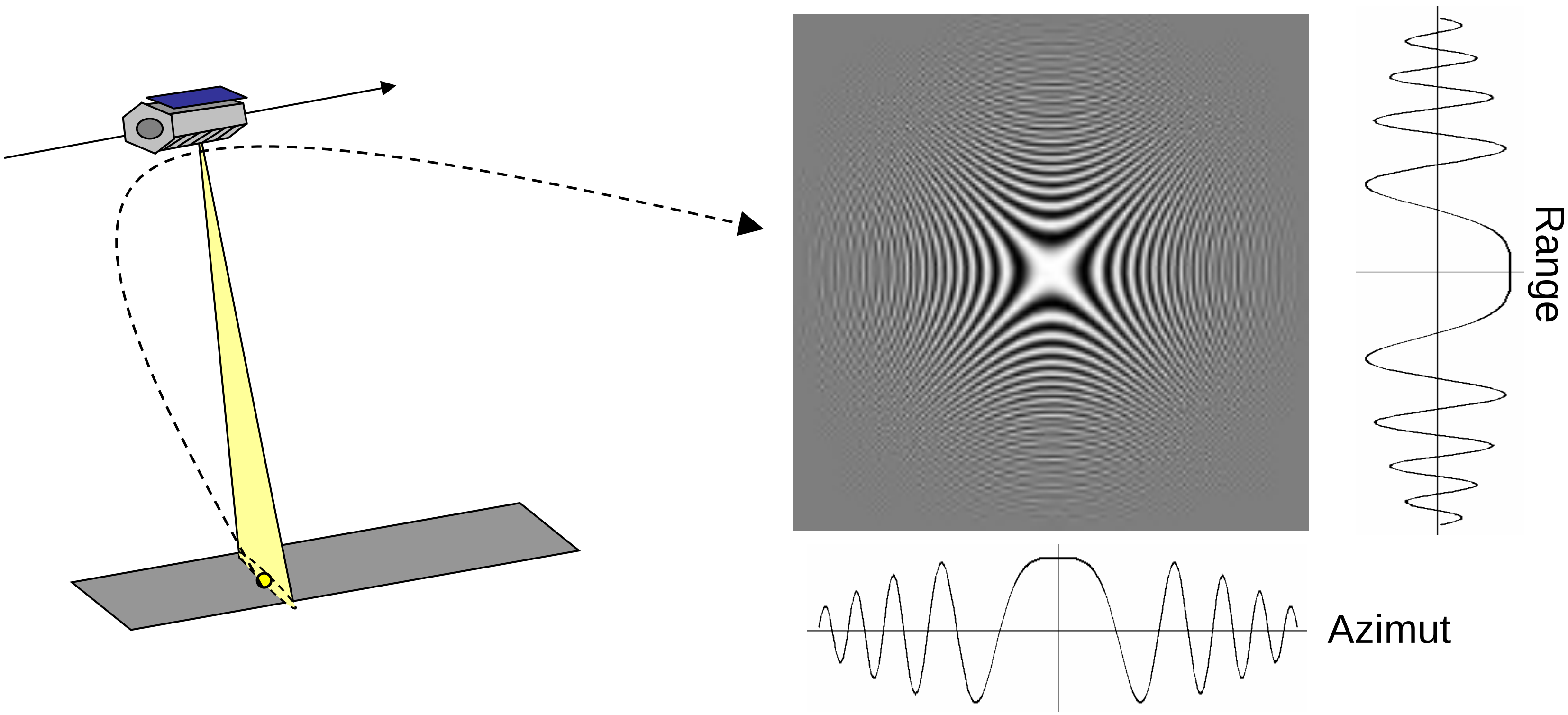

SAR Raw Data (After Range Compression)

→ azimuth

data ERS-1 © ESA

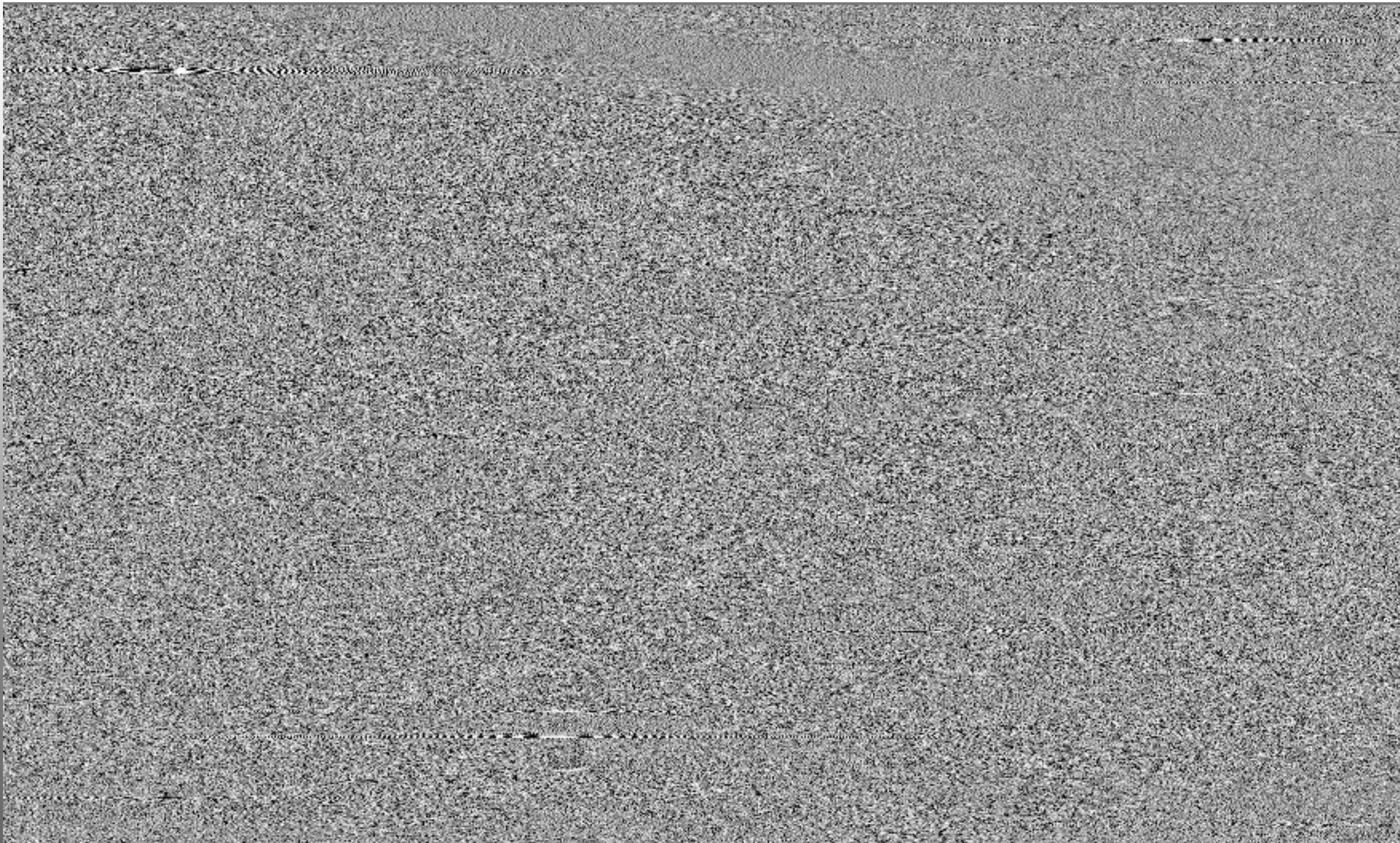

Remote Sensing Technology

Focussed SAR Data

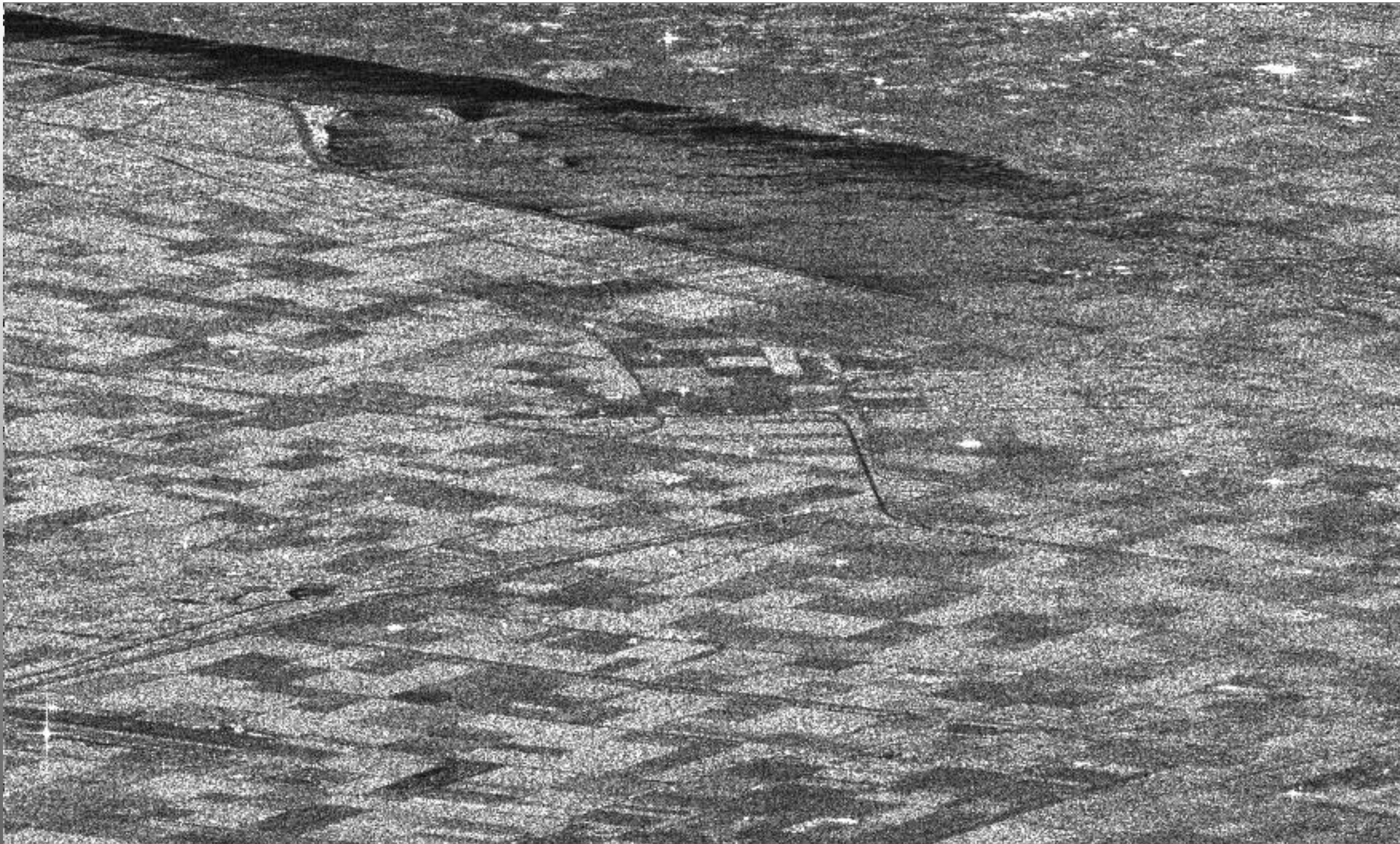

Focussed SAR Data

→ azimuth

data ERS-1 © ESA

after
azimuth pixel averaging by 4
to achieve approximately
square pixels

Point Target Response after Range Compression

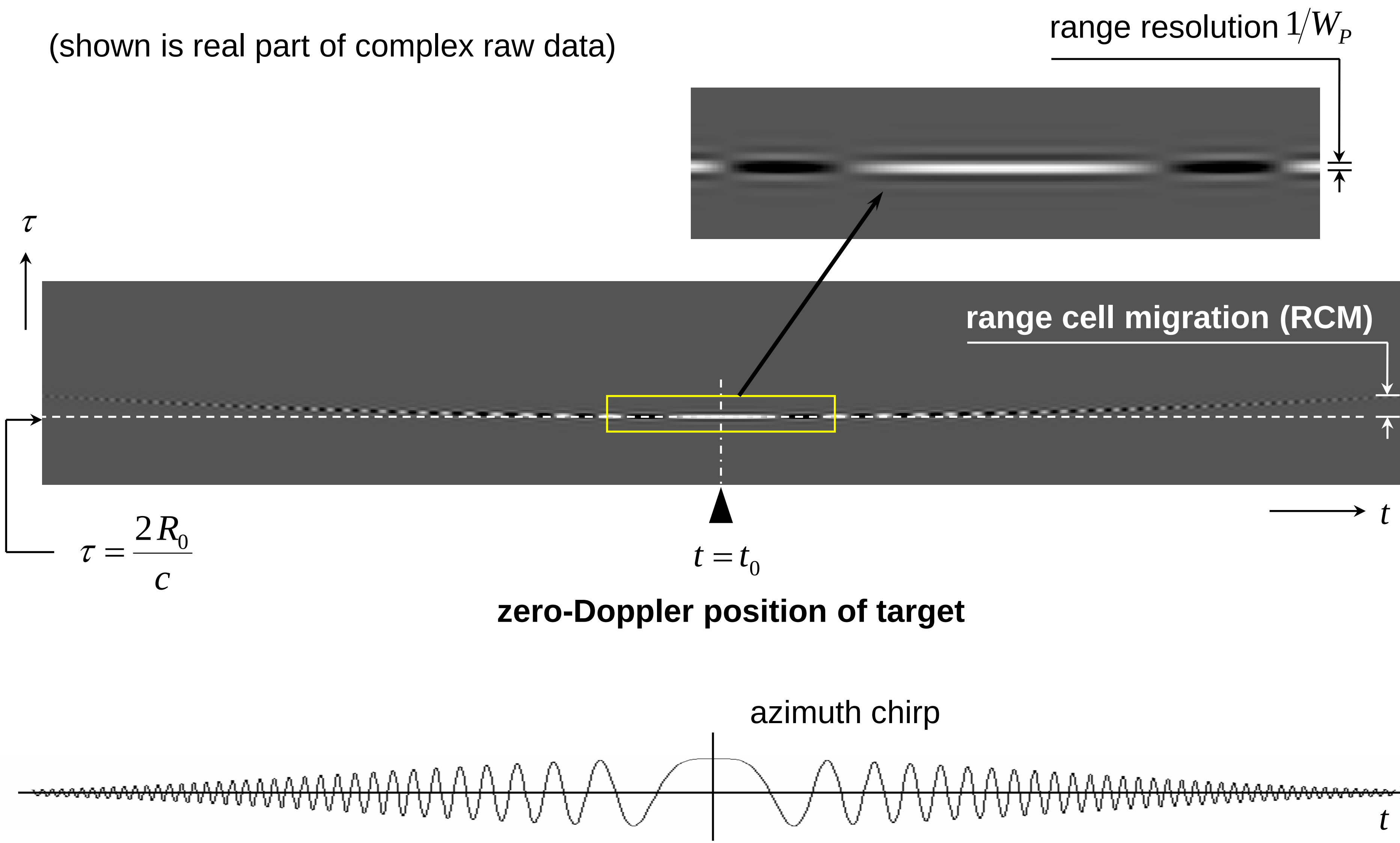

Current and Future Civil Spaceborne SARs

satellite	owner	band	resolution	look angle	swath	lifetime
ERS-1	ESA	C	25 m	23°	100 km	1991-2000
ERS-2	ESA	C	25 m	23°	100 km	1995-2012
Radarsat-1	Canada	C	10 m - 100 m	20°- 59°	50 - 500 km	1995-2013
ENVISAT	ESA	C	25 m - 1 km	15°- 40°	100 - 400 km	2002-2012
ALOS	Japan	L	10 m -100 m	35°- 41°	70 - 360 km	2006-2011
Cosmo	Italy	X	ca. 1 m - 16 m	…	…	2007-
TerraSAR-X & TanDEM-X	Germany	X	1 m - 16 m	15°- 60°	10 - 100 km	2007/2010-
Radarsat-2	Canada	C	3 m - 100 m	15°- 59°	10 - 500 km	2007-
ALOS-2	Japan	L	3 m – 100 m	8°-70°	25 – 350 km	2014?-
Sentinel-1a/b	ESA	C	5 m – 50 m	20°-46°	20 - 400 km	‘14/’16-

ENVISAT

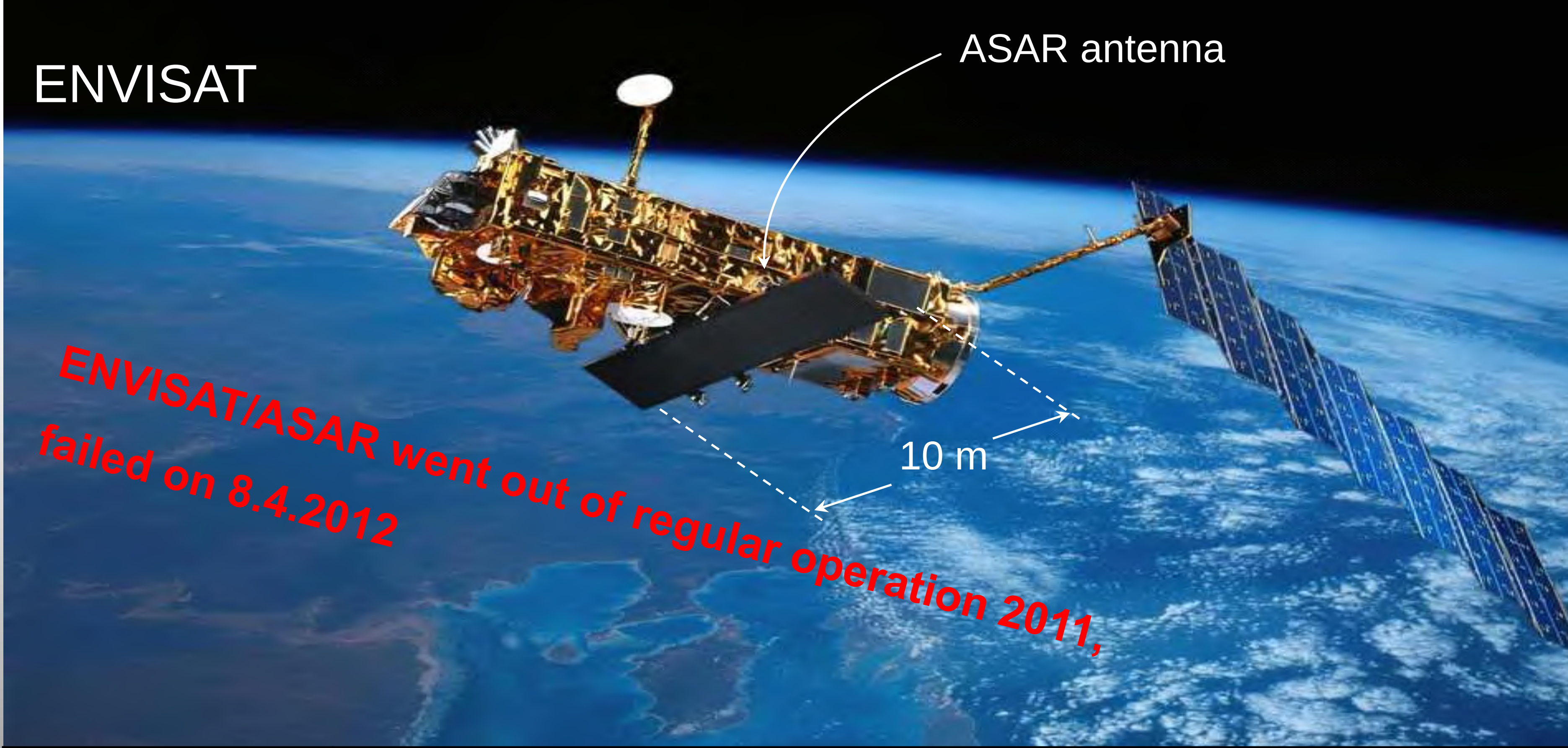

Image Mode (IM)	Spatial resolution of approximately 30 m (for precision product). VV or HH polarisation from any of 7 selectable swaths. Swath width approx. 56-100km.
Alternating Polarisation Mode (AP)	Spatial resolution of approximately 30 m (for precision product). HH/VV, HH/HV, or VV/VH polarisation pairs. Two co-registered images per acquisition, from any of 7 selectable swaths.
Wide Swath Mode (WS)	Spatial resolution of approximately 150 m by 150 m 400 km by 400 km wide swath image. VV or HH polarisation.
Global Monitoring Mode (GM)	Spatial resolution of approximately 1000 m by 1000 m. Up to a full orbit of coverage. HH or VV polarisation.
Wave Mode (WV)	Small imagette (dimensions range between 10 km by 5 km to 5km by 5km), esp. for ocean monitoring. May be positioned anywhere in an Image Mode swath. HH or VV polarisation may be chosen.

ENVISAT – ASAR: St. Petersburg (Rus)

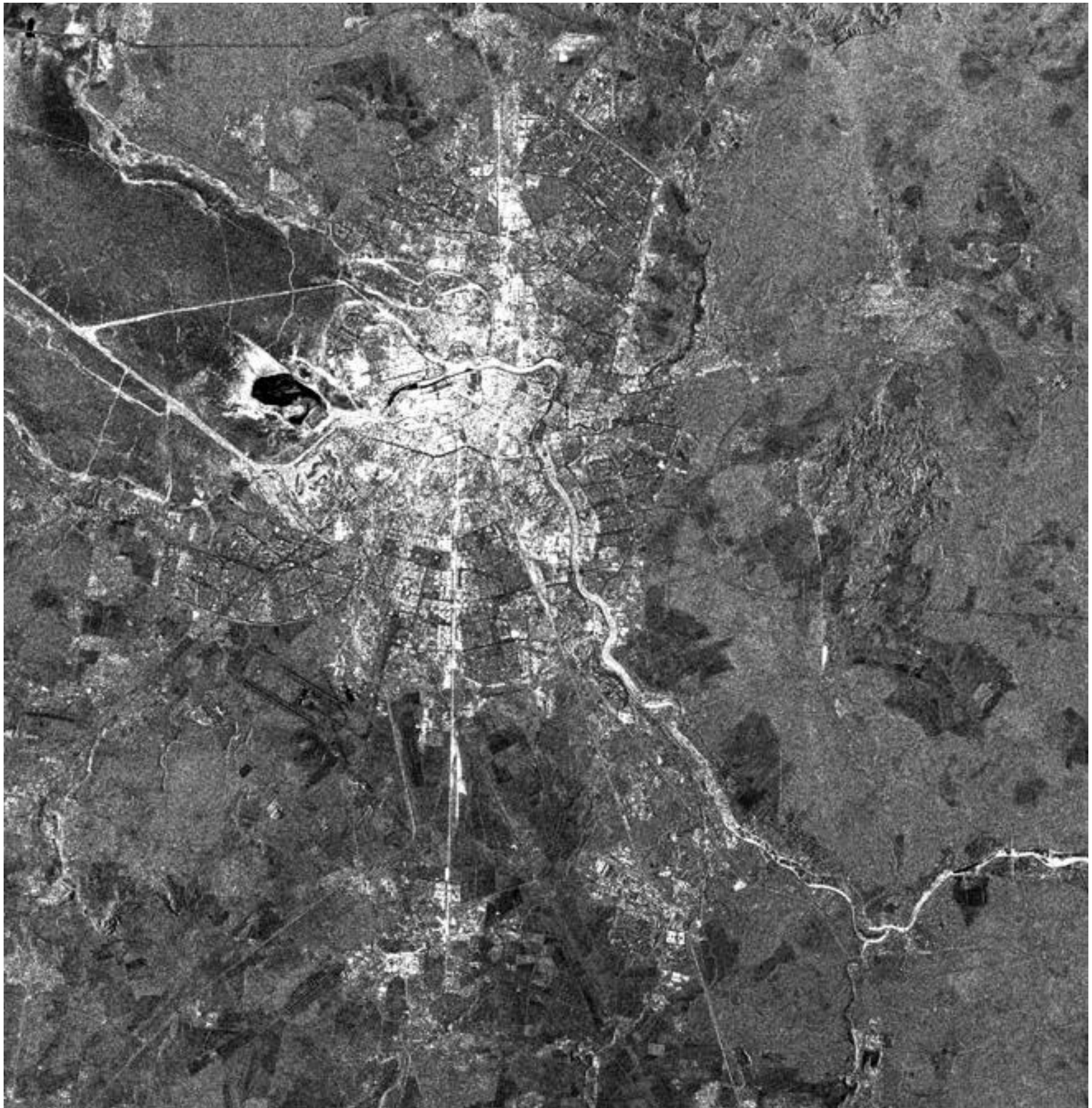

Sentinel-1A

Antarctica Peninsula from Sentinel-1A
Data © ESA

ALOS

ALOS-Satellite: three remote-sensing instruments

PRISM:
3 High-resolution(monochrome) images (also for DEMs)

AVNIR-2:
Multi-band(color) images, capability of pointing

PALSAR:
Cloud-free, Day-and-Night radar sensor

ALOS failed 12.5.2011 followed by ALOS-2

Major Specifications of PALSAR

Observation Mode	High Resolution	SCANSAR
Frequency	L-band (1.27GHz)	
Polarization	HH,VV,HH&HV, VV&VH	HH,VV
Spatial Resolution	10m	100m
Number of Looks	2	8
Swath Width	70km	250x350km
Off-nadir Angle	10 - 51 deg	
NEsigma0	Approx. -23dB	

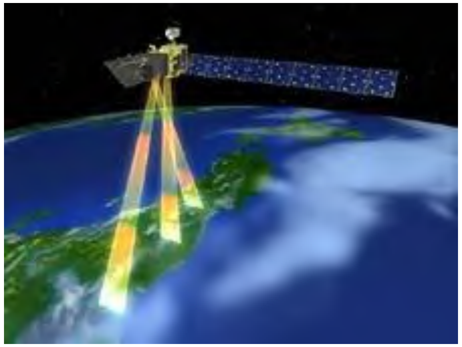

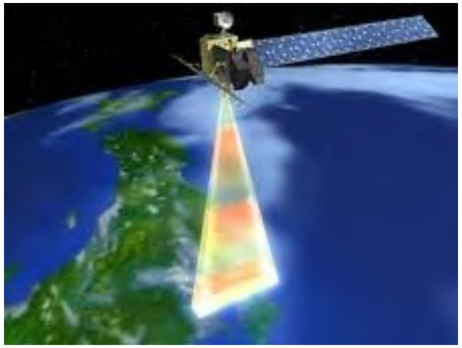

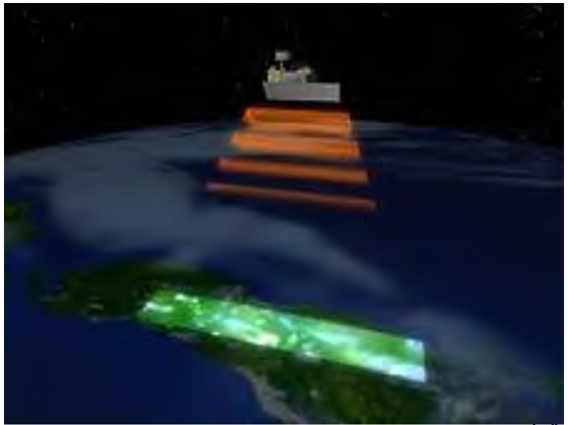

ALOS – PALSAR

500m Browse Mosaic of South America
(FBS/HH Ascending)
for cycle40 (Dec. 16, 2010 ~ Jan. 30, 2011)

→ Forest / biomass mapping

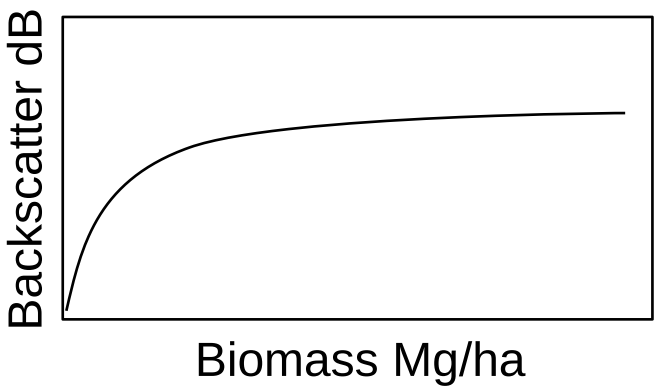

From: http://www.eorc.jaxa.jp/ALOS/en/img_up/mosaic_500_c40.htm

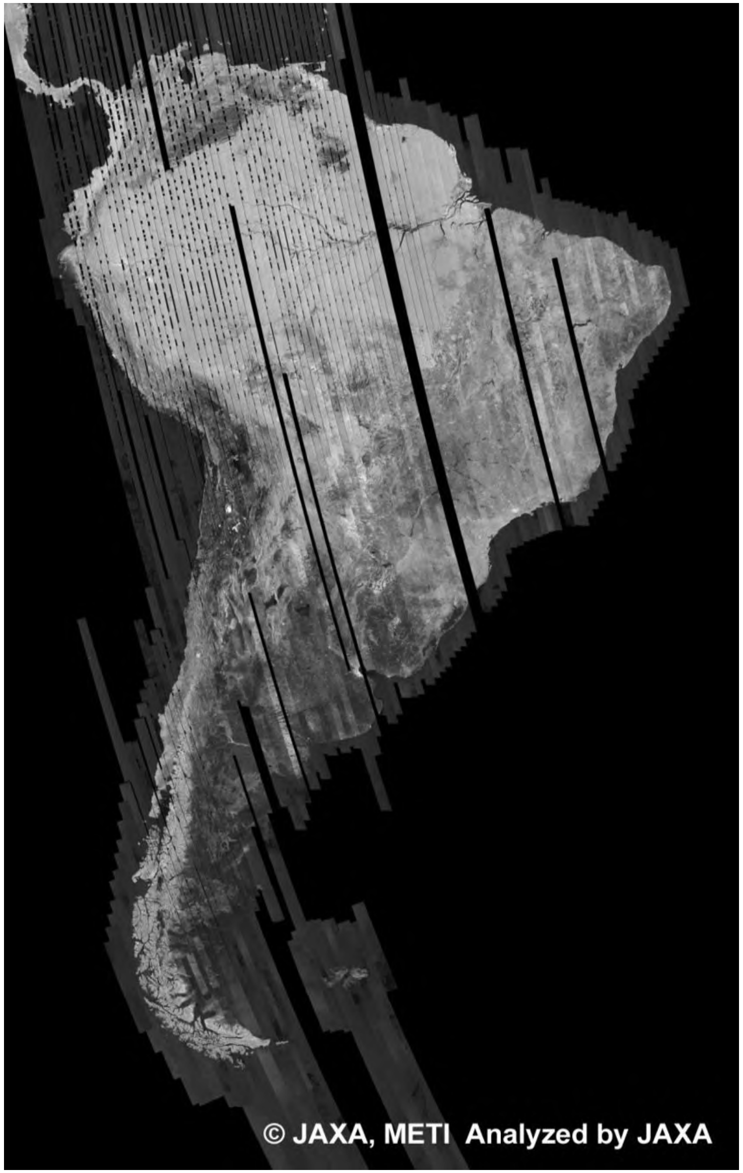

TerraSAR-X Satellite

Satellite
- 514 km altitude
- 11 days repeat orbit
- 800 W average power
- 320 Gbit memory
  (600 s of stripmap data)
- Rollable to left looking

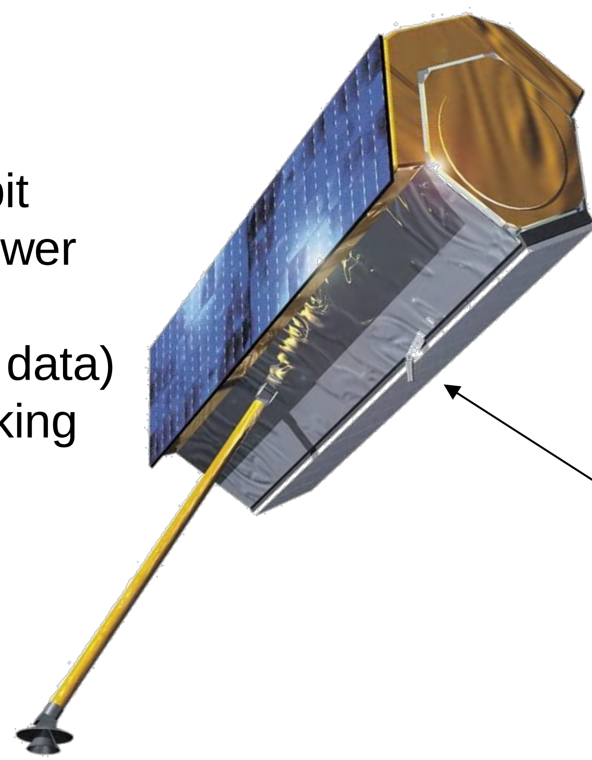

300 MBit/s downlink

Active array SAR antenna
- 384 sub-arrays
- 150 MHz bandwidth (300 MHz)
- right looking
- >100 elevation beams
  - ScanSAR
- > 100 azimuth beams
  - Spotlight
- transmit and receive in H or V
  - Dual polarization
- experimental dual receive antenna & redundant receiver
  - Quad polarization
  - GMTI

Advanced SAR Modes: e.g. TerraSAR-X

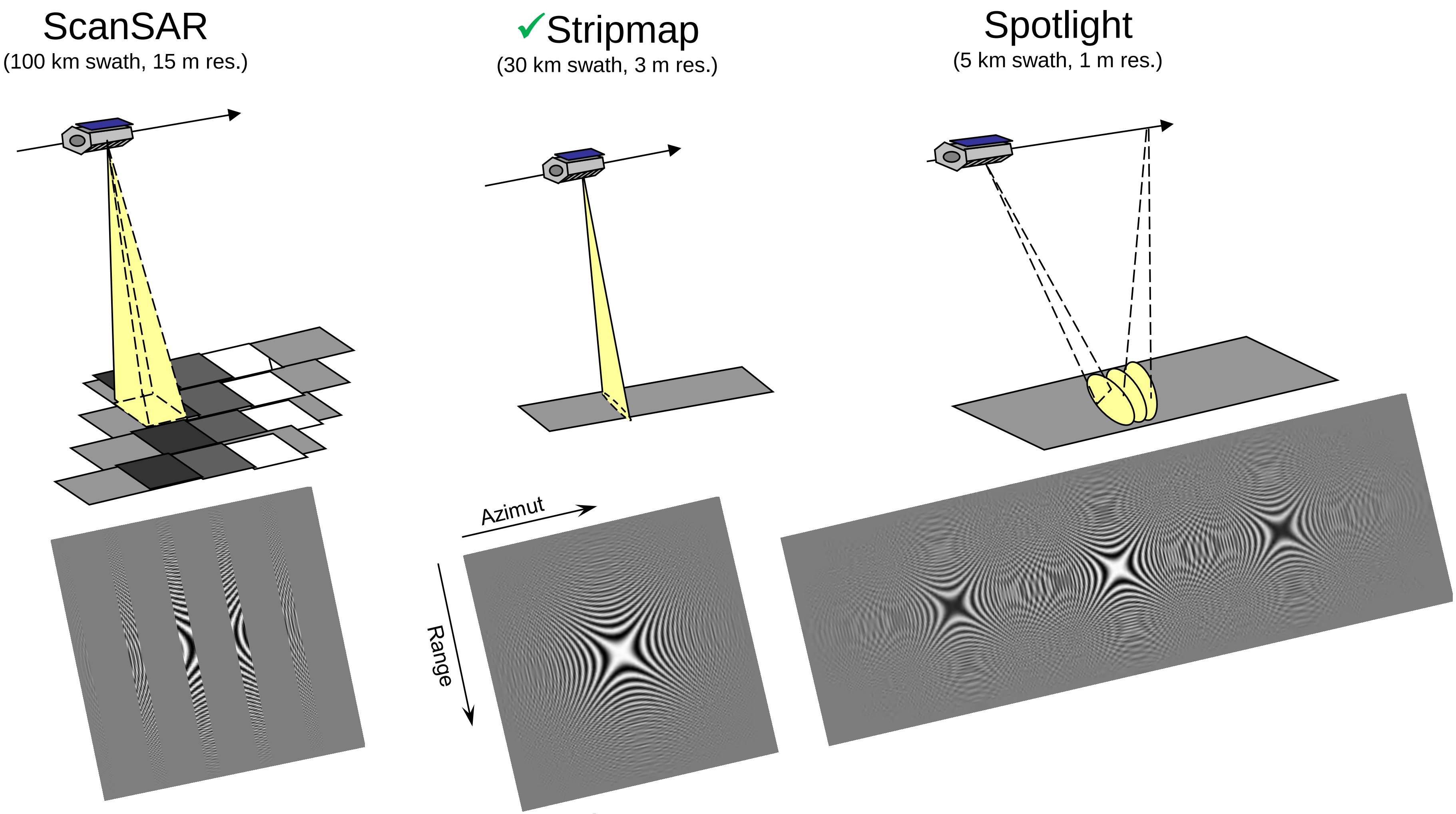

Point target response

ScanSAR Mode

ScanSAR

(100 km swath, 15 m res.)

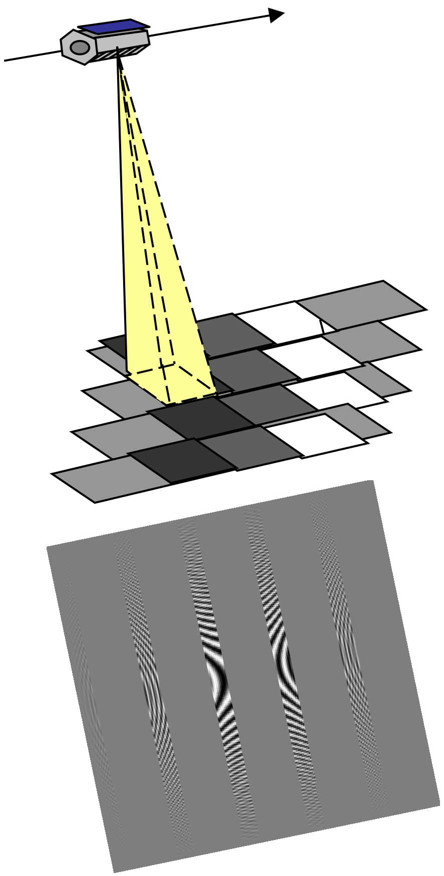

- Periodic switching of antenna elevation look direction:
- Illuminate/receive only part (e.g. ¼) of synthetic aperture with bursts
- Use remaining time to look („Scan“) at other ranges by steering the antenna electronically

→ **+** increased swath width (e.g. × 4)

→ **-** reduced resolution (e.g. ÷ 4)

Spotlight Mode

Spotlight
(5 km swath, 1 m res.)

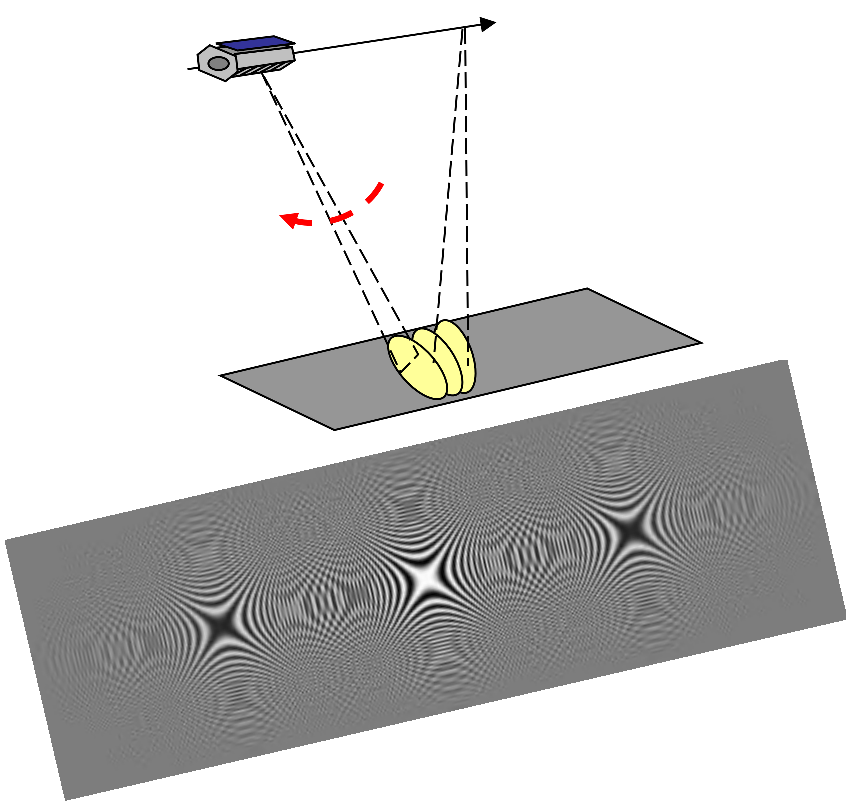

- Increase aperture time by steering the antenna ectronically **backward** in azimuth → longer illumination time, longer chirp
- Higher chirp frequencies & aliasing with PRF need special processing techniques

→ + increased resolution (e.g. × 3)

→ - continuous operation not possible, limited azimuth image size (e.g. 5 km)

TOPS Mode (e.g. Sentinel-1)

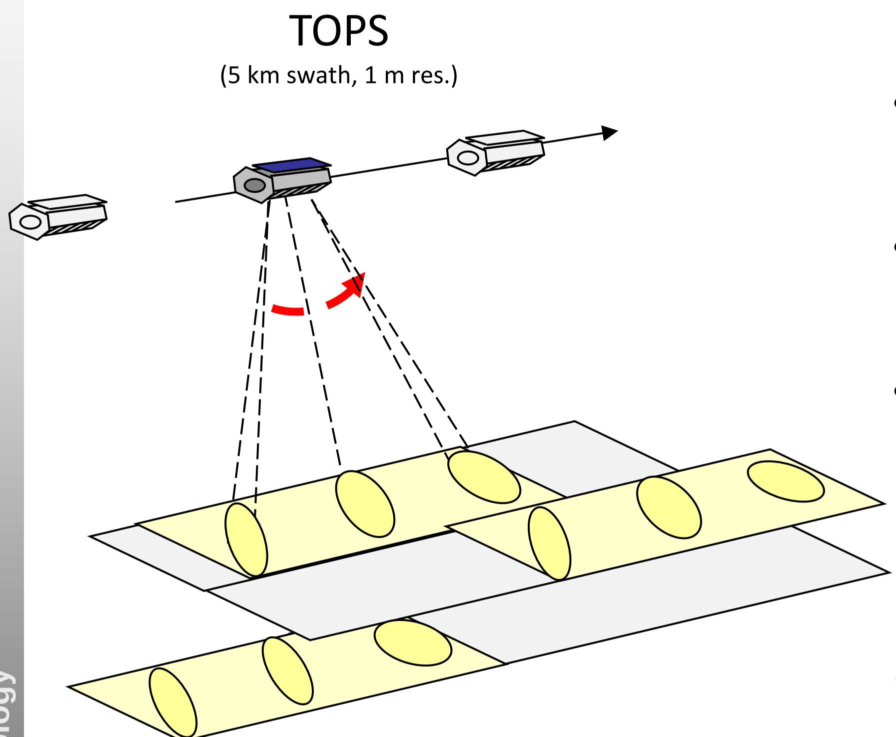

- Reduce aperture time by steering the antenna ectronically **forward** in azimuth
- More azimuth distance, less illumination time per target
- Saved time can be used to electronically steer the antenna to other elevation directions

→increased swath width (e.g. S1: 3 x = 250 km)

→reduced resolution (e.g. S1: 17 m)

Stadtentwicklung Dubai 2007-2008

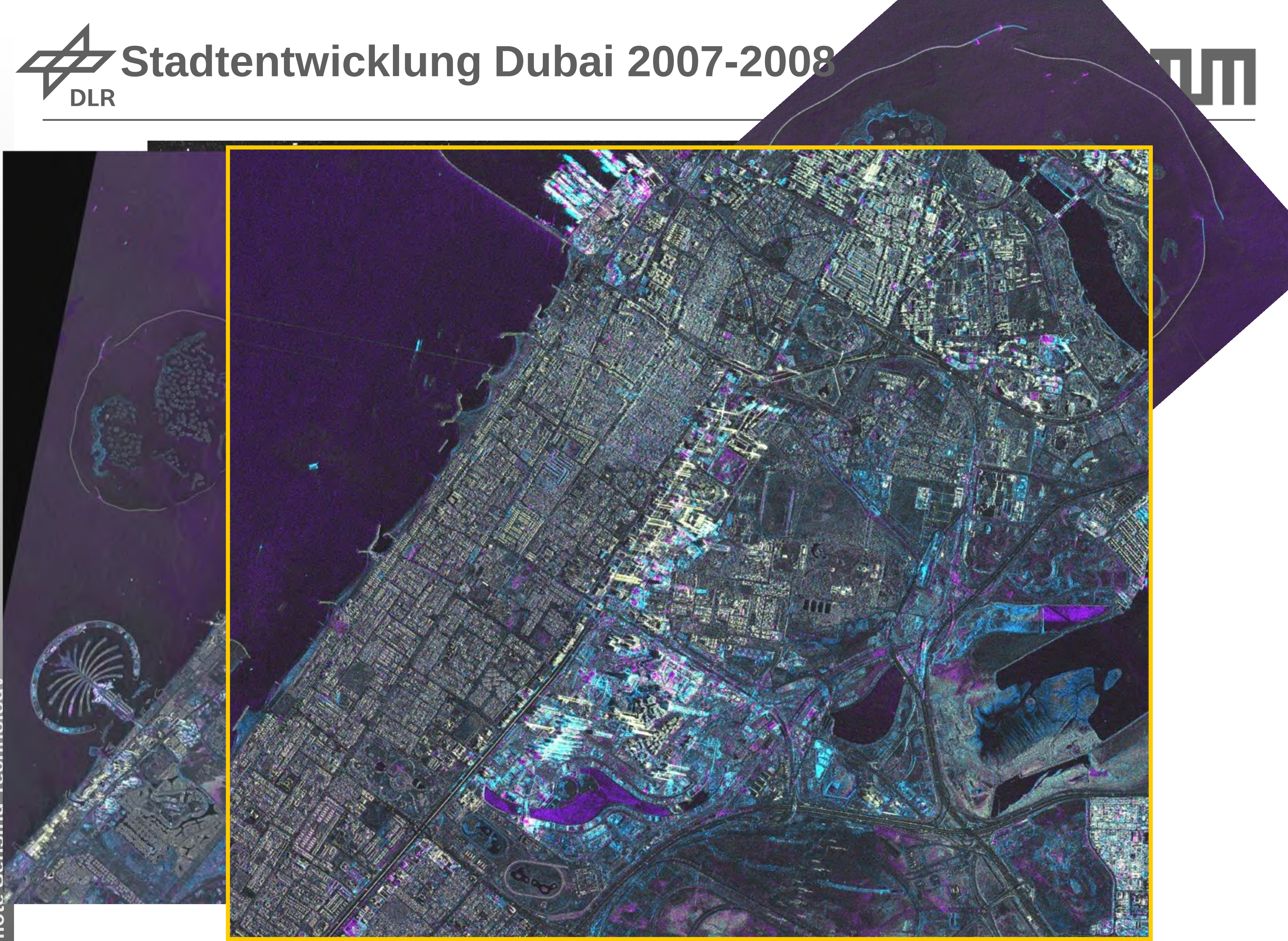

Application: Mapping of Urban Areas

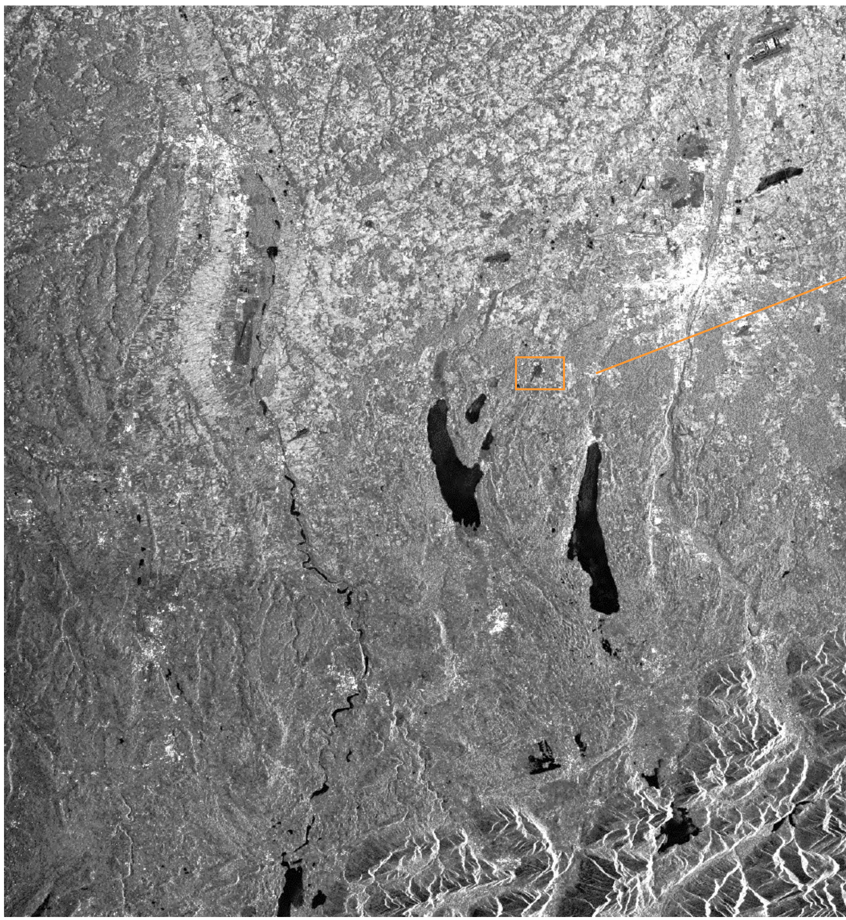

ENVISAT / ASAR IM 2 Oberpfaffenhofen 100 km x 100 km;
25 m resolution (© ESA)

Remote Sensing Technology

Synthetic Aperture Radar (SAR)

SAR Image Characteristics

azimuth

range

ERS-1 data © ESA

Issues:

- resolution (shape of point scatterer response)
- radiometry
- geometry
- polarimetry
- artifacts

SAR Image Point Scatterer Response

point scatterer

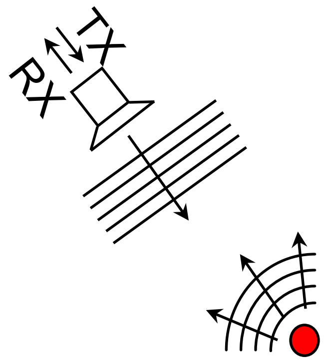

size << $\rho_{x,R}$

SAR image of point scatterer (simulated)

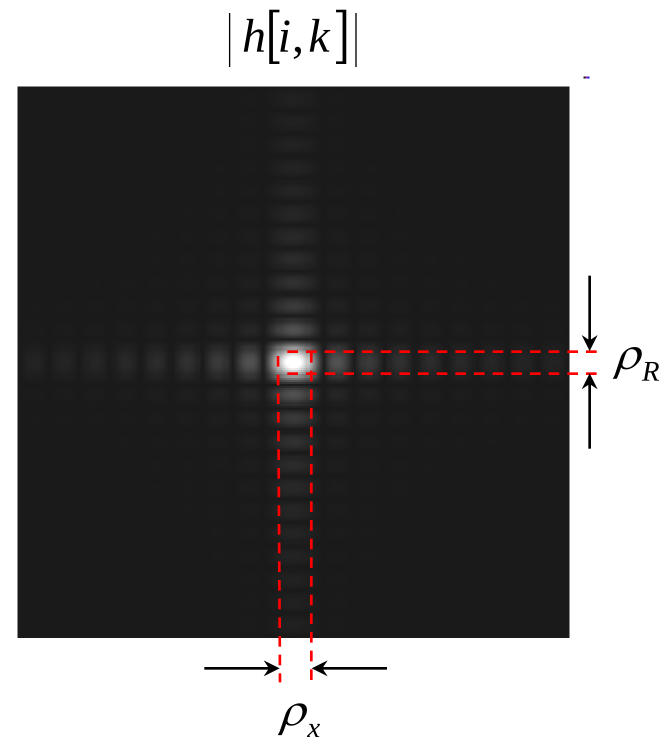

radar cross section: $\sigma \quad [m^2] \quad \text{or} \quad [dBm^2]$

energy: $\Delta x\,\Delta R \times \sum_i \sum_k |h[i,k]|^2 \propto \sigma$

phase at peak: $\phi = -\frac{4\pi}{\lambda} R + \phi_{scat}$

3-D View of Point Response Function

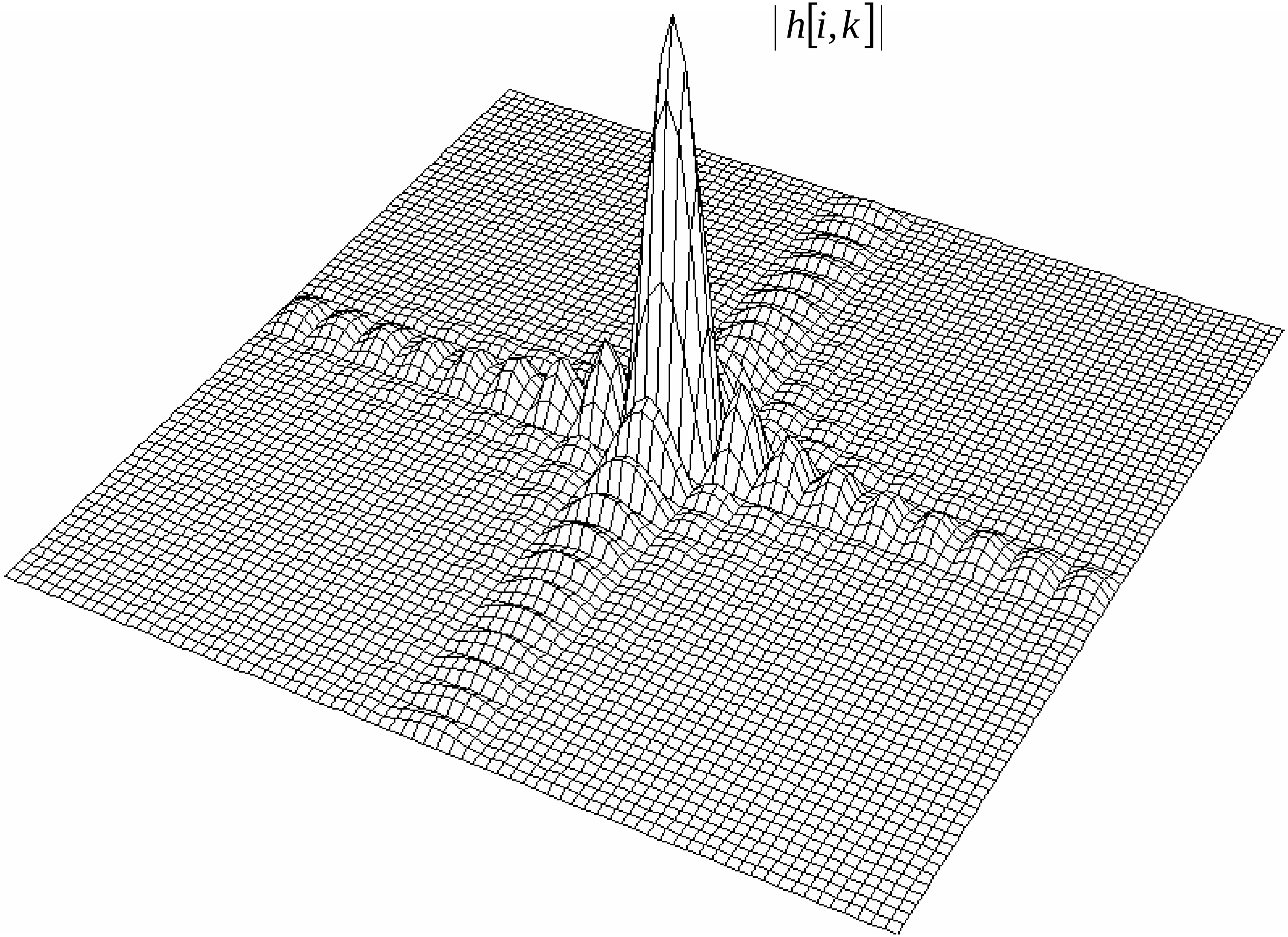

Characteristics of Point Scatterer Response

- resolution = width of mainlobe, often defined as 3dB-width (half power)
- location accuracy
- sidelobe structure:
  - PSLR: peak-sidelobe-ratio
  - ISLR (1-D or 2-D):
    integrated sidelobe-ratio,
    ratio of energy in sidelobes to
    energy in mainlobe
- phase at peak

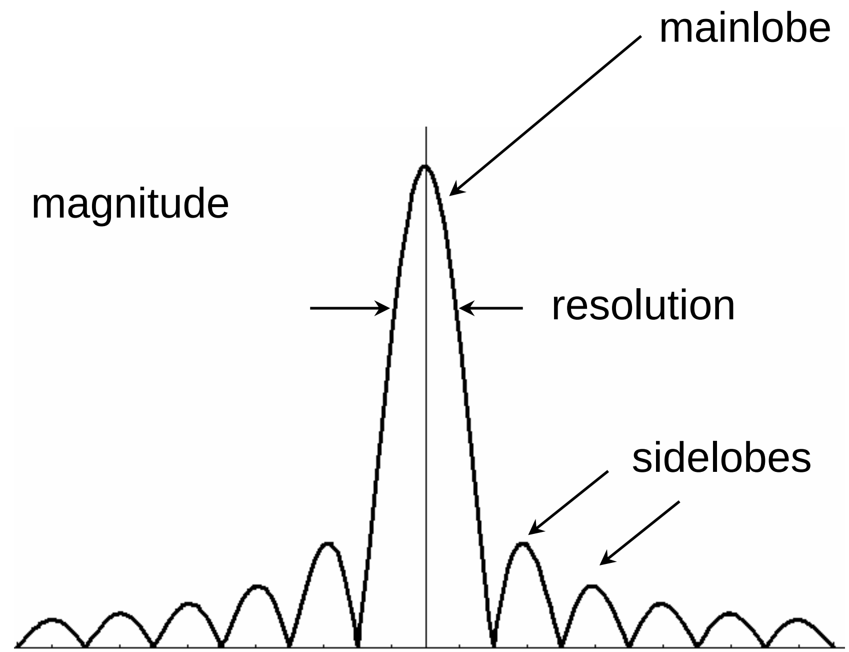

1-D cut through 2-D point response function

Example of a SAR Point Target Analysis Tool

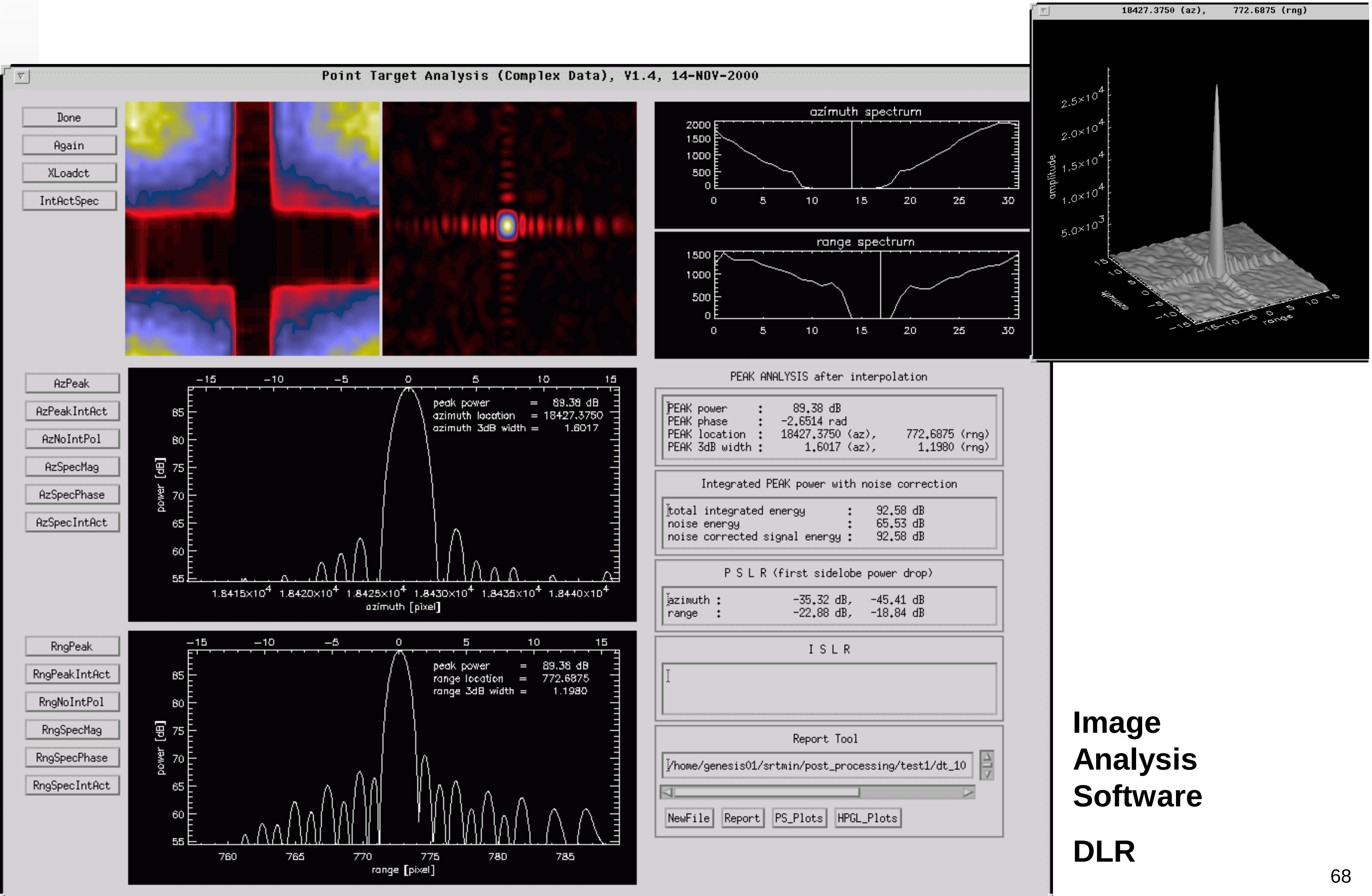

Image Analysis Software

DLR

Radar Cross Section of Single Scatterers

- Metal sphere:

e.g. R=1 m → σ=3.1 m²

$$\sigma = R^2\pi \quad [m^2]$$

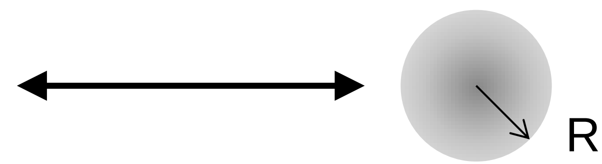

- Corner reflector:

e.g. L=1 m, λ=5.6 cm →σ=74 m²

$$\sigma = \frac{4\pi\, L^4}{3\,\lambda^2} \quad [m^2]$$

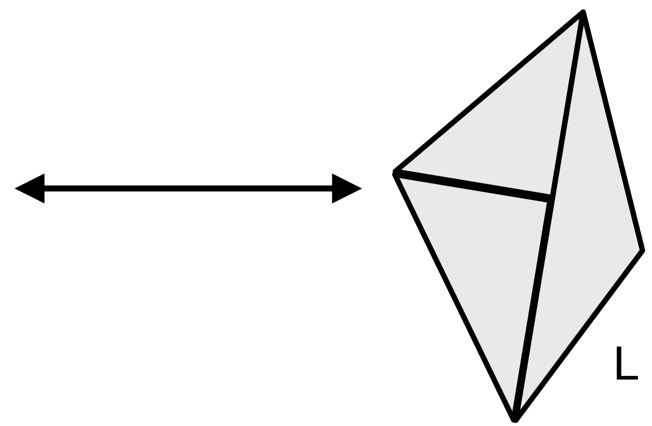

Backscatter of Distributed Objects

- Natural scenes (rough surfaces, vegetation) contain ‘many‘ scatterers in every resolution element (often referred to as “clutter”).
- scatterer <u>density</u> = normalized radar cross section or **backscatter coefficient “sigma naught”**:

$$\sigma^0 = \frac{\sum\limits_{n \in \text{area}} \sigma_n}{\text{area}} \qquad \left[\frac{m^2}{m^2}\right]$$

e.g. cornfield

$\sigma_c^0 = -10dB$

σ_c^0	σ_c^0	σ_c^0	σ_c^0
σ_c^0	σ_c^0	σ_c^0	σ_c^0
σ_c^0	σ_c^0	σ_c^0	σ_c^0
σ_c^0	σ_c^0	σ_c^0	σ_c^0

Resolution cells

Ideal Histogram

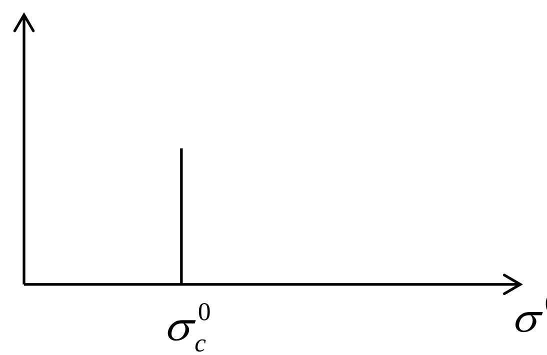

Speckle Effect within Resolution Element

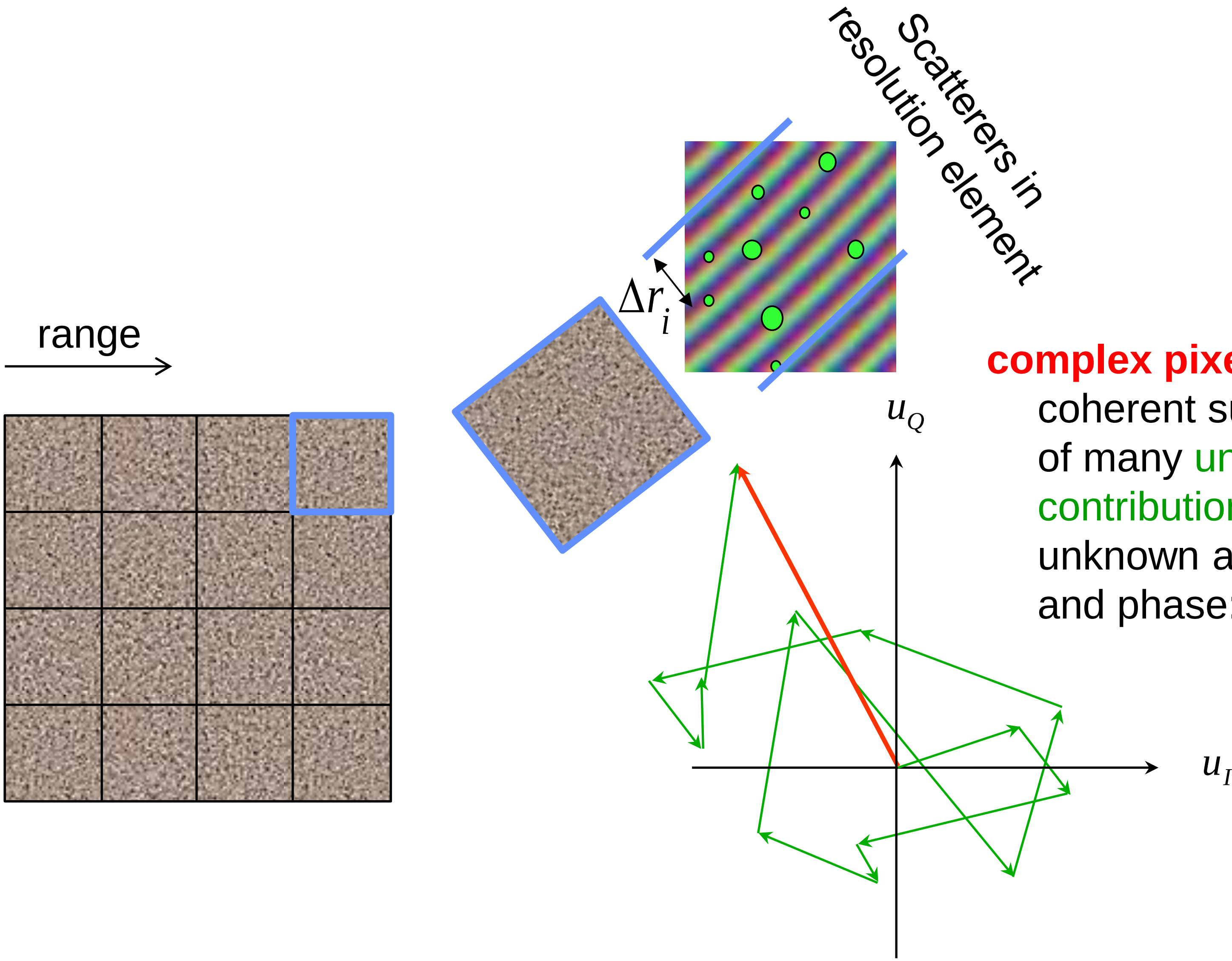

complex pixel value =
coherent summation of many uncorrelated contributions of unknown amplitude and phase:

Speckle Statistics

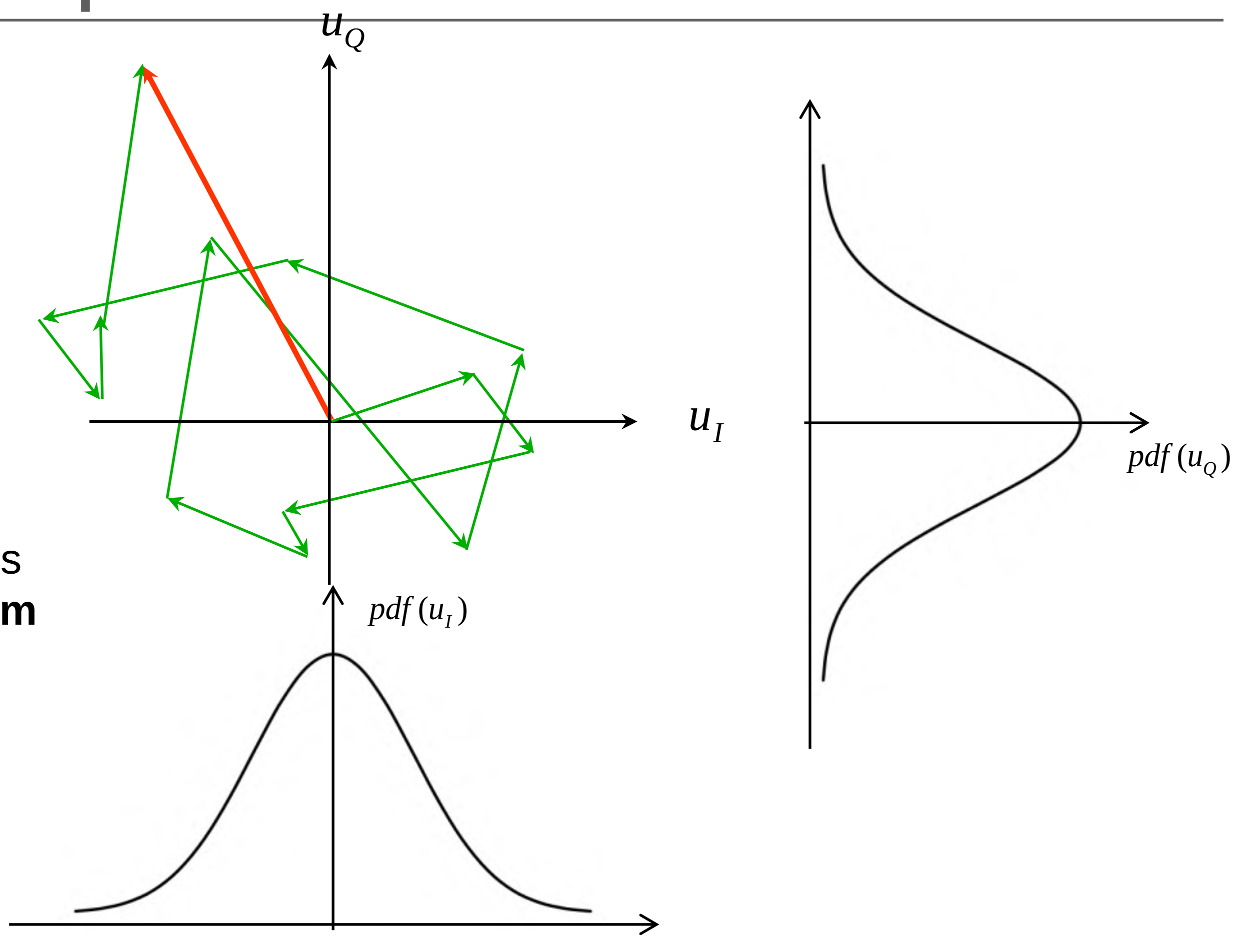

large number of contributions
→**circular Gaussian random process**

- u_I and u_Q are zero-mean mutually uncorrelated Gaussian processes, where (for a given incidence angle):

$$E\left\{u_I^2 + u_Q^2\right\} \propto \sigma^0$$

72

Consequences of Speckle Statistics

Random positive and negative interference of wave contributions from many individual scatterers within one resolution cell →

- varying brightness from pixel to pixel even for constant σ^0

$\Rightarrow$ granular appearance

- random equal distribution of phase:

$$\boxed{\phi_{scatt}} = \arg\left\{ \sum A_i e^{\boxed{-j\frac{4\pi\Delta r_i}{\lambda}}} \right\}$$

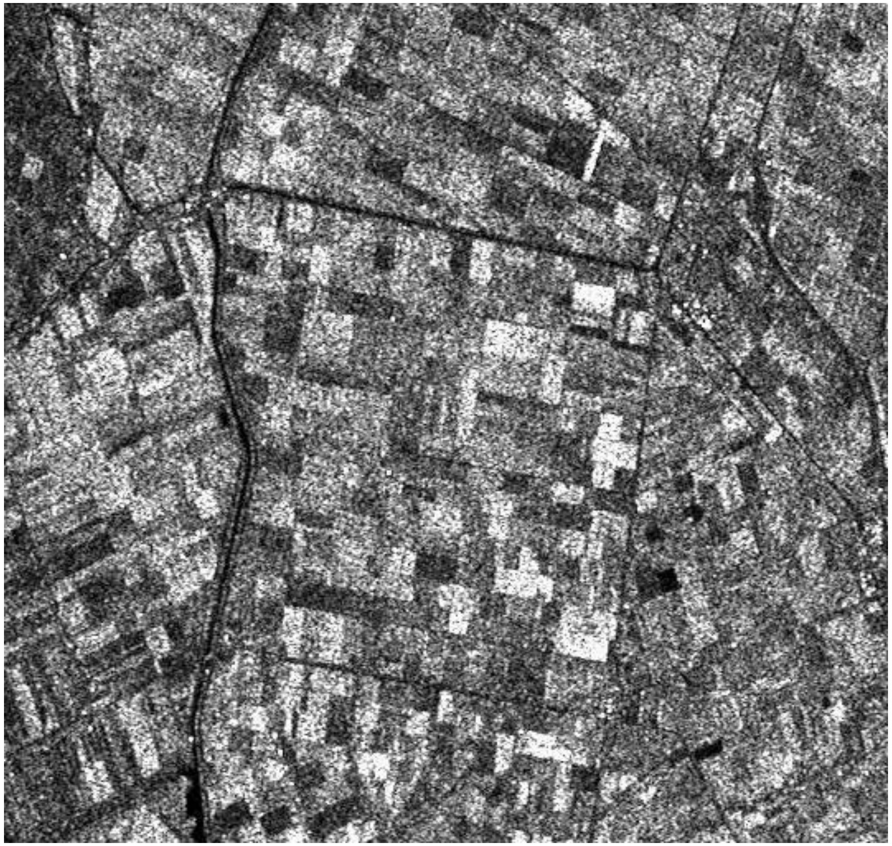

ERS data © ESA

Speckle Intensity Statistics

	magnitude	intensity
quantity ⇨	$\sqrt{u_I^2 + u_Q^2}$	$I = u_I^2 + u_Q^2$
probability distribution ⇨	**Rayleigh**	**exponential**

$$pdf_I\left(I \middle| \sigma^0\right) = \frac{1}{\sigma^0} \exp\left\{-\frac{I}{\sigma^0}\right\}$$

averaging of N_L independent samples (looks)

$$pdf_I\left(I \middle| \sigma^0, N_L\right) = \frac{I^{N_L - 1} {N_L}^{N_L}}{\Gamma(N_L) {\sigma^0}^{N_L}} \exp\left\{-\frac{I N_L}{\sigma^0}\right\}$$

Gamma function $\left(\Gamma(x+1) = x \cdot \Gamma(x)\right)$

$$pdf_I\left(I \middle| \sigma^0, N_L\right)$$

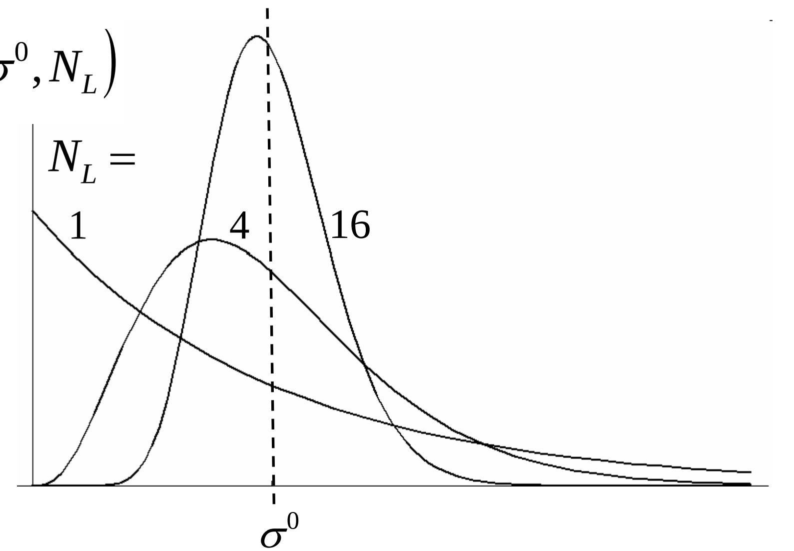

$N_L = 1 \quad \Rightarrow \quad$ standard deviation = mean !

Speckle Reduction

- speckle “masks” underlying σ^0-image
- speckle reduction = estimation of σ^0
  - $\Rightarrow$ assumptions (models) about the structure of σ^0 are required to separate it from speckle (Maximum A Posteriori estimation: MAP)
- optimum speckle reduction for simple model: σ^0 = const.:
  - averaging of adjacent pixels (box filter) or **multi-looking** $\Rightarrow$ **loss of resolution**
- more complex models (try to limit resolution degradation):
  - σ^0 Γ-distributed $\Rightarrow$ Gamma-Gamma-MAP filter
  - Gibbs random fields for describing textures
  - heuristic smoothness criteria $\Rightarrow$ e.g. wavelet denoising
  - full Bayesian approach allows for automatic selection between models of different complexity

Speckle Reduction by Temporal Multilooking (ERS)

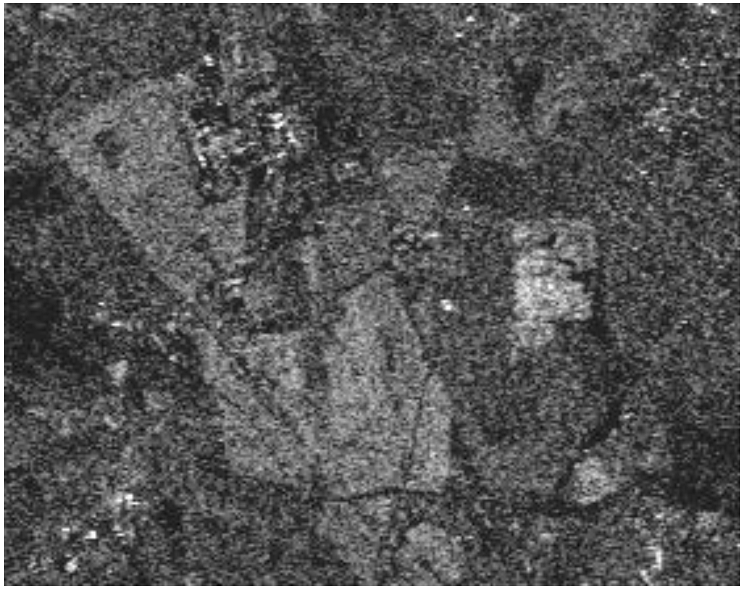

L=5 looks
20 x 20 m ground resolution
2 dB radiometric resolution

L=320 looks
20 x 20 m ground resolution
0.3 dB radiometric resolution

Adaptive Speckle Reduction

Example for Bayesian method. Others are *Lee* or *Frost* filter.

original SAR image
SAR data © AeroSensing GmbH

speckle filtered
Bayesian algorithm

SAR Polarimetry (I)

- (1) Sensor transmits horizontally (H) polarized pulse
- (2) H-Pulse is scattered and polarization angle may change
- (3) Sensor receives horizontal and vertical echo components in 2 channels → scattering vector

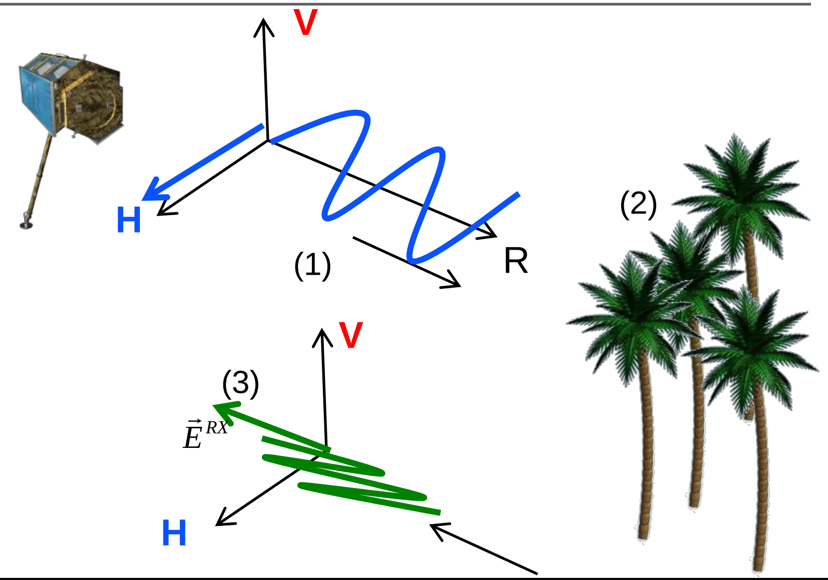

- (4) Sensor transmits vertically (V) polarized pulse
- (5) V-Pulse is scattered and polarization may change
- (6) Sensor receives horizontal and vertical echo components in 2 channels → scattering vector

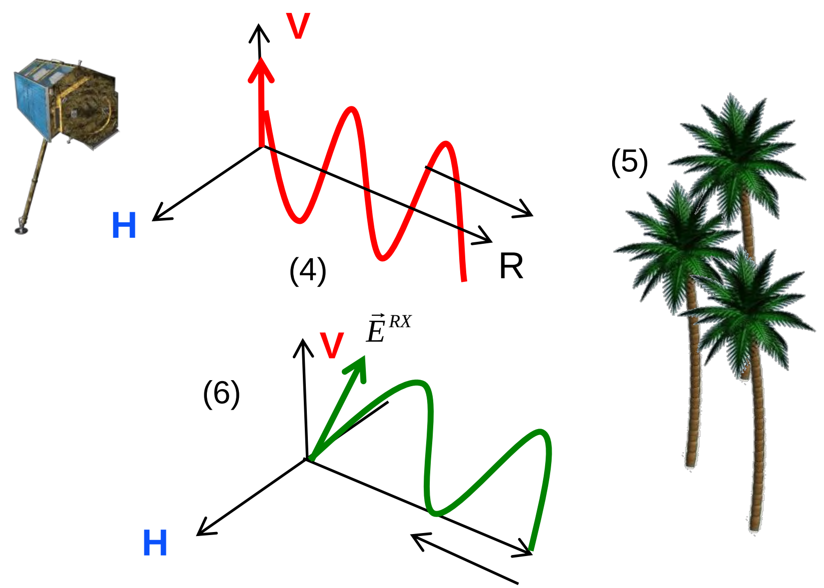

SAR Polarimetry (II)

- **Result: 2 x 2 scattering matrix [S]**

$$\begin{bmatrix} E_H^{RX} \\ E_V^{RX} \end{bmatrix} = \begin{bmatrix} S_{HH} & S_{HV} \\ S_{VH} & S_{VV} \end{bmatrix} \begin{bmatrix} E_H^{TX} \\ E_V^{TX} \end{bmatrix}$$

- **Describes polarimetric signature of scattering object**

- **Examples:**
  - **Single reflection on metallic plate (or odd number of reflections)**

$$S = \begin{bmatrix} 1 & 0 \\ 0 & 1 \end{bmatrix}$$

  - **Random scattering of vegetation**

$$S = \begin{bmatrix} a & b \\ b & d \end{bmatrix}$$

Calibration of SAR Systems

Instrument parameters to be calibrated:

- transmit power
- receiver gain
- elevation antenna pattern (roll angle !)

Calibration objects:

- corner reflectors
- active radar calibrators (ARCs)
- rain forest

Heavy Clouds and Rain Cells in X-Band SAR Images

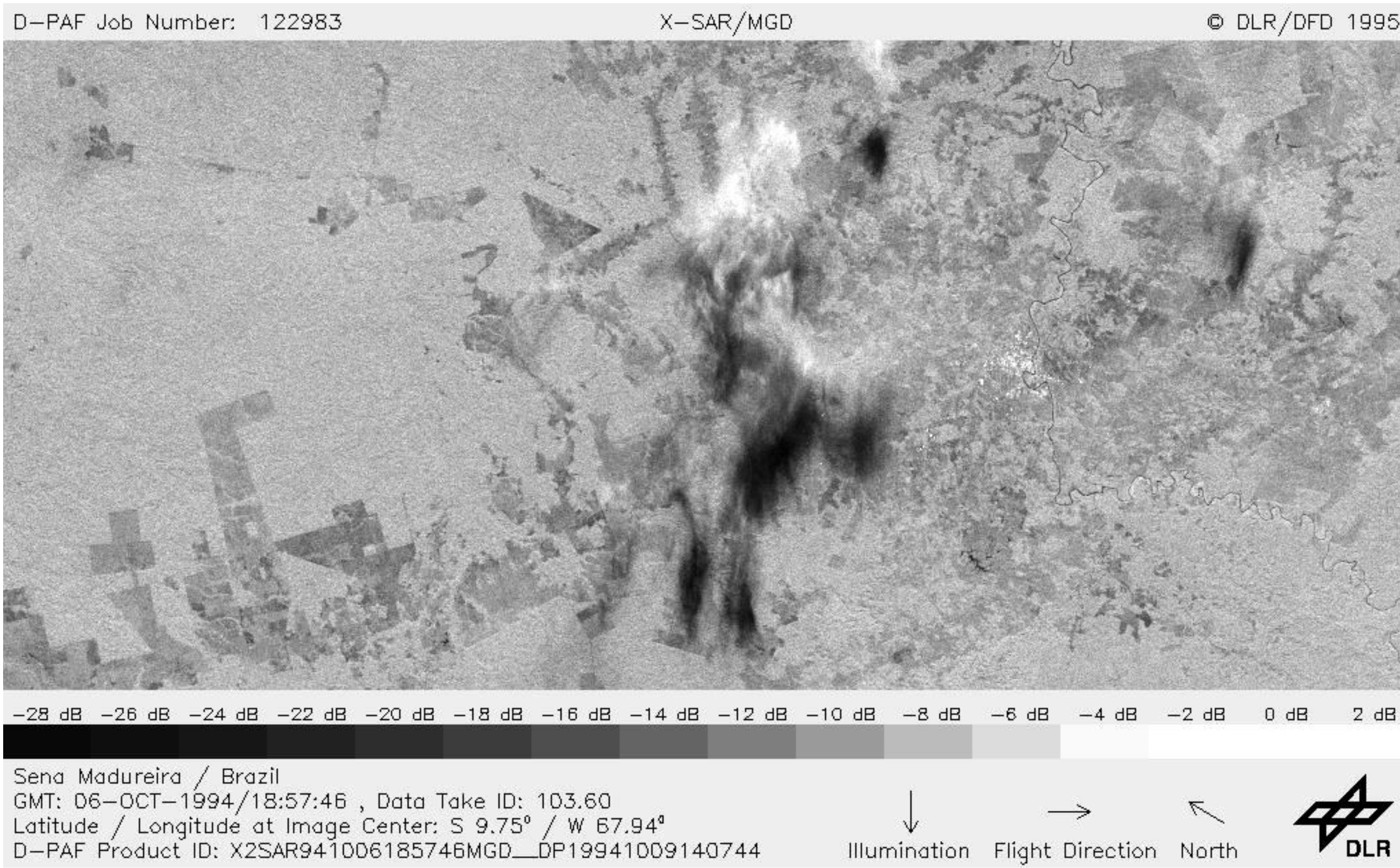

Remote Sensing Technology

Penetration of Microwaves

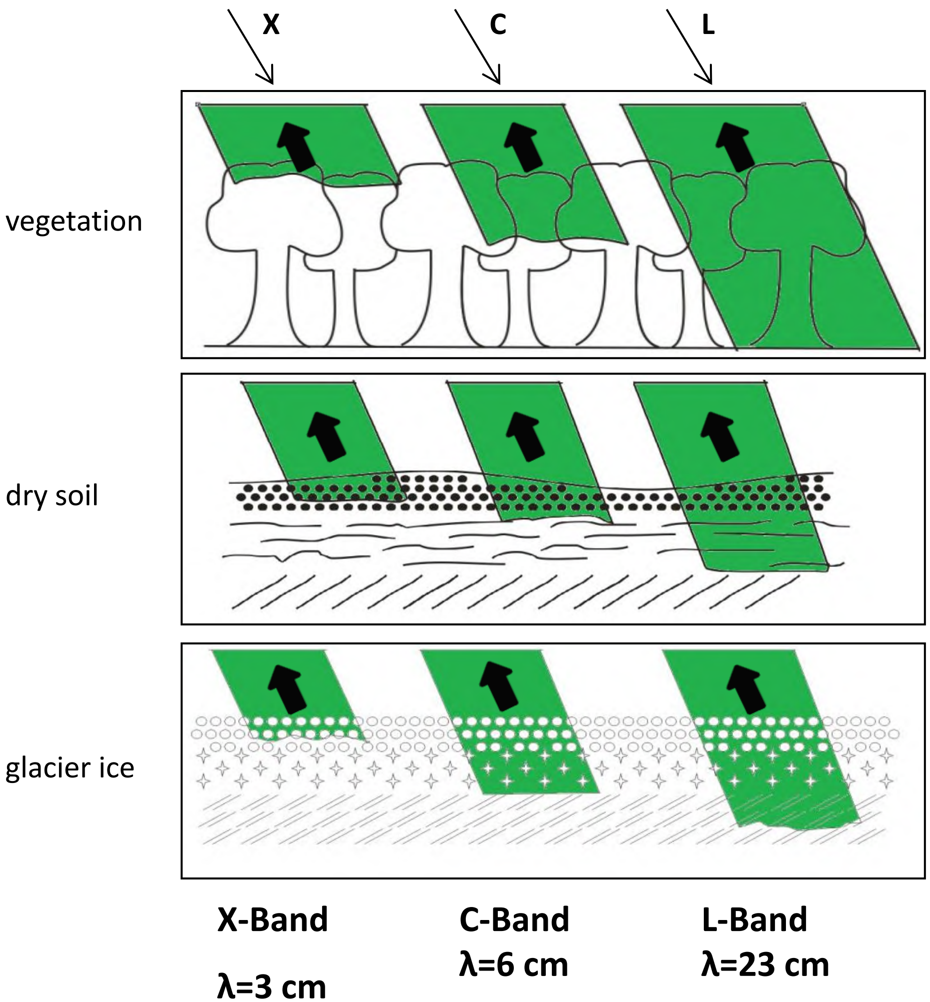

Scattering Mechanisms in Forests

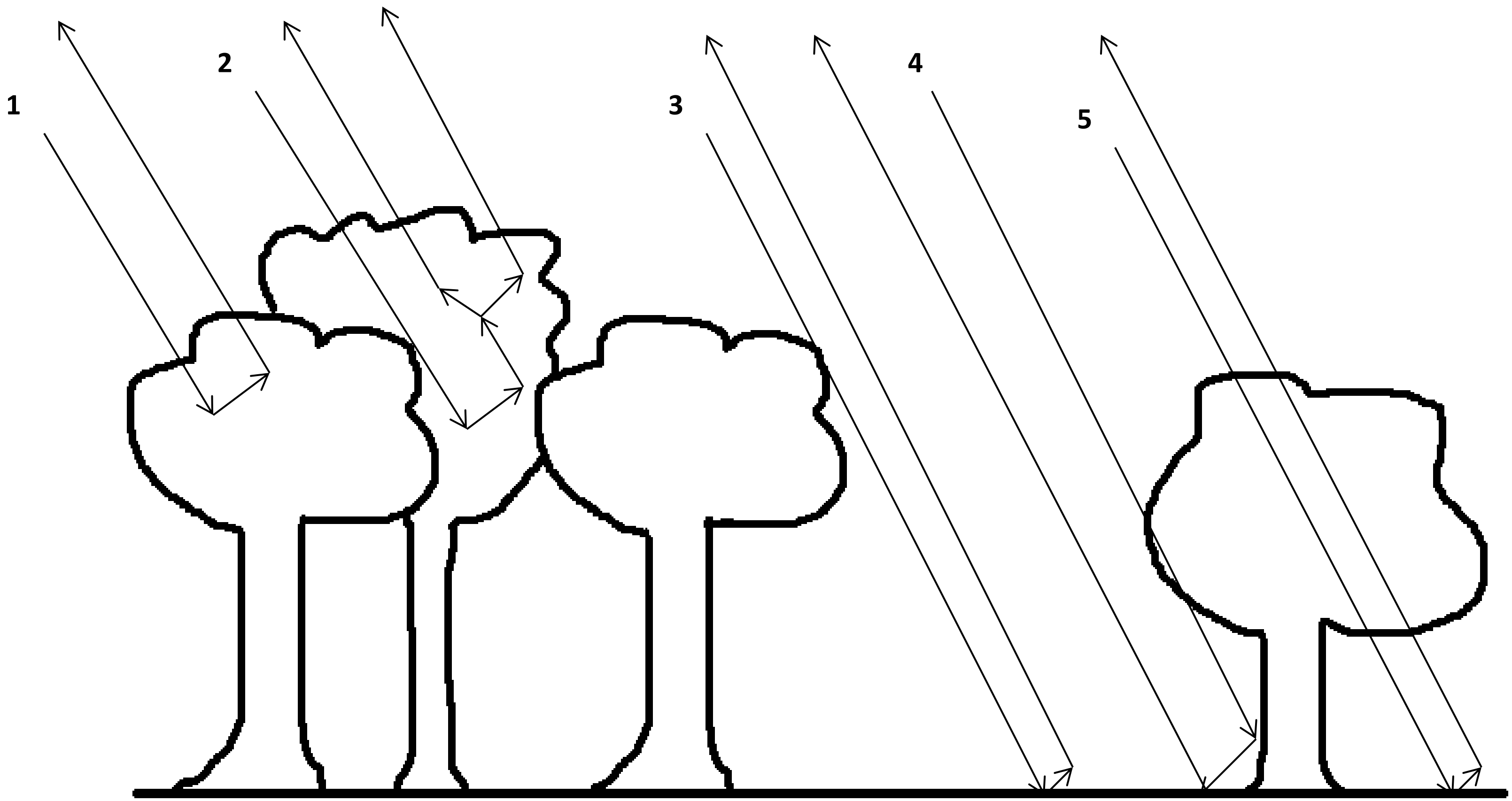

1: direct single scatter

2: multiple bounce

3: direct ground reflection

4: double bounce trunk - ground

5: attentuation of ground scatter by canopy

Synthetic Aperture Radar (SAR)

Geometry of SAR Images - Range-Doppler Equations

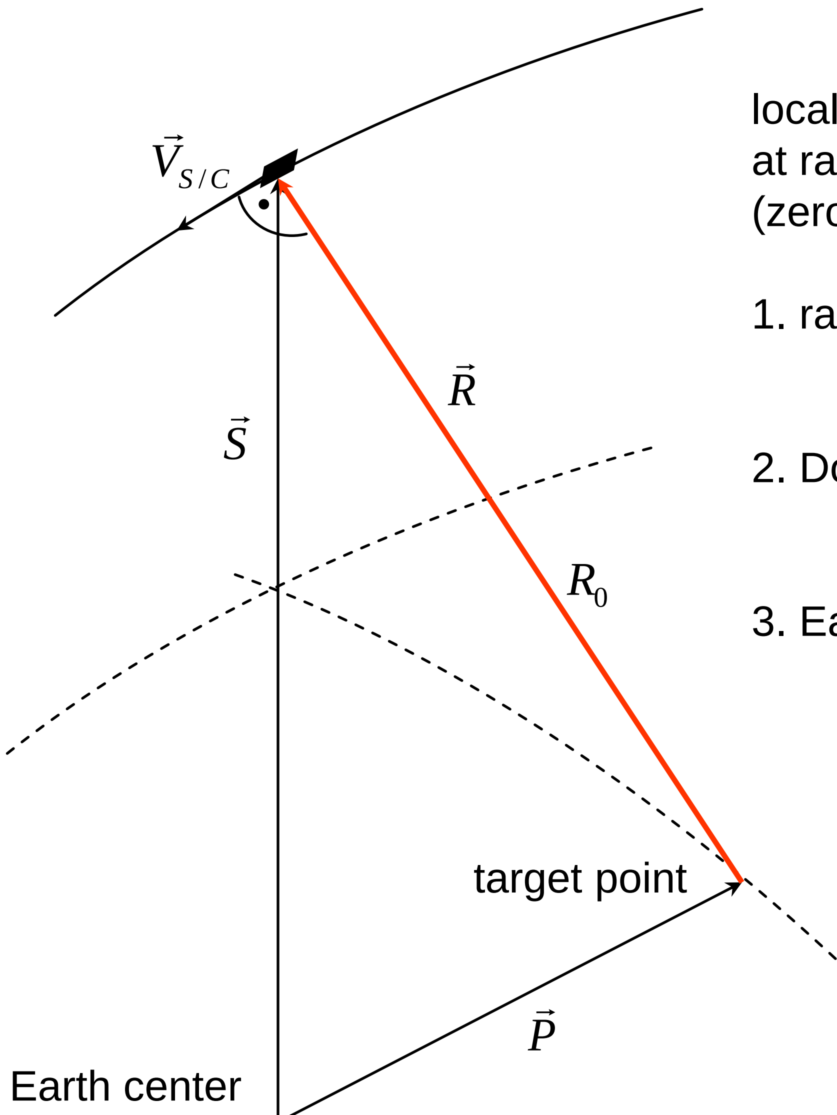

localization of a point $\vec{P}$ from a SAR image
at range R_0 and azimuth t_0 with satellite position $\vec{S}(t_0)$
(zero-Doppler image geometry assumed):

1. range equation: $\left|\vec{S}-\vec{P}\right| = \left|\vec{R}\right| = R_0$

2. Doppler equation: $\left(\vec{S}-\vec{P}\right)\cdot\left(\dot{\vec{S}}-\dot{\vec{P}}\right) = 0$

3. Earth equation: $\left|\vec{P}\right| = \text{local Earth radius}$

in Earth fixed co-ordinates: $\dot{\vec{S}}-\dot{\vec{P}} = \dot{\vec{S}} = \vec{V}_{S/C}$

Geometry of SAR Images - Radar Co-ordinates

for SAR images processed to 'zero-Doppler' geometry: $\begin{pmatrix} x \\ y \\ z \end{pmatrix} \rightarrow \begin{pmatrix} x \\ R \end{pmatrix}$

where $R = \sqrt{(y_0 + y)^2 + (H - z)^2}$

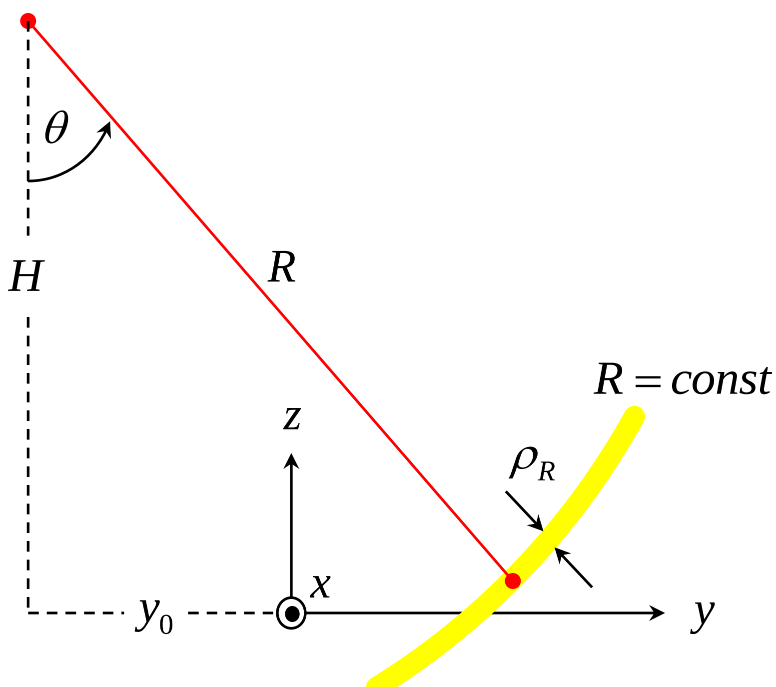

Geometry of SAR Images - Foreshortening

= geometric distortions of slopes from ground to "slant range"

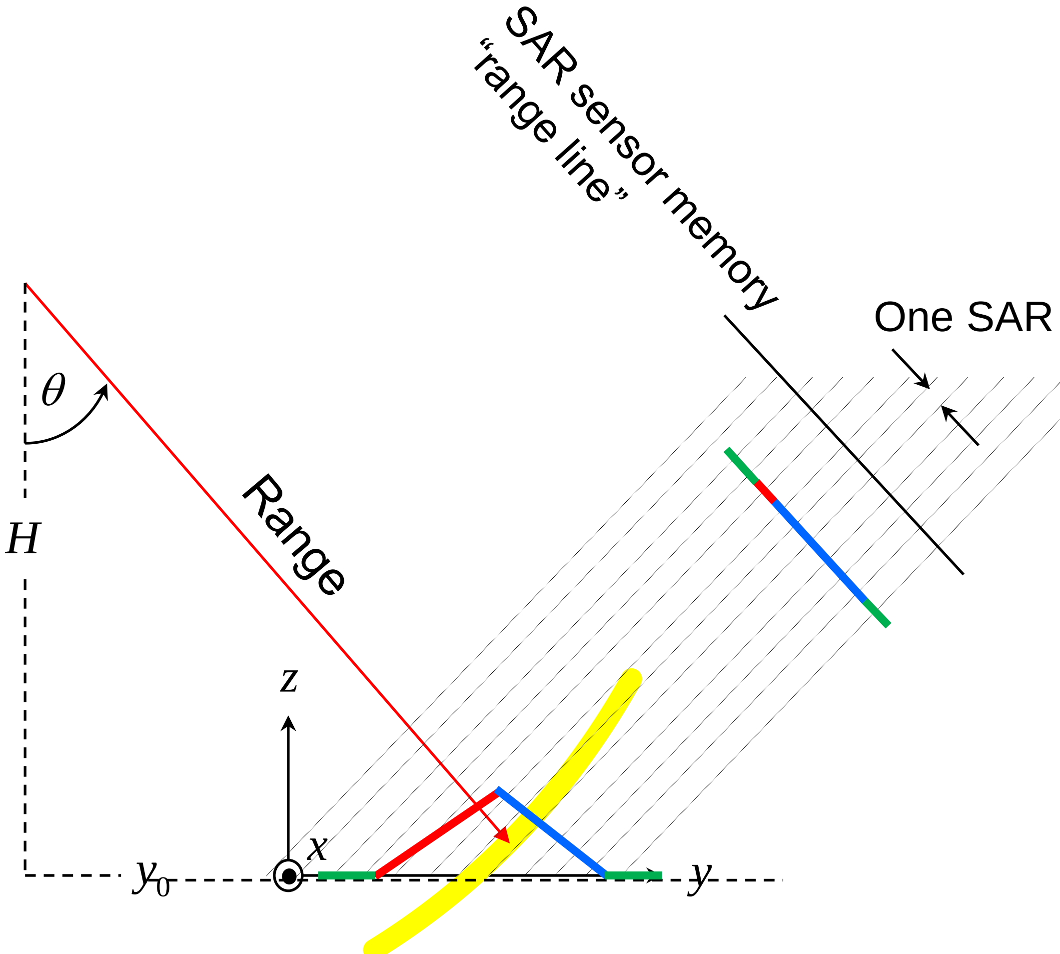

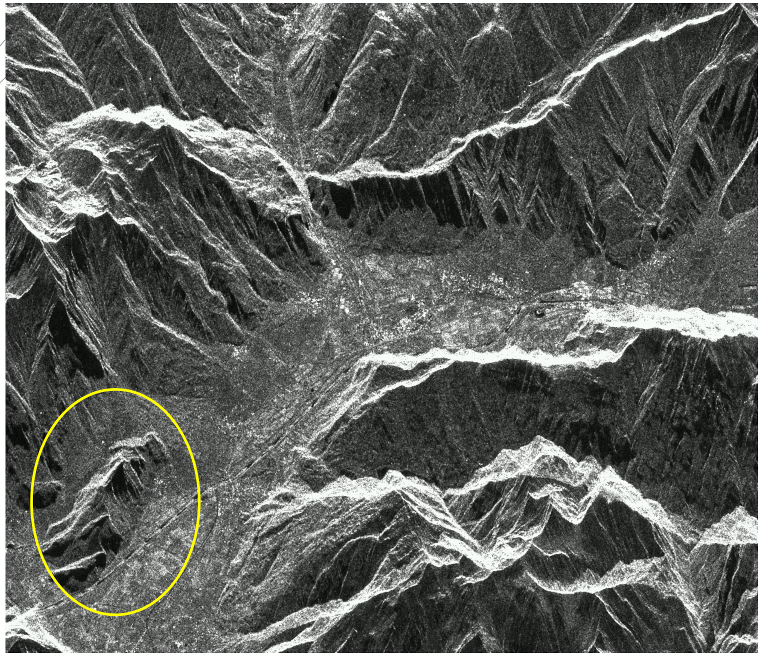

$\theta = 23\,\mathrm{deg}$ ERS-1

Geometry of SAR Images - Layover

= overlay of multiple areas from ground to slant range

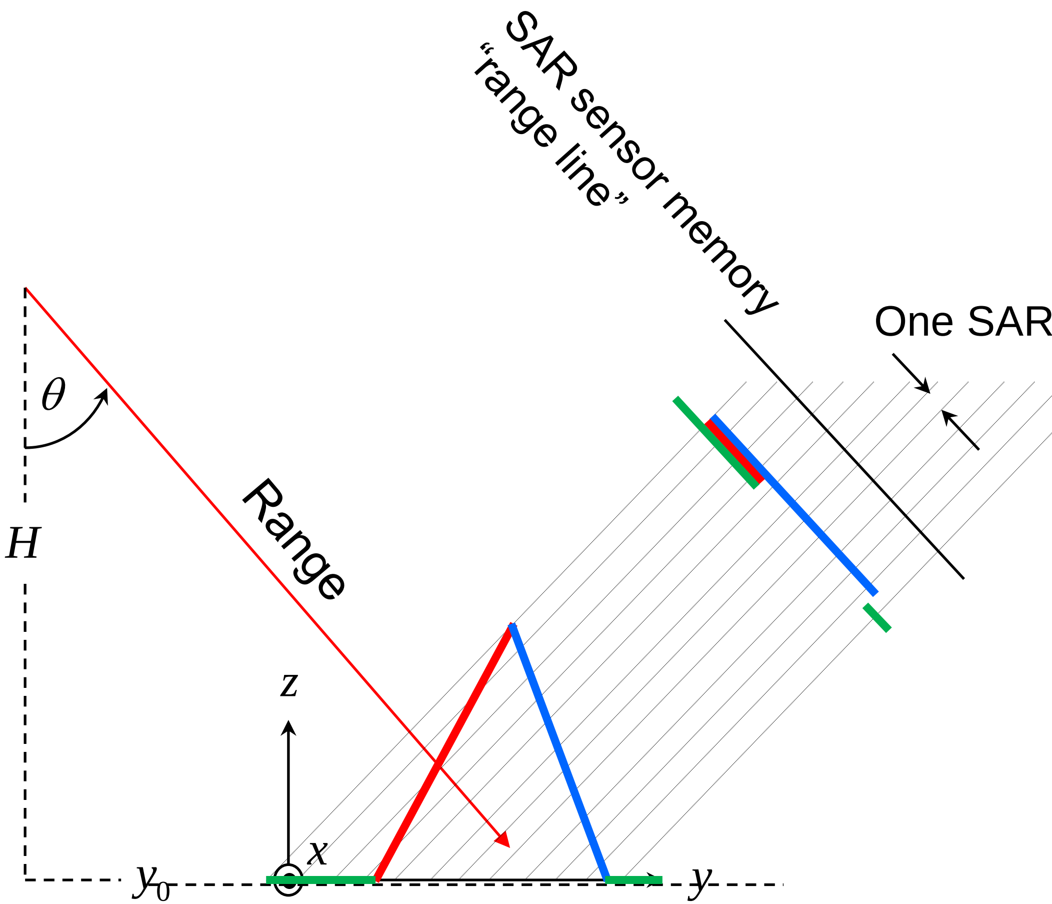

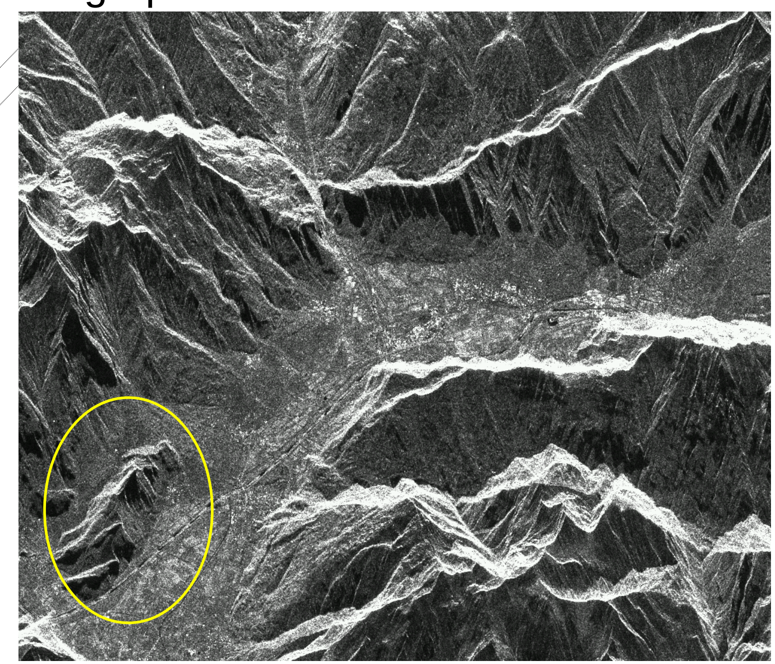

$\theta = 23\,\mathrm{deg}$ ERS-1

Geometry of SAR Images - Shadow

= no reflection from back-slopes not illuminated by SAR

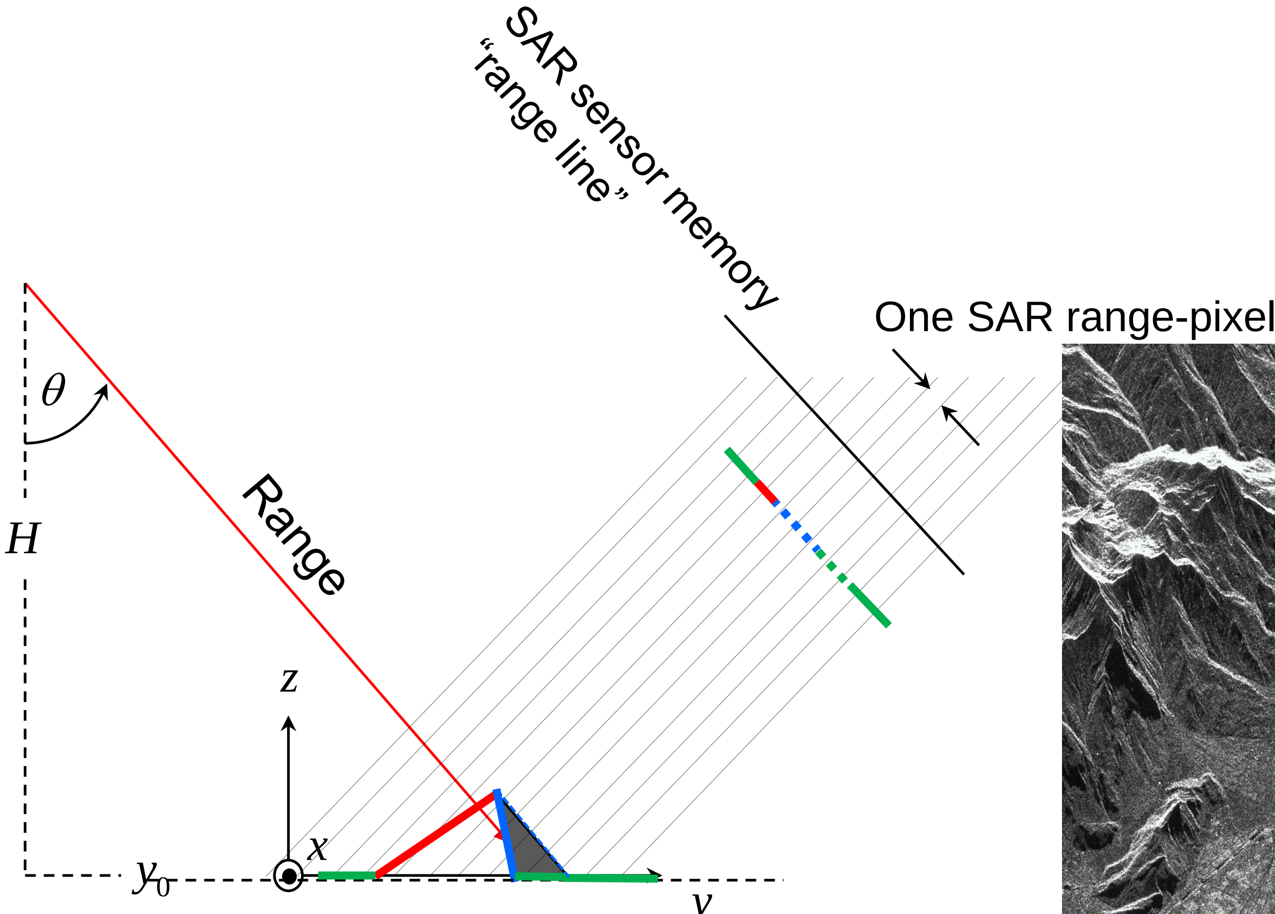

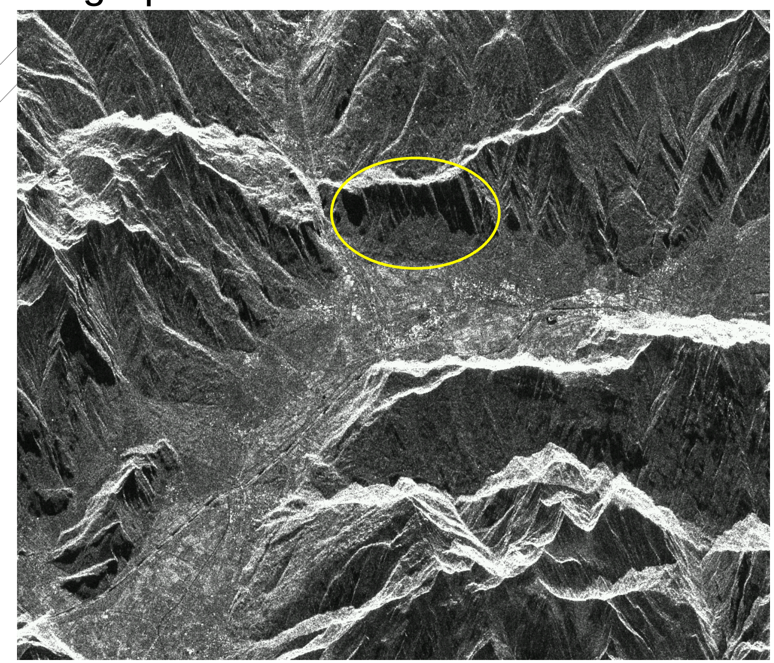

$\theta = 23\,\mathrm{deg}$ ERS-1

Lay-Over Mask Computed from DEM

100m DEM

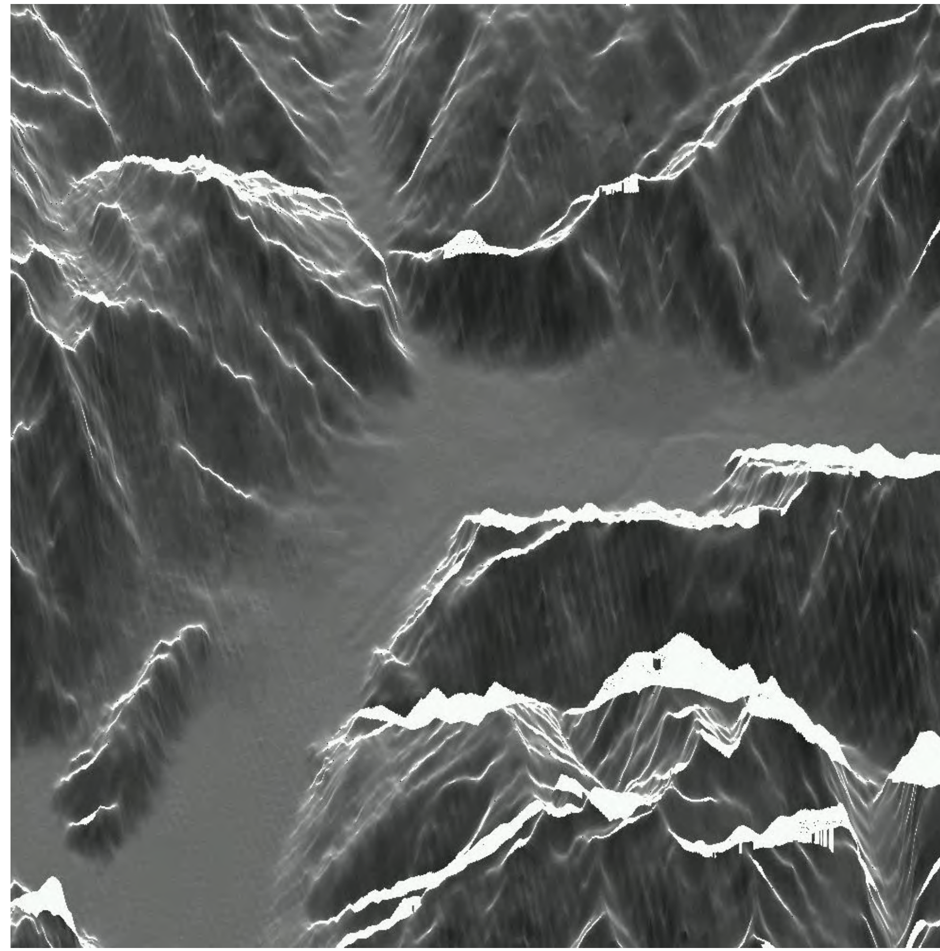

simulated ERS-Image
white: lay-over

Books on SAR

- John C. Curlander, „Synthetic Aperture Radar: Systems and Signal Processing“, Wiley-Interscience, 1991
- Ian G. Cumming, „Digital Processing of Synthetic Aperture Radar Data: Algorithms and Implementation“, Artech House, 2005

Range Compression by Matched Filtering

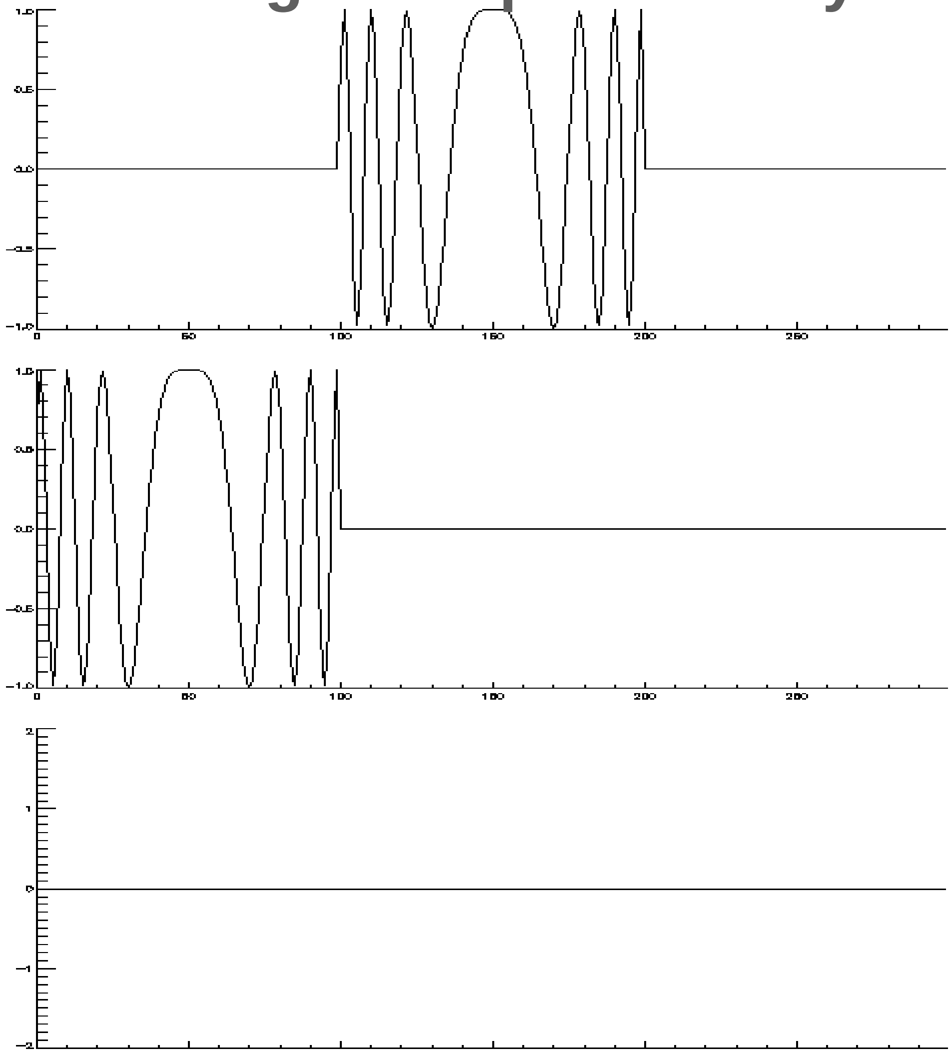

received signal $r(\tau)$

reference chirp $c(\tau)$

s cross-correlation $\int r^*(\tau) c(\tau + s) d\tau$

Linear System →Superposition Law

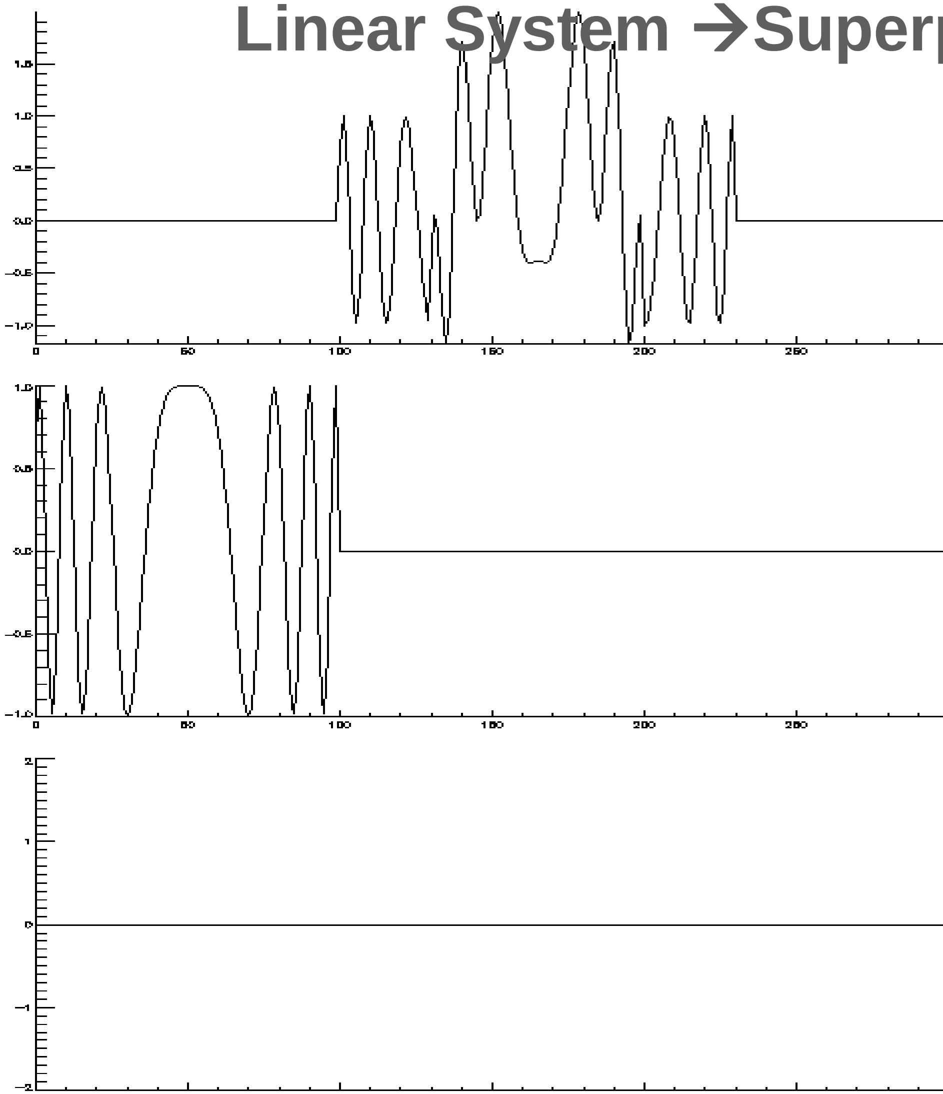

received signal $r_1(\tau)+r_2(\tau)$

reference chirp $c(\tau)$

cross-correlation

$$\int (r_1^*(\tau)+r_2^*(\tau))c(\tau+s)d\tau =$$

$$\int r_1^*(\tau)c(\tau+s)d\tau + \int r_2^*(\tau)c(\tau+s)d\tau$$

Back

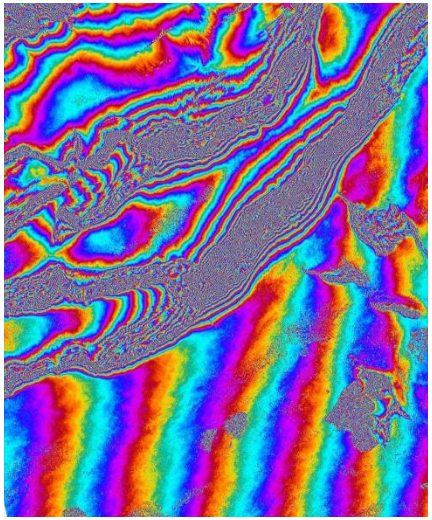

Signal Processing and Microwave Remote Sensing WS 19/20

III. SAR Interferometry - InSAR

Prof. Dr. Michael Eineder

Institut für Methodik der Fernerkundung
Deutsches Zentrum für Luft- und Raumfahrt DLR

Microwave Satellite Remote Sensing

Phase of one Pixel of a SAR Image

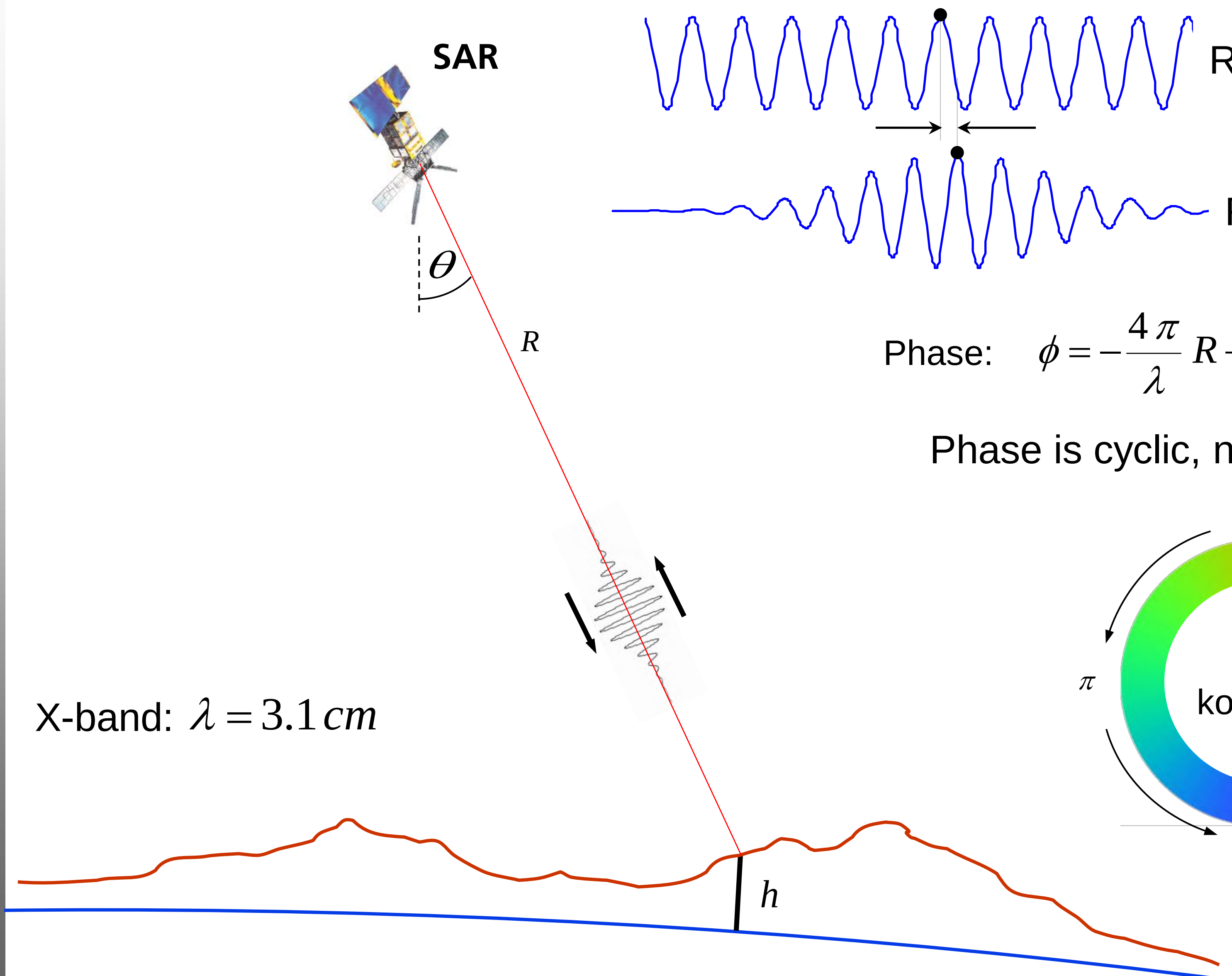

Phase: $\phi = -\frac{4\pi}{\lambda} R + \phi_{scatt} - n \cdot 2\pi$

Phase is cyclic, n unknown!

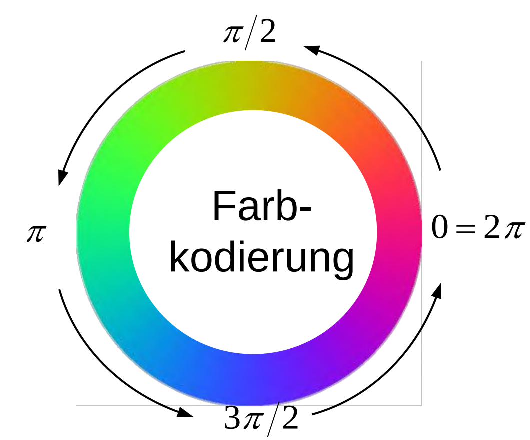

X-band: $\lambda = 3.1\,cm$

InSAR = Phase difference between multiple images

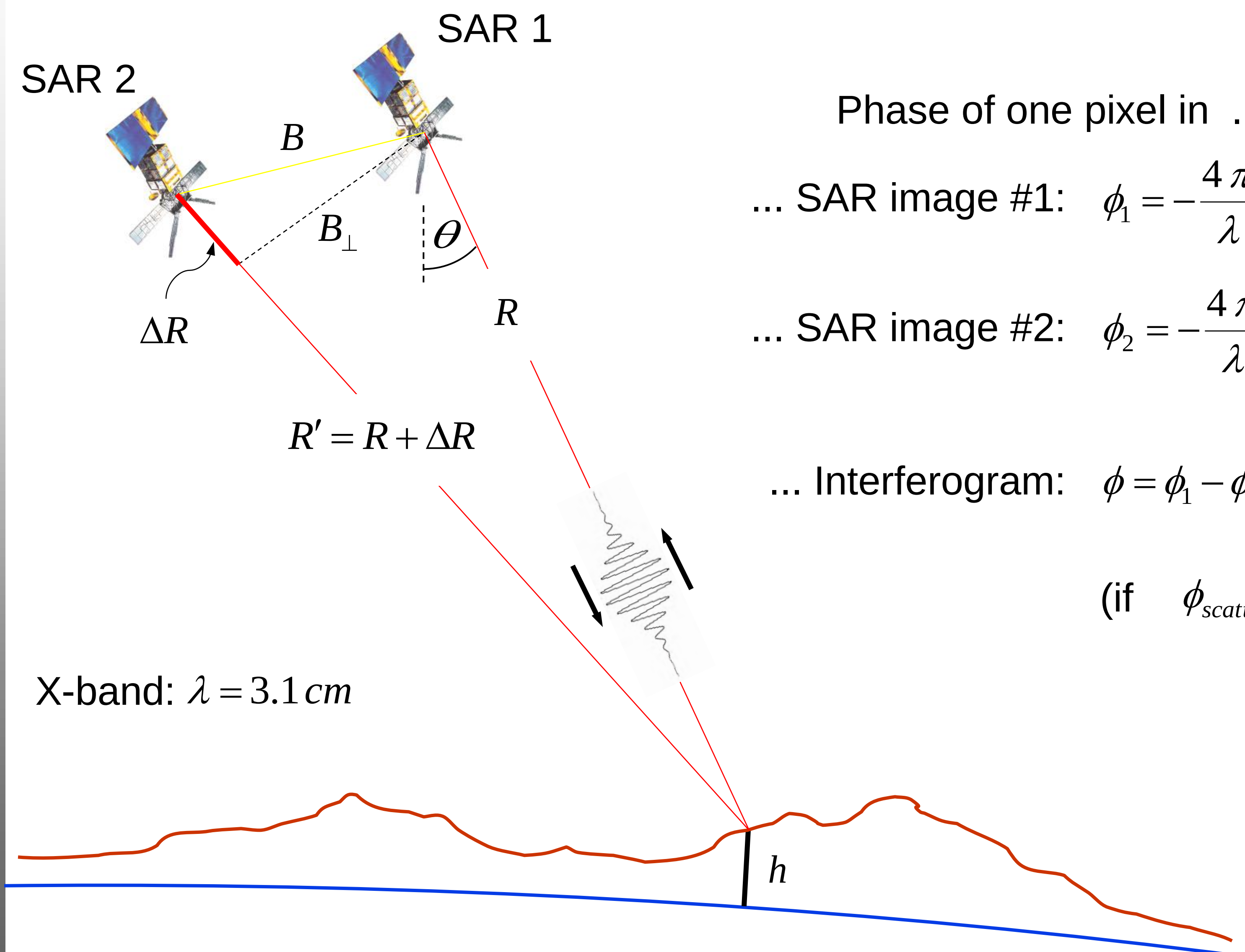

Phase of one pixel in ...

... SAR image #1: $\phi_1 = -\frac{4\pi}{\lambda} R + \phi_{scatt,1}$

... SAR image #2: $\phi_2 = -\frac{4\pi}{\lambda} \left(R + \underline{\Delta R}\right) + \phi_{scatt,2}$

... Interferogram: $\phi = \phi_1 - \phi_2 = \frac{4\pi}{\lambda} \Delta R$

(if $\phi_{scatt,1} = \phi_{scatt,2}$!)

X-band: $\lambda = 3.1\,cm$

SAR Interferogram Formation

phase of a complex SAR image pixel: $\phi_{1,2} = \underbrace{-\frac{4\,\pi}{\lambda} R_{1,2}}_{\text{range}} + \underbrace{\phi_{scatt_{1,2}}}_{\text{scattering}}$ note: non-ambiguous phase!

complex SAR image #1: $u_1[i,k] = |u_1[i,k]| \cdot \exp(j\,\phi_1[i,k])$

complex SAR image #2: $u_2[i,k] = |u_2[i,k]| \cdot \exp(j\,\phi_2[i,k])$

interferogram: $v[i,k] = u_1[\cdot]\,u_2^*[\cdot] = |u_1[\cdot]|\,|u_2[\cdot]|\,\exp(j\,\phi[\cdot])$

interferometric phase: $\phi[\cdot] = \phi_1[\cdot] - \phi_2[\cdot]$

Different Type of Baselines:

- InSAR measures phase difference from different positions and/or at different times
  - Differential (temporal) interferometry → deformation
    - Many scenes: Persistent Scatterer Interferometry (PSI)
  - Across track interferometry → Digital Elevation Models
    - One satellite at different times →repeat pass InSAR
    - Two antennas or antennas at same time → single pass InSAR

Application 1: Across-Track InSAR →Topografy

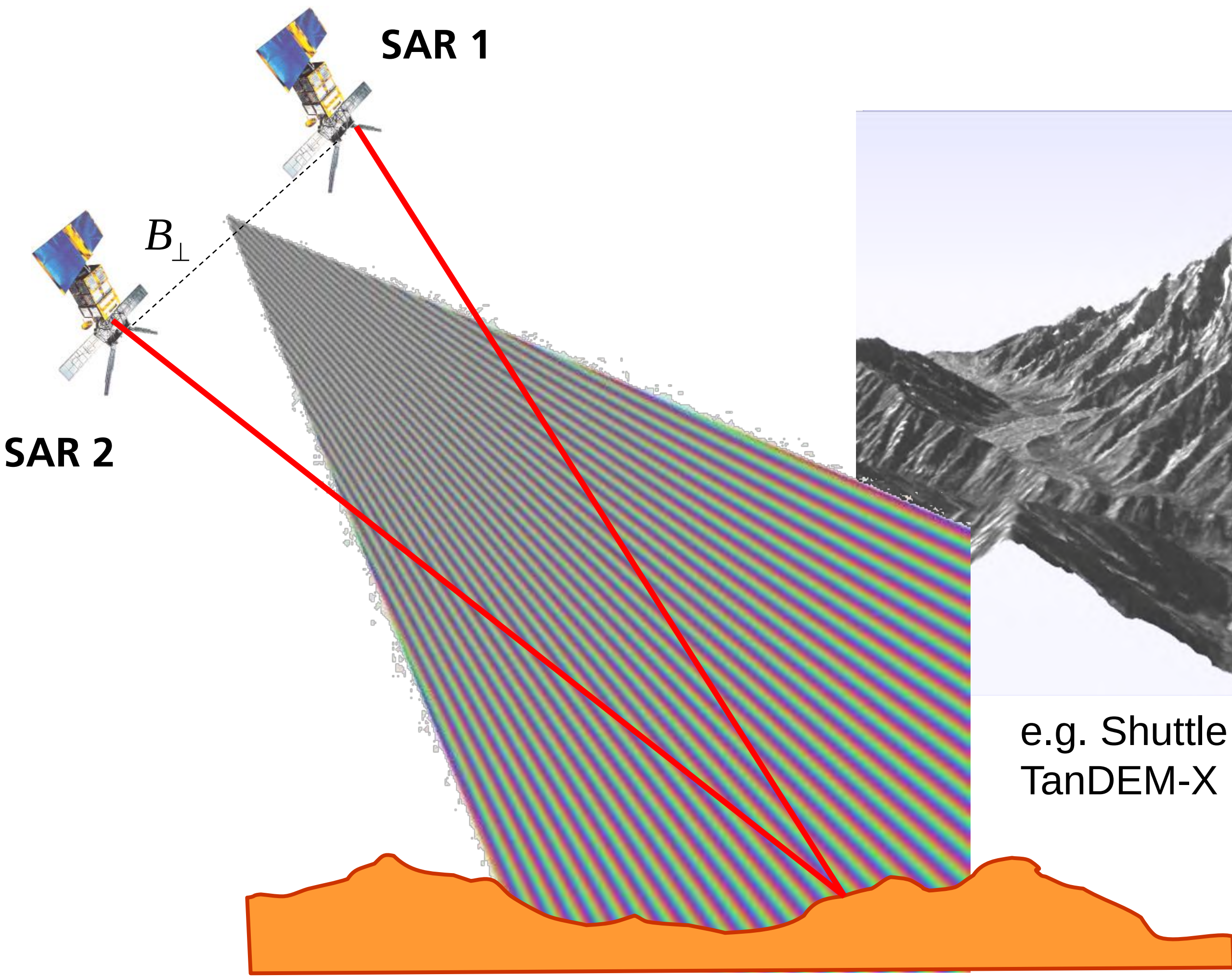

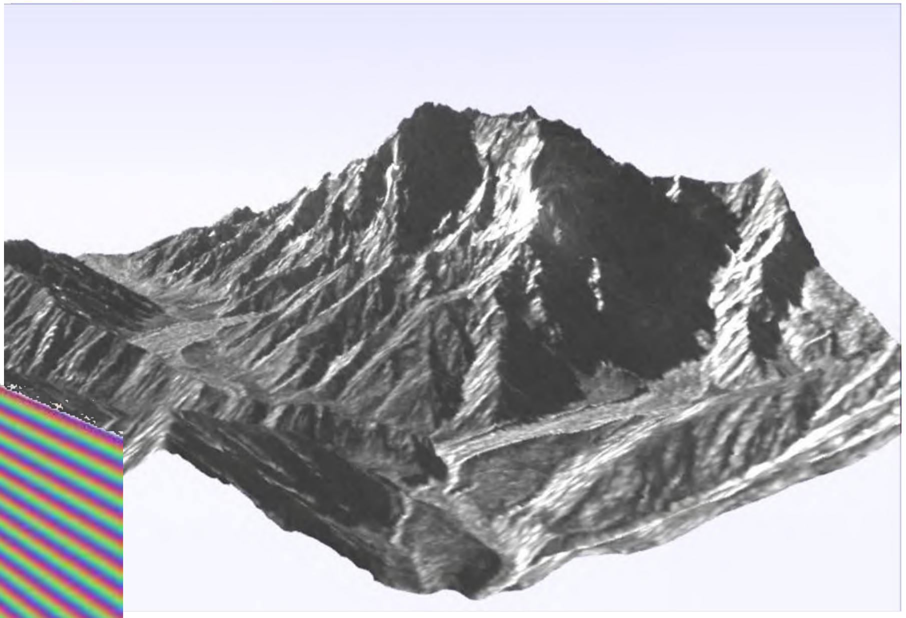

e.g. Shuttle Radar Topografy Mission,
TanDEM-X Mission

Single Pass Missions

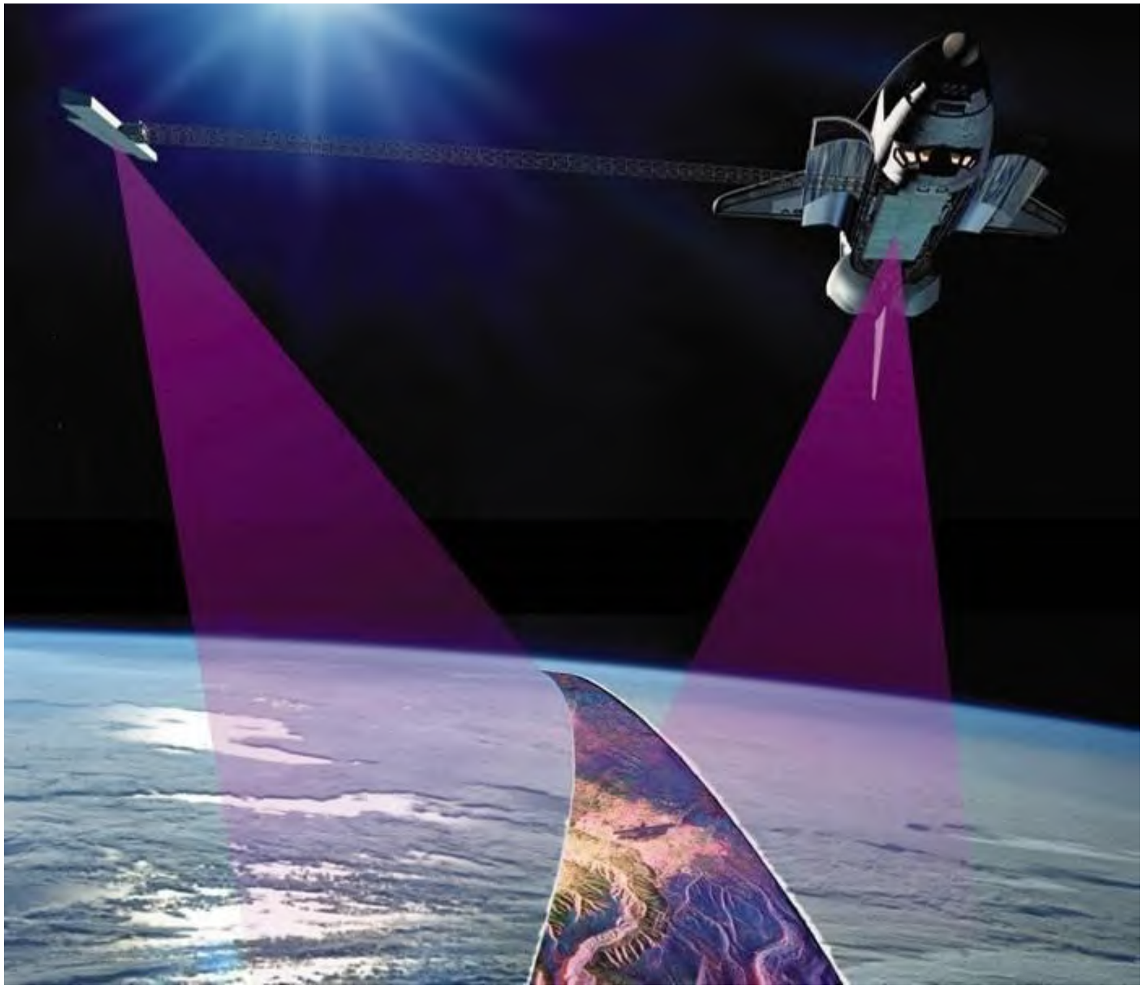

SRTM

- USA/Germany/Italy, 11 days in 2000
- X+C-Band,
- dedicated single pass interferometer
- Global DEM between +-60°
- 1“/3“ (30m/90m) raster
- 6m / 16m accuracy (rel/abs)

TanDEM-X Mission

- Goal:
  - Global DEM: 12 m grid,
    2 m point-to-point acc. (90%)
- Method:
  - Bistatic SAR interferometer from TerraSAR-X and twin satellite
- Mission plan:
  - 2-3 years global imaging with different baselines and angles
  - Scientific experiments (extreme baselines, along-track-InSAR)

TanDEM-X

- Start of mapping 12/2010
- After 3 months: 3/2011:

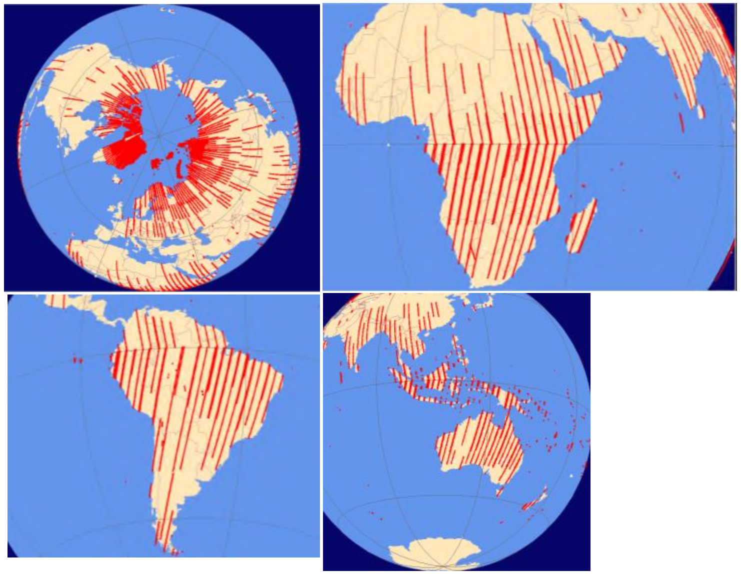

After 5 years

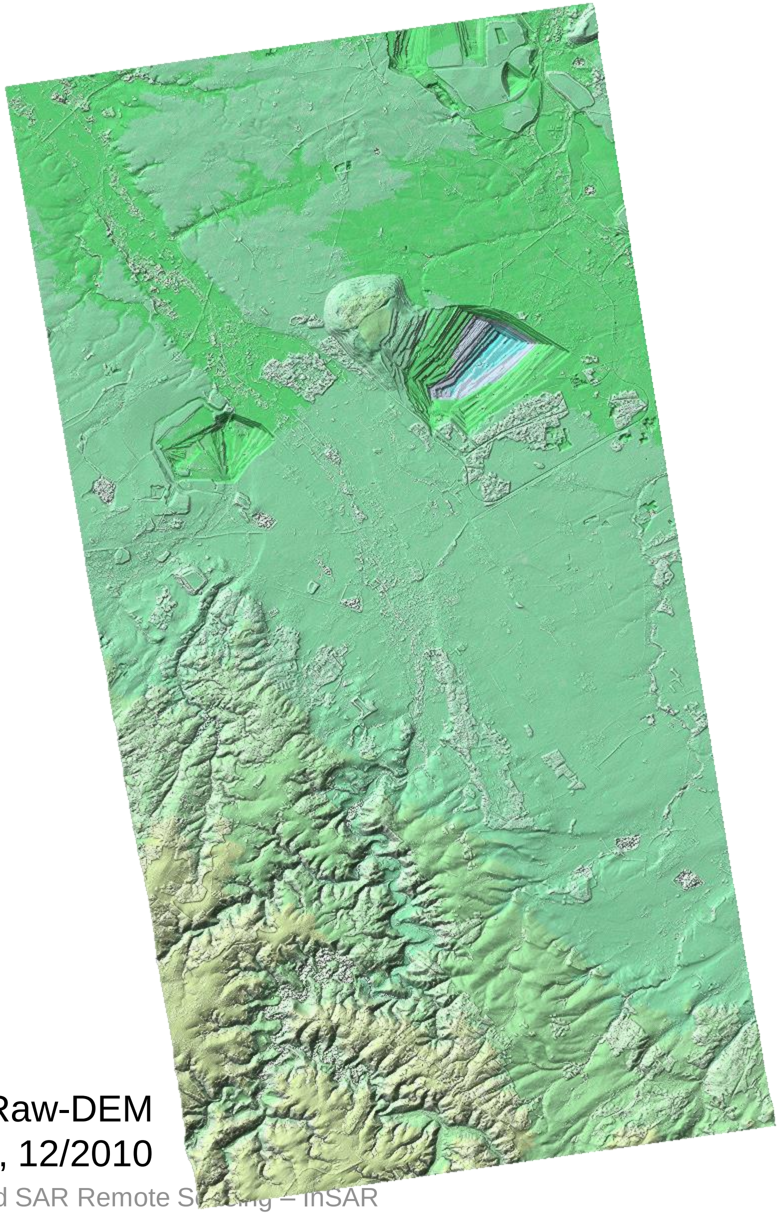

TanDEM-X Raw-DEM
Hambach, 12/2010

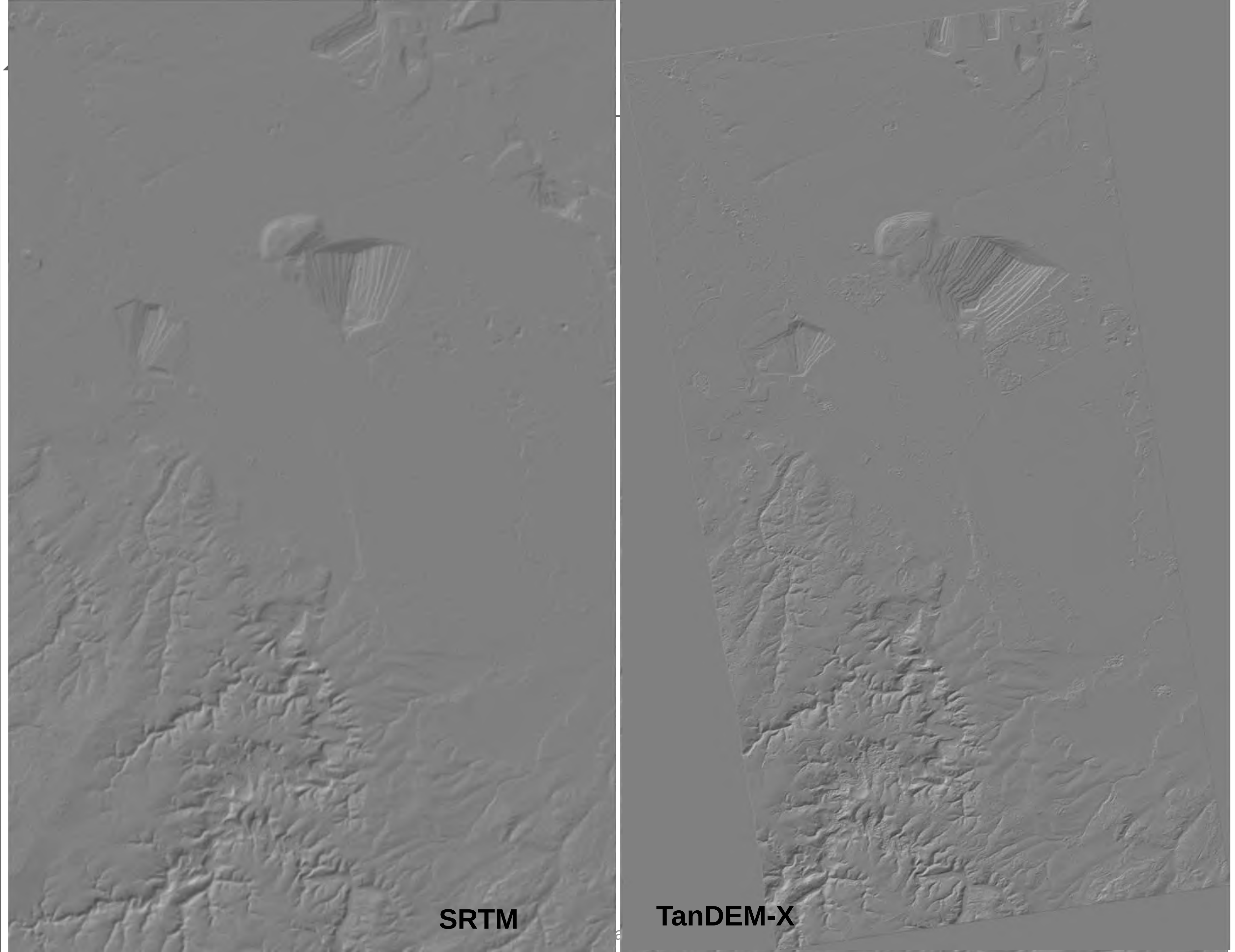
SRTM
TanDEM-X

TanDEM-X DEM - Änderungen seit SRTM 2000

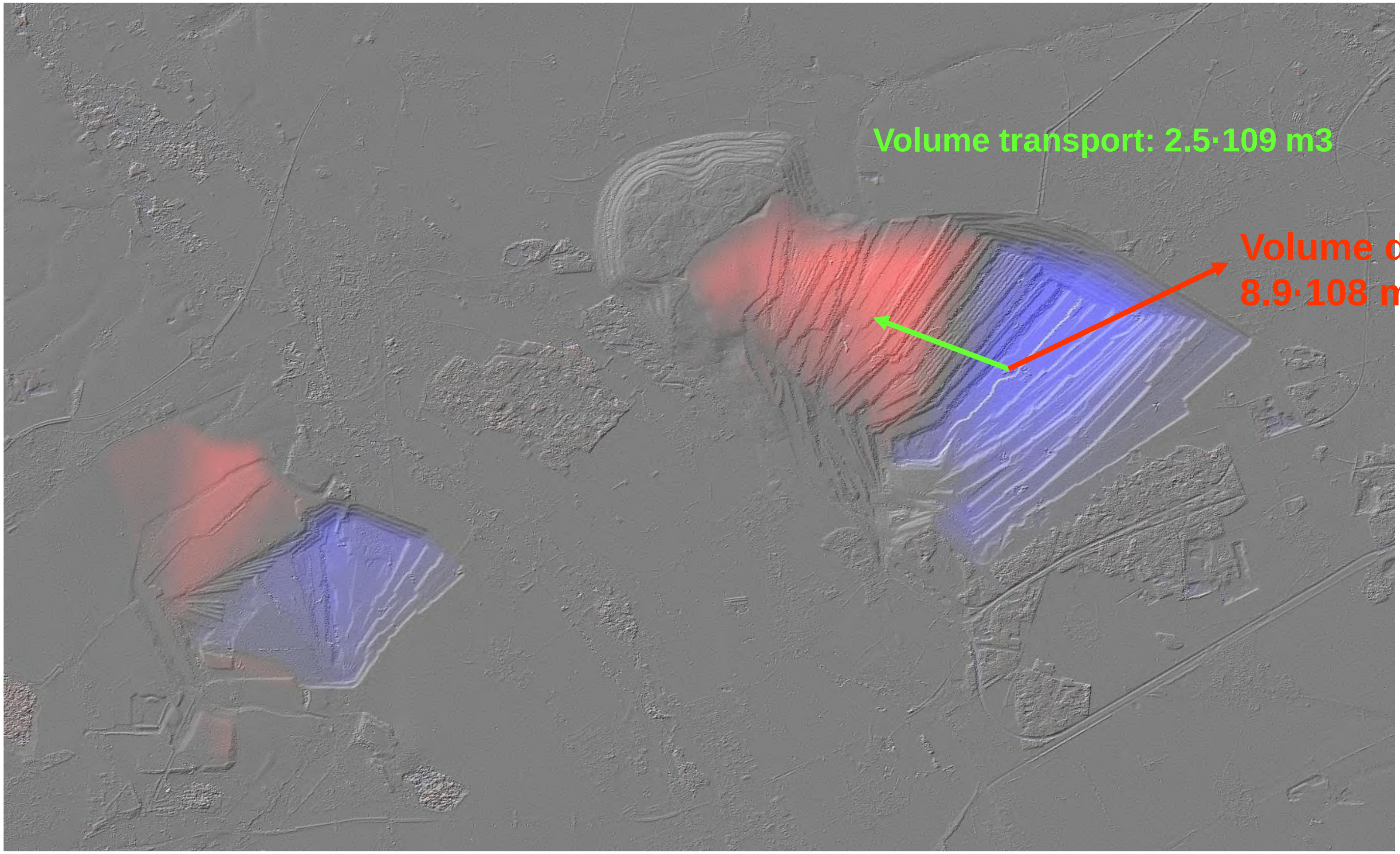

Application 2: dInSAR → Surface Deformation

Range change in line of sight

→ Phase change $$\phi_{defo} = -\frac{4\pi}{\lambda} \Delta R_{defo}$$

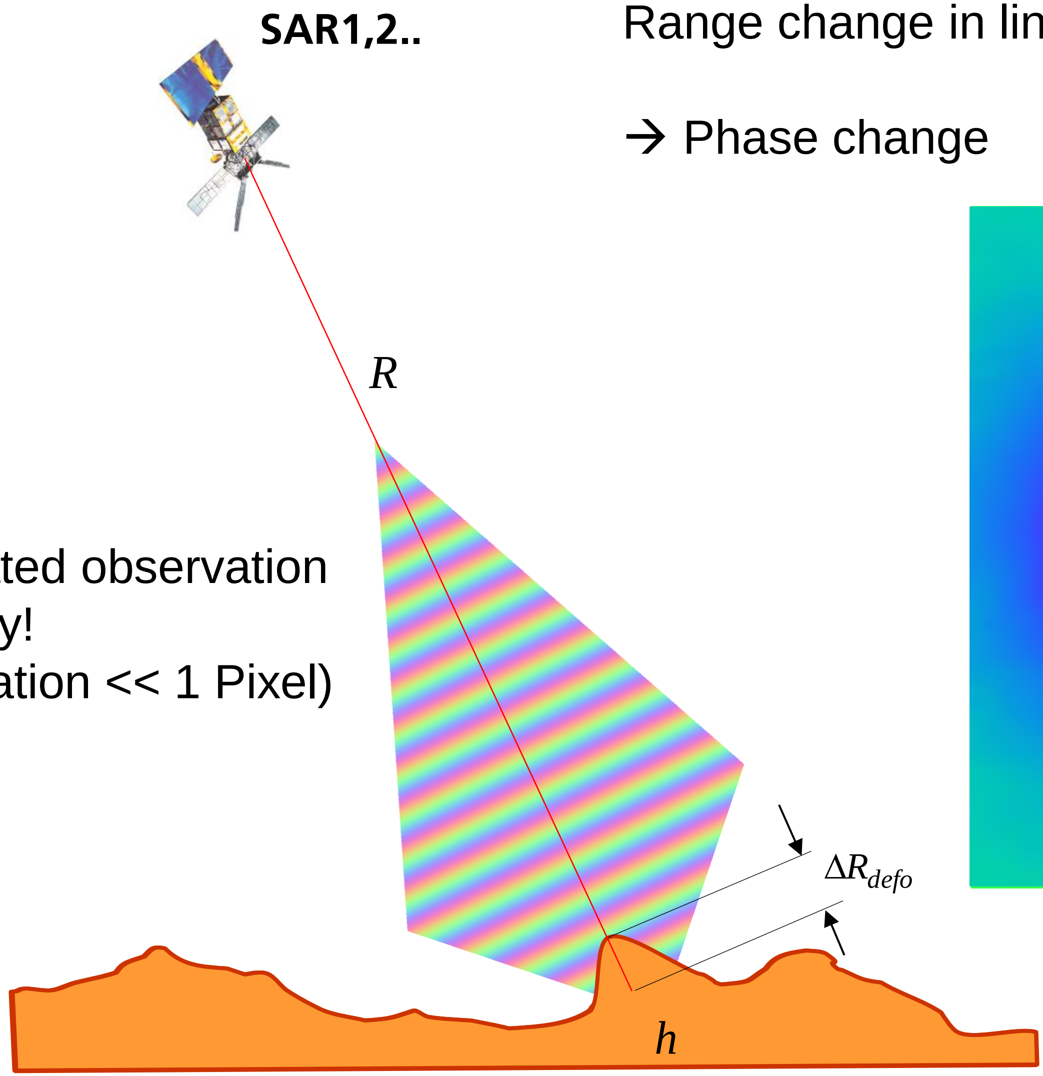

Exagerated observation geometry!
(deformation << 1 Pixel)

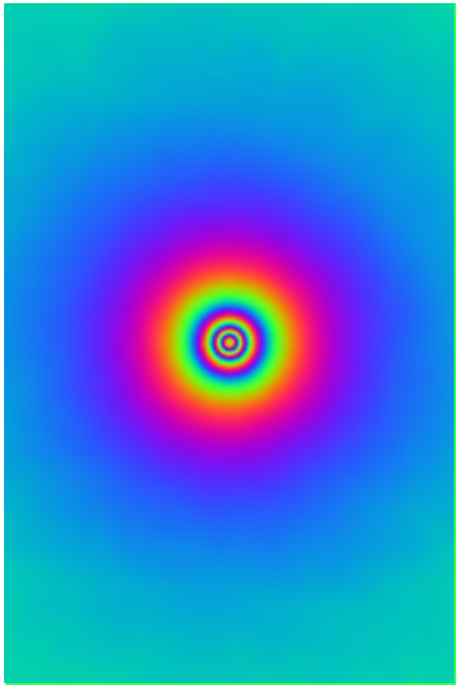

Interferogram

In reality: Motion and Topografy

$$\phi = \phi_{defo} + \phi_{topo} = -\frac{4\pi}{\lambda}\Delta R_{defo} + 4\pi\frac{hB_\perp}{\lambda R\sin\theta}$$

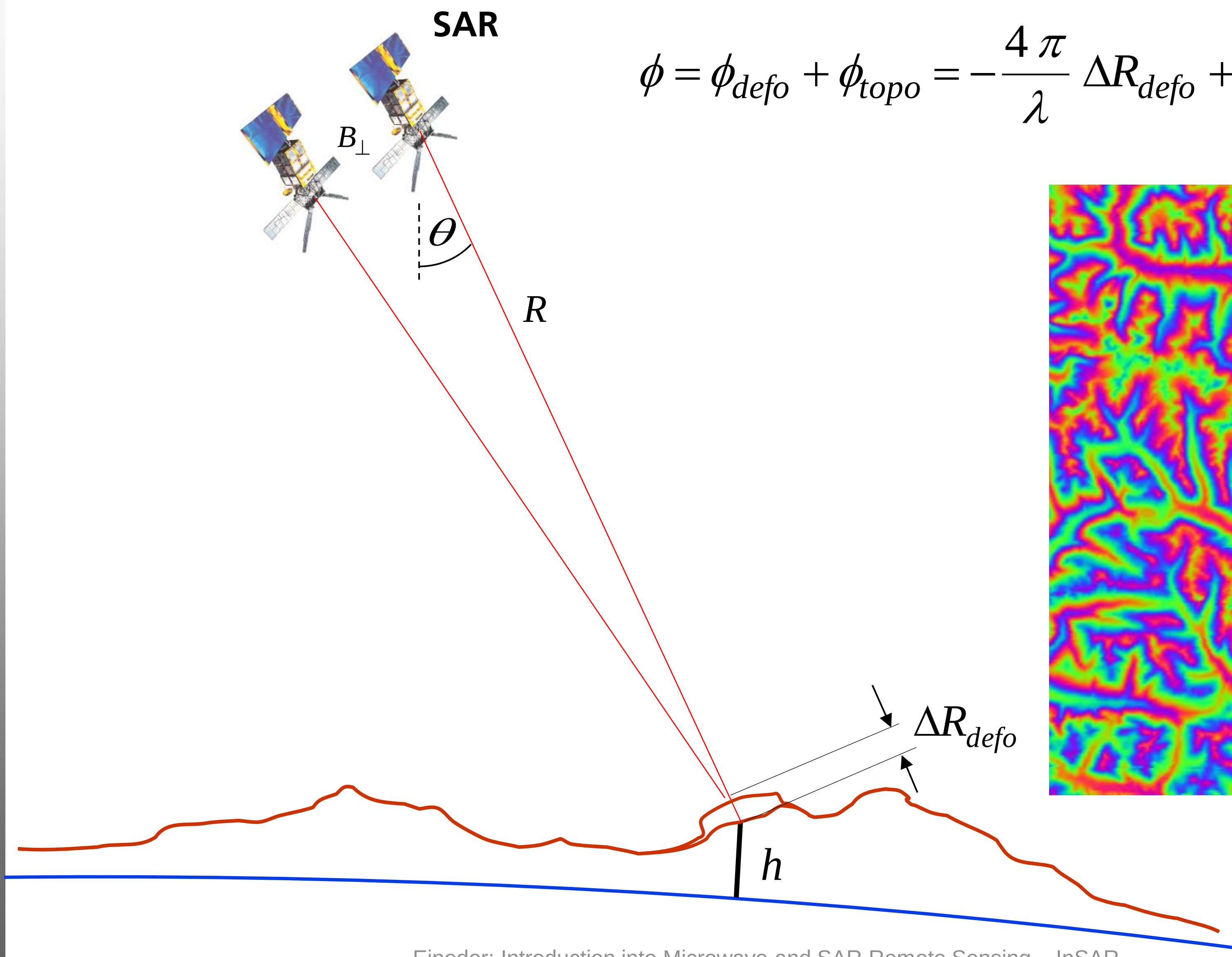

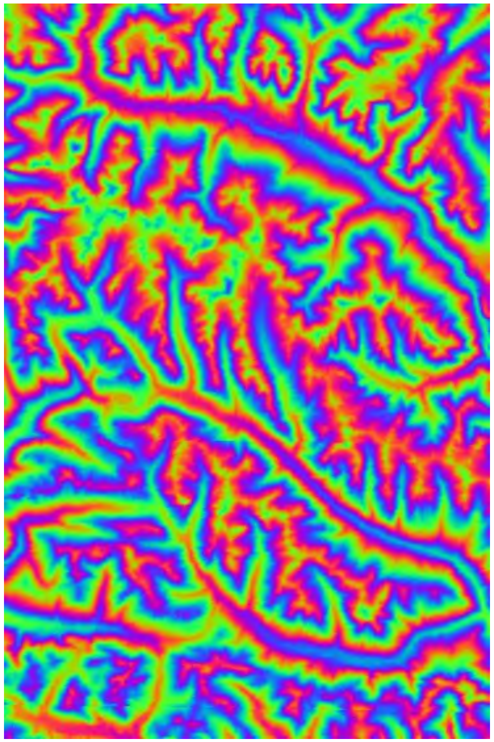

Co-Seismisc deformation of earthquake in Bam, Iran on 26.12.2003

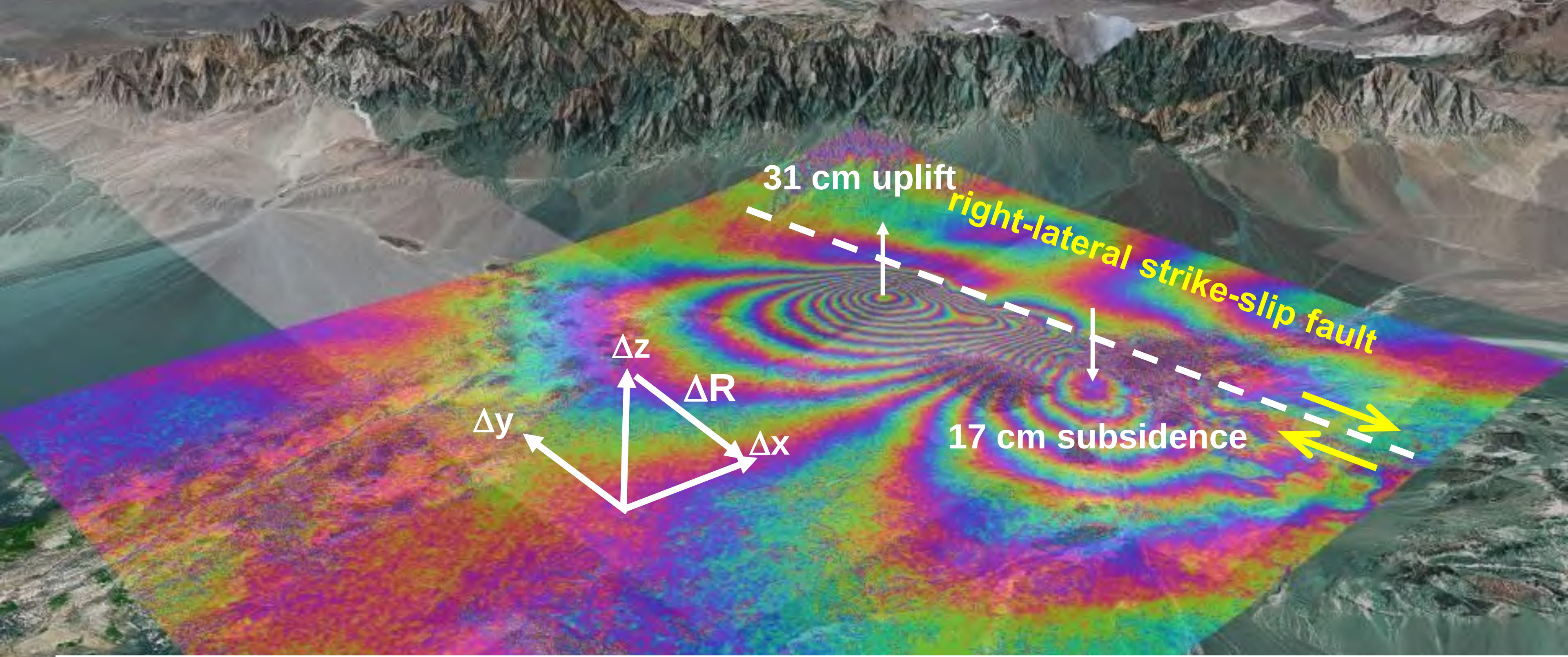

InSAR measures ΔR-component of 3D deformation field in line of sight.

→ Interpretation based on a-priory knowledge or additional (GPS-) measuements

→ 3D-Vector derivation from InSAR possible through combination of multiple viewing directions

InSAR error sources

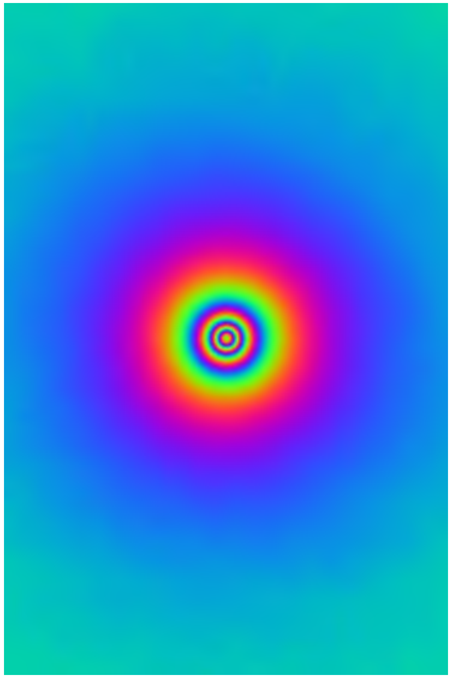

1. Phase ambiguities

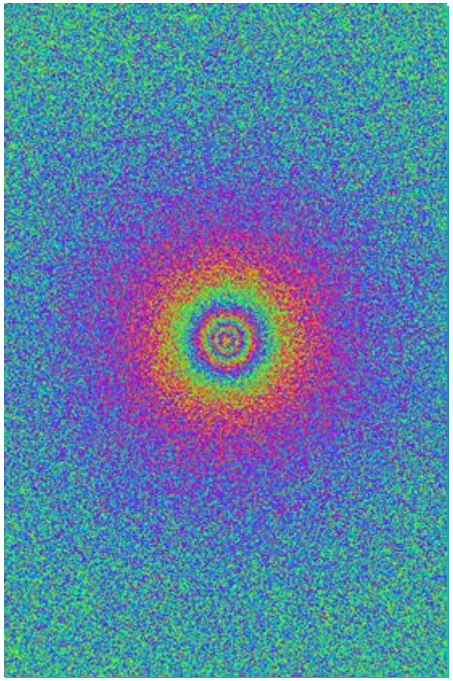

2. Random motion of e.g. vegetation (→phase decorrelation)

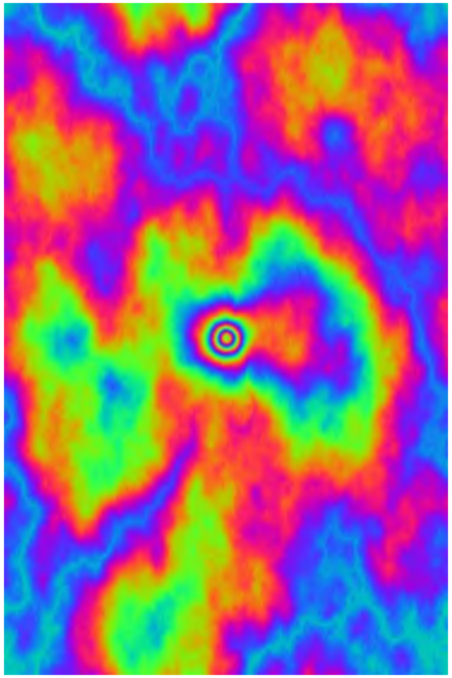

3. Water vapour in atmosphere (large scale error)

→ Time series and motion models requried: Persistent Scatterer Interferometry (PSI)

Persistent Scatterer Interferometry (PSI)

- Selection of points with stable (temporal) phase (very small percentage)
- Connection of points with short arcs network
- Parameter estimation of temporal phase model (linear, periodic …) on each arc
- 2D network integration of model parameters
- Interpolation of results

Persistent Scatterer Interferometry with ERS-1/ERS-2

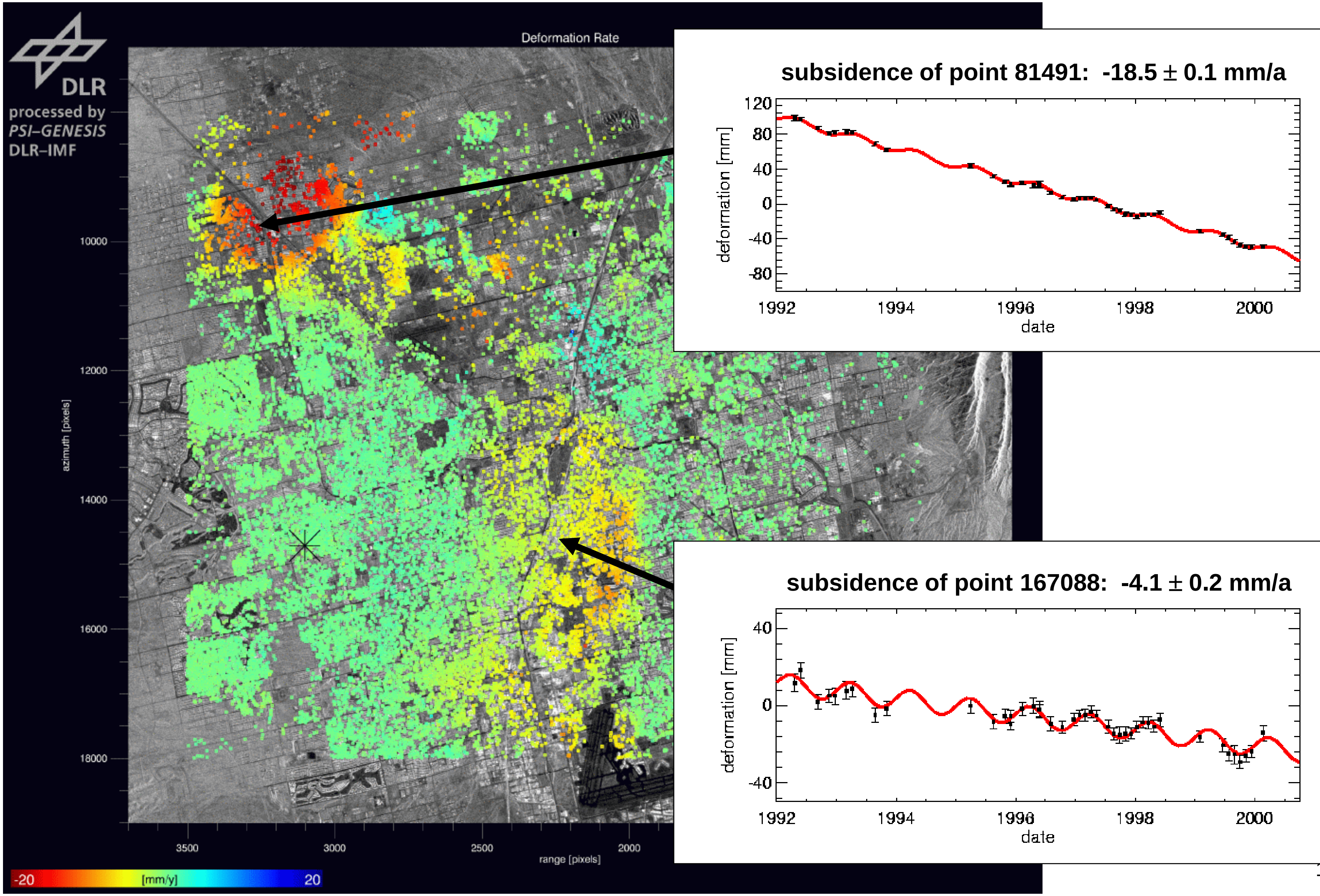

High Resolution PSI with TerraSAR-X

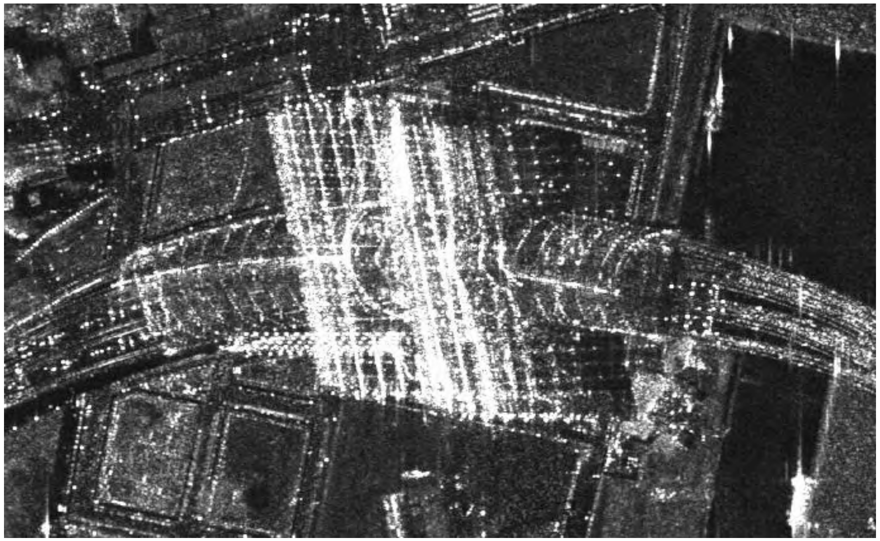

TerraSAR-X

Google Earth

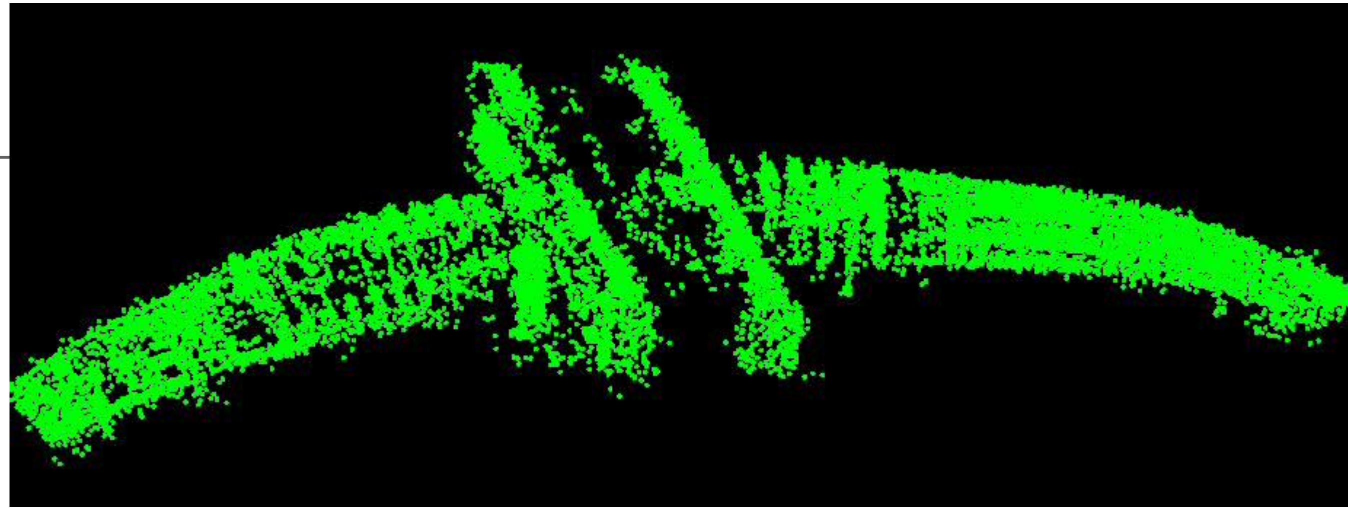

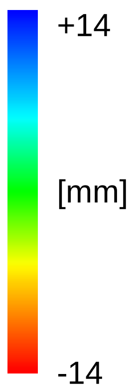
+14
[mm]
-14